2011-02-22

Development of Monolithic Stationary phases for Cation-Exchange Capillary Liquid Chromatography of Peptides and Proteins

Xin Chen
Brigham Young University - Provo

DEVELOPMENT OF MONOLITHIC STATIONARY PHASES FOR CATION-EXCHANGE

CAPILLARY LIQUID CHROMATOGRAPHY OF PEPTIDES AND PROTEINS

Xin Chen

A dissertation submitted to the faculty of
Brigham Young University
in partial fulfillment of the requirements for the degree of

Doctor of Philosophy

Milton L. Lee, Chair
Steven W. Graves
H. Dennis Tolley
Matthew R. Linford
Adam T. Woolley

Department of Chemistry & Biochemistry

Brigham Young University

April 2011

ABSTRACT

DEVELOPMENT OF MONOLITHIC STATIONARY PHASES FOR CATION-EXCHANGE
CAPILLARY LIQUID CHROMATOGRAPHY OF PEPTIDES AND PROTEINS

Xin Chen

Department of Chemistry & Biochemistry
Doctor of Philosophy

This dissertation focuses on the preparation of polymeric monolithic capillaries for ion exchange chromatography of peptides and proteins, since polymeric monoliths have shown promise for providing improved protein separations. Characteristics of monolithic columns include low back pressure, simplicity of fabrication and biocompatibility. Preparation of strong and weak cation-exchange monolithic stationary phases in 75 μm I.D. capillaries by direct *in situ* copolymerization was achieved using various functional monomers including sulfopropyl methacrylate, phosphoric acid 2-hydroxyethyl methacrylate, bis[2-(methacryloyloxy)ethyl] phosphate and 2-carboxyethyl acrylate with polyethylene glycol diacrylate and other PEG materials. The resulting monoliths provided excellent ion exchange capillary LC of peptides and proteins with good run-to-run [relative standard deviation (RSD) < 1.99%] and column-to-column (RSD < 5.64%) reproducibilities. Narrow peaks were obtained and peak capacities of over 20 were achieved. Dynamic binding capacities of over 30 mg/mL of column volume for lysozyme were measured.

A single monomer was used to synthesize a phosphoric acid containing monolith to improve its stability and reproducibility. The monolith was synthesized from only BMEP in 75 μm I.D. UV transparent fused-silica capillaries by photo-initiated polymerization. A dynamic binding capacity (lysozyme) of approximately 70 mg/mL of column volume was measured. Efficiencies of 52,900 plates/m for peptides and 71,000 plates/m for proteins were obtained under isocratic conditions. Good reproducibilities were achieved.

Zwitterionic monolithic columns based on photo-initiated copolymerization of N,N-dimethyl-N-methacryloxyethyl-N-(3-sulfopropyl)ammonium betain and poly(ethylene glycol) diacrylate were prepared in 75 μm I.D. fused silica capillaries for hydrophilic interaction chromatography. Inverse size exclusion chromatography was used to characterize the pore structure of the resulting monolith. A typical hydrophilic interaction chromatography mechanism was observed when the organic content in the mobile phase was higher than 60%. Good separations of amides, phenols, and benzoic acids were achieved. The effects of mobile phase pH, salt concentration, and organic modifier content on retention were investigated.

Keywords: monolith, ion exchange, hydrophilic interaction, liquid chromatography

ACKNOWLEDGMENTS

Finally, I must thank my family and Ying's family. The help and love given by both families during the past five years is indescribable. My deepest gratitude belongs to my wife, Ying, who is a graduate student as well in the Department of Chemistry & Biochemistry. It was a challenge to bear two children and take care of them while pursuing graduate studies during the past five years. Without her excellent work at home and without her personal sacrifice, it would have been impossible for me to finish this project. Deep gratitude also belongs to my parents-in-law and to my parents. Bearing great loneliness, they traveled to America, which was unfamiliar to them, to help take care of our children. Their unselfish love and understanding were the greatest impetus for me to finish this dissertation. This dissertation is dedicated to my parents-in-law, my parents, my wife, and my two children, Elvin and Kaelyn.

TABLE OF CONTENTS

LIST OF ABBREVIATIONS

AIBN	2-2'-azo-bis-isobutyrylnitrile
AMPS	2-acrylamido-2-methyl-1-propanesulfonic acid
ATRP	atom transfer radical polymerization
BACM	4-[(4-aminocyclohexyl)methyl]cyclohexylamine
BMA	butyl methacrylate
BMEP	bis[2-(methacryloyloxy)ethyl] phosphate
BNE	biotin NHS ester
BPO	dibenzoyl peroxide
BVPE	1,2-bis(p-vinylphenyl)ethane
CE	capillary electrophoresis
CEA	2-carboxyethyl acrylate
CEC	capillary electrochromatography
CHD	trans-1,2-cyclohexanediamine
CLC	capillary liquid chromatography
CTAB	cetyltrimethyl ammonium bromide
DBC	dynamic binding capacity
DEGDMA	diethylene glycol dimethacrylate
DMA	decyl methacrylate
DMN-H6	1,4,4a,5,8,8a-hexahydro-1,4,5,8-exo,endo-dimethanonaphthalene
DMPA	2,2-dimethyl-2-phenylacetophenone
DMPA	2,2-dimethoxy-2-phenylacetophenone

DVB	divinylbenzene
EDMA	ethylene glycol dimethacrylate
EOF	electroosmotic flow
GA	glutaric anhydride
GC	gas chromatography
GMA	glycidal methacrylate
HEA	2-hydroxyethyl-acrylate
HEMA	hydroxyethyl methacrylate
HIC	hydrophobic interaction chromatography
HILIC	hydrophilic interaction chromatography
HPLC	high performance liquid chromatography
IEC	ion-exchange chromatography
ISEC	inverse size exclusion chromatography
LPO	lauroyl peroxide
MBA	N,N'-methylenebisacrylamide
MEMAC	(methacryloyloxy)ethyltrimethylammonium chloride
META	2-(methacryloyloxy)ethyltrimethylammonium methyl sulfate
MPA	2-methoxy-2-phenylacetophenone
MPC	methacryloyloxyethyl phosphorylcholine
NBE	norborn-2-ene
OD	octadecene
ONDCA	7-oxanorborn-2-ene-5,6-carboxylic anhydride

PAHEMA   phosphoric acid 2-hydroxyethyl methacrylate

PDITC   1,4-diisothiocyanate

PEDAS   pentaerythritol diacrylate monosterate

PEGA   polyethylene glycol acrylate

PEGDA   polyethylene glycol diacrylate

PETA   pentaerythritol triacrylate

polyHIPE   polymerized high internal emulsions

POSS   polyhedral oligomeric silsesquioxane

ROMP   ring-opening metathesis polymerization

RPC   reversed-phase chromatography

RSD   relative standard deviation

SCX   strong cation-exchange

SDS   sodium dodecyl sulfate

SEM   scanning electron microscopy

SEMA   2-sulphoethyl methacrylate

SMA   stearyl methacrylate

SPE   N,N-dimethyl-N-methacryloxyethyl-N-(3-sulphopropyl)ammonium betain

SPMA   3-sulfopropyl methacrylate

TEPIC   tris(2,3-epoxypropyl) isocyanurate

TPM   3-(trimethoxysilyl)propyl methacrylate

TVBS   tetrakis(4-vinylbenzyl)silane

VS   vinyl sulfonic acid

LIST OF TABLES

LIST OF FIGURES

CHAPTER 1 BACKGROUND AND SIGNIFICANCE

1.1 Liquid Chromatography

1.1.1 History of Column Liquid Chromatography

Liquid Chromatography (LC) is a chromatographic technique that is widely used to identify, quantify, and purify individual components of mixtures of components. It was first studied systematically by a Russian botanist, Mikhail Tswett, whose work was reported in 1906.[1] In his study, a solid adsorbent packed into a glass column was used as stationary phase. Separation of chlorophyll extracts from plants using petroleum spirits was obtained. During the period from 1910 to 1930, the LC method was slow to develop, although some work describing the use of LC for the separation of pigments in plants and dairy products was published.[2] One of the reasons for the lack of interest in LC is that scientists at that time were interested in large-scale synthetic organic chemistry, and not in small-scale physical separation methods. In 1931, Lederer et al. continued to use LC to investigate pigments in egg yolk, because the new technique made it possible to avoid degradation of carotene molecules due to its relatively high speed.[3] From this time on, other forms of chromatography were developed. In 1938, planar chromatography as well as thin layer chromatography was developed, in which the stationary phase material was spread on a glass plate.[4]

The major breakthrough that led to development of modern chromatography came in 1941 with the work of Martin and Synge,[5] who produced the first mathematical treatment of chromatographic theory using the plate theory, for which they won the Nobel Prize in 1952. Many of the developments in chromatography were predicted, which was realized later. With developments in technology, it was possible to apply chromatographic theory to the further

development of LC. Of particular importance was the use of small particles for the stationary phase. Due to the low permeability of small particle packed beds, a pump was required to generate sufficient pressure to produce a reasonable flow rate. This technique was initially called "high-pressure LC". Soon after, this terminology was replaced with "high-performance LC" due to the improvement in performance in terms of resolving power, detection, quantitation and speed. During the 1960s, many developments in technique were made by pioneers such as Huber, Kirkland, Knox, Snyder, and Scott. At the same time, instrument manufacturers also played an important role in the development of LC. With improvement in pumps, injectors, and detectors, LC became a very popular chromatographic technique by the mid-1970s. At the end of 1980s, it was the most widely used chromatographic technique, with an estimated 65% of the worldwide separation science market.[6] Currently, LC is used by a variety of industries, including biotechnological, biomedical, pharmaceutical, cosmetics, energy, food, and environmental.

1.1.2 Classification of LC Modes

Depending on the type of packing material, LC can be classified into two categories: (1) liquid-liquid chromatography and (2) liquid-solid chromatography. The former was developed by Martin and Synge in 1941,[4] and depends on the partitioning of solutes between a liquid mobile phase and an immobilized liquid stationary phase that is distributed on an inert support. Liquid-solid chromatography is the oldest form of LC. The separation mechanism involves differential, reversible adsorption of solutes on solid adsorbents. The strength of such sorptive interactions depends on the polarity of the solutes, the mobile phase, and the stationary phase.

Based on retention mechanism, three categories of LC have been delineated: adsorption, partition, and size exclusion. In adsorption chromatography, the stationary phase has an active surface, which can adsorb analytes from the mobile phase. Adsorption LC includes affinity

chromatography, argentation chromatography, hydrophobic interaction chromatography, ion-exchange chromatography, ion chromatography, ion-pair chromatography, ligand exchange chromatography, and metal chelate chromatography. In partition chromatography, the separation relies on the differential solubility of solutes between mobile and stationary phases. Partition chromatography mechanisms are used in countercurrent chromatography, micellar liquid chromatography, normal-phase liquid chromatography, reversed-phase chromatography, and supercritical fluid chromatography. Size exclusion chromatography (third category) is determined by the physical sizes of the solutes and pore sizes in the stationary phase.

1.1.3 Ion-Exchange Chromatography (IEC)

IEC is an LC technique used to separate analytes with electrical charges (i.e., ions). Ion exchange behavior was first observed in soil in the middle of the 19th century by Thompson.[7] It was put into industrial use in 1905, when artificial ion exchangers were made by melting aluminates and silicates together.[8] They were used to soften water, exchanging the ions of calcium and magnesium in hard water with sodium ions. In 1935, synthetic organic ion exchangers made it possible to remove salts completely from water by combining cation and anion exchange.[9] In 1938, Taylor and Urey used this technique to separate lithium and potassium isotopes.[10] IEC developed rapidly from this time for the separation of rare earth ions due to the urgent need to furnish such materials in the Manhattan project.[11] The success in separating adjacent rare earths suggested that isotopes of N might also be separated using IEC. In 1955, Spedding et al. separated ^{15}N from ^{14}N,[12] and shortly thereafter, IEC was used to separate metal ions using both anion and cation-exchange chromatography. Researchers in Oak Ridge demonstrated that a number of elements could be taken up and separated as their anionic fluoride, bromide, nitrate or sulfonate complexes.[13] Samuelson published a book in 1963 to help

popularize the use of IEC in analytical chemistry.[14] It did not take long to recognize that IEC could be used to separate biomolecules. For example, Cohn[15] used IEC to separate nucleic acids, and Sober et al.[16] used it to separate spleen enzymes. It was not until the middle of the 1970s that methods were developed to pack columns that could withstand pressures exceeding 35 MPa, which enabled much faster separations than possible in the past.[17] From then on, IEC became a routine method for the separation of peptides and proteins.[18,19]

The two main categories of ion exchangers are based on the electrical charges on ion exchange functionalities. Cation exchangers contain sulfonic acid, phosphoric acid, or carboxylic acid groups, while anion exchangers contain tertiary or quaternary amines. Retention in IEC depends on ionic interactions between the analytes and the ion exchanger. Analytes are eluted by displacing them from the ion exchanger with competing ions in the mobile phase. Thus, the chromatographic retention of an analyte relies on the strength of the interaction between the analyte and the ion exchanger.

IEC has been used for the analysis of both small and large analytes, including inorganic ions, organic ions, and biomolecules. The conditions employed in IEC are not prone to denature proteins, which is important to preserve the activities of the biomolecules. IEC has been used to separate other biomolecules, such as peptides, nucleotides, and amino acids. Carbohydrates can also be separated in the IEC mode when using a high-pH mobile phase.[20] IEC is almost always used as the first dimension in two-dimensional separations due to its orthogonality to reversed-phase liquid chromatography (RPLC).[21]

An ion exchanger consists of an insoluble support, to which charged groups are covalently bound. The support may be based on an inorganic matrix, synthetic resin, or organic polymer. The characteristics of the support affect its chromatographic properties, including

efficiency, capacity, recovery, chemical stability, mechanical strength, and flow properties. Today, most of the commercially available columns for IEC are prepared with packed particulate media. Both silica and polymer particles are used as supports. Pohl arranged the available LC supports into eight different categories, based on how they were manufactured.[22] These categories included silica particles modified using silane reagents, polymer chains grafted onto a support surface, polymeric supports encapsulated with a polymer film, and particles with electrostatically attached colloidal particles. Compared to silica supports used in ion-exchange applications, the stability of polymeric supports at high pH is a distinct advantage, especially when alkaline eluents are needed, because silica deteriorates in alkaline pH.

1.2 Monoliths

1.2.1 General Introduction of Monoliths

A wide variety of LC chromatographic sorbents is commercially available,[23] among which packed columns are the norm. Modern LC columns provide high efficiency, and they are available in various lengths and internal diameters. The particulate media used as packing materials can be prepared reproducibility in large quantities under controlled conditions. However, there are several drawbacks in using spherical packing materials as LC stationary phases. For example, the diffusive mechanism of molecular penetration into the inner volume of the porous particles, especially for large biomolecules that have low diffusion coefficients, significantly limits the separation speed. Because intra-particle diffusive transport is orders of magnitude slower than inter-particle convective transport, band broadening is large at high mobile phase velocity. Various supports have been developed to improve mass transfer, such as micropellicular,[24] superporous,[25] nonporous,[26] and perfusion packings.[27] However, these materials have only partially solved the issue of slow mass transfer. Another problem with

particulate media is the large void volume between the particles that broadens the chromatographic zones and decreases the separation efficiency. One approach to solve this problem is to use very small particles (i.e., < 2 µm diameter). However, this increases the backpressure.

At the end of the 1980s, a novel monolithic chromatographic media was developed to solve problems associated with particulate packing materials. Monoliths are solid, porous rods containing large through-pores, through which the mobile phase flows, and small pores that provide high surface area for solute-stationary phase interaction. Monoliths are prepared by *in situ* polymerization or consolidation. If necessary, the resultant surface can be functionalized with desired chemical moieties. The initial preparation of "single piece" media was reported in the late 1960s and early 1970s. In 1967, Kubin et al. prepared a swollen poly(2-hydroxyethyl methacrylate) polymer for size exclusion chromatography of proteins under low pressure. However, the permeability was too low for practical use.[28] Hileman et al. prepared monolithic polyurethane foams for both LC and gas chromatography (GC).[29] Unfortunately, the monolithic medium swelled excessively in some solvents. It was not until 1989 that a monolithic medium was successfully used in chromatographic separations.[30] This work reported a complex process, requiring multiple steps including a compression process. This early work was followed by extensive studies conducted by Svec and Fréchet,[31,32] who reported a simple procedure to fabricate rigid monolithic columns. A rigid porous polymer was prepared in a capillary column that was initially filled with a monomer mixture including 2-2'-azo-bis-isobutyrylnitrile (AIBN) as initiator. In the mid 1990s, Minakuchi and Tanaka et al. prepared monoliths from inorganic materials,[33] such as silica. The resultant monoliths were successful for separation of small molecules.

From the time that polymeric monoliths were first prepared in 1989, they have steadily increased in interest. To date, monoliths have been prepared in various geometries, such as in disks, rods, and capillary columns. One significant advantage of monolith preparation is the simple synthesis. Monoliths, especially polymer monoliths, can be formed *in situ* in any shape from 8 L[34] to a few nL in the channel of a microfluidics chip.[35] This feature is particularly important for the preparation of micro and nanoscale devices, for which the packing of particulate sorbents is difficult, and leads to poor reproducibility.[36] Organic polymer-based monoliths have been formed from polymethacrylates, polystyrenes, and polyacrylamides, and they have been primarily used for chromatographic separations of macromolecules, such as proteins, nucleic acids, and polysaccharides.[37-39] Silica-based monoliths provide high permeability and good efficiency in separation of small molecules.[33,40] However, they typically cannot be used with alkaline eluents, similar to silica particle packed columns. Organic polymer-based monoliths are stable under a wide range of pH. However, they can possess poor mechanical stability due to swelling and shrinking in some organic solvents, and they often demonstrate relatively low separation efficiency for small molecules. Fortunately, with the advantages of wide pH stability, inertness to biomolecules, ability to functionalize, and mild preparation conditions, considerable efforts have been directed to improving the mechanical strength of polymer-based monoliths. Since this dissertation addresses the separation of biomolecules, only polymer-based monoliths are considered further.

1.2.2 Monolith Preparation

1.2.2.1 Polymerization Methods

The preparation of rigid macroporous polymers by a facile molding process is simple. The mold, typically a tube or a fused capillary is filled with a polymerization mixture and sealed

at both ends. The polymerization is then triggered by one of a variety of initiation methods. After the monolith is formed in the mold, the seals are removed and the monolith is flushed with solvent to remove the porogens and other soluble compounds remaining in the pores.

Thermal-initiation polymerization. Thermal initiation is the most widely used method to produce free radicals for the preparation of rigid polymer-based monoliths.[30,31] The simple procedure is the same as used for preparation of porous beads using suspension polymerization. However, the resultant monolith has different properties. For example, in 1992, glycidyl methacrylate (GMA) and ethylene glycol dimethacrylate (EDMA) were used to prepare monoliths with cyclohexanol and dodecanol as porogens using both suspension and bulk polymerization.[31] The resultant beads and monoliths exhibited different pore size distributions. One explanation for the difference in porosity between the monolith and beads is the difference in interfacial tension.[41] Thus, the existing knowledge about pore formation in porous beads prepared by suspension polymerization cannot be transferred to the synthesis of monoliths directly. As a result, the prediction of pore properties still strongly depends on experience.

The polymerization temperature is probably the most effective parameter that can be used to control the pores in the resulting monolith through its effect on the polymerization kinetics.[42,43] For example, the decomposition half-life of AIBN in styrene is 5.7 h at 70 ℃, while it is approximately 3.2 min at 110 ℃. Higher temperature leads to more rapid decomposition of the initiator, leading to a larger number of growing polymer chains and growing nuclei. The effect of temperature can be explained in terms of the nucleation rate.[43] The free-radical initiator decomposes at a particular temperature, and the resulting radicals initiate the polymerization in solution. However, the polymers that are formed become insoluble and precipitate as a result of both cross-linking and choice of porogen, which is typically a poor solvent for the polymer.

Precipitation leads to the formation of nuclei, which grow to the size of globules as the polymerization proceeds further. The globules and their clusters constitute the elemental morphological units of the macroporous polymer. Because higher reaction temperature leads to the formation of a larger number of free radicals by decomposition of the initiator, a larger number of growing nuclei and globules are formed. Since the volume of monomer used is the same for each polymerization, the formation of a larger number of globules is compensated for by their smaller size. Because macroporous materials are composed of arrays of interconnected globules, smaller voids or pores are obtained if the globules are smaller and more numerous. Therefore, the shift in pore size distribution induced by changes in the polymerization temperature can be accounted for by the difference in the number of nuclei that result from such changes.

Porogenic solvents play an important role in controlling the pores of the resultant monolith. Phase separation during polymerization may be initiated at either an early or late stage, determined by the porogen solvents. In principle, the choice of porogen(s) depends on the polarity of both monomer and cross-linker. Typical porogen mixtures, e.g., cyclohexanol/dodecanol, dimethylsulfoxide/dodecanol, and methanol/THF, have been used.[44-46] Supercritical CO_2 was also used as an alternative to organic porogenic solvents. Phase separation was suggested to be governed only by monomer concentration, and the specific surface area was dependent on the CO_2 pressure.[47,48] Phase separation of cross-linked nuclei is a prerequisite for formation of the macroporous morphology. The polymer phase separates from the solution during polymerization due to its limited solubility in the polymerization mixture. This limited solubility may result from a molecular weight that exceeds the solubility limit of the polymer in the given solvent system or from insolubility derived from cross-linking. With the addition of a

poorer solvent to the porogens, earlier phase separation of the polymer is induced. The new phase swells with the monomers because these are thermodynamically much better solvents for the polymer than the porogenic solvents. As a result of this swelling, the local concentration of monomers in the swollen gel nuclei is higher than that in the surrounding solution. Therefore, the polymerization reaction proceeds mainly in the swollen nuclei rather than in the solution. The newly formed nuclei in the solution are likely to be adsorbed by the large preglobules formed earlier, which further increases their size. Overall, the globules that form in such a system are larger and, consequently, the voids between them are larger as well. As the solvent quality improves, the good solvent competes with the monomers in the solvation of nuclei, the local monomer concentration is lower and the globules are smaller. As a result, porous polymers formed in more solvating solvents have smaller pores. Obviously, the porogenic solvent controls the porous properties of the monolith through the solvation of the polymer chains in the reaction medium during the early stages of polymerization.

Although temperature and porogenic solvents affect the porous properties of the resultant monolith, the composition of the monolith stays constant. However, any variation in ratio of monomer to cross-linker alters both porous structure and composition. With a higher content of cross-linker, more highly cross-linked polymers in the early stages of polymerization are formed, which leads to earlier phase separation. Although this is similar to the effect of poor solvent, the nuclei are more cross-linked and, because this affects their swelling with the monomers, they remain relatively small in size. The preglobules can still capture the nuclei generated during the later stages of polymerization. However, true coalescence does not occur. Since the final macroporous structure consists of smaller globules, it also has smaller voids. Viklund et al.[43] clearly documented a shift in the pore size distribution toward smaller pore sizes as the

percentage of cross-linker increased. Their results implied that the pore size distribution is controlled by the swelling of cross-linked nuclei.

Svec et al. observed that polymerization time had a significant effect on pore structure.[41] A monolith polymerized in 1 h at 55 ºC yielded a surface area of over 500 m^2/g and a pore volume of 3.8 mL/g. Although the conversion of monomers to polymer was nearly quantitative after approximately 10 h, some additional structural changes still occurred within the rod if the system was kept longer at the polymerization temperature. However, no significant changes were observed with reaction times exceeding 22 h. Surface area and pore volume were significantly lower at 120 m^2/g and 1.1 mL/g, respectively. Trojer et al.[49] studied the pore properties of monolithic poly[*p*-methylstyrene-*co*-1,2-(*p*-vinylphenyl) ethane] capillary columns prepared with polymerization times varying from 45 min to 24 h. The surface area dropped from 76 to 23 m^2/g and pore volume from 70 to 40% as time increased from 45 min to 24 h. The separation of small molecules was accomplished with high efficiency using the column polymerized for 45 min. With an increase in polymerization time, the separation efficiency decreased and became unacceptable when the column was polymerized for 24 h.

Photo-initiation polymerization. Compared to thermal-initiated polymerization, photo-initiated polymerization is significantly faster and usually can be finished in minutes. Since it is conducted at room temperature, liquids with low boiling points such as methanol and ethyl ether can be used as porogenic solvents.[46] Another advantage of photo-initiated polymerization is that the monolith can be prepared within specific locations. For example, the incorporation of monoliths in microfluidics often requires monolith formation in certain sections with no monolith in other sections. Using a mask, monomers do not react beneath the mask. One limitation of this method is that a UV transparent mold is required.

In 1997, Viklund et al.[50] first studied the preparation of a poly(glycidyl methacrylate-co-trimethylolpropane trimethacrylate) monolith by *in situ* photo-polymerization. They demonstrated that photo-initiated polymerization was much faster than thermal-initiated polymerization. The ease of preparation, short time needed for reaction, and possibility of running the reaction at a low temperature were some of the main advantages of photo-initiated *in situ* polymerization.

The photo-initiator was studied for preparation of monoliths. AIBN was used for both thermal-initiated and photo-initiated polymerization. Geiser et al.[51] prepared poly[butyl methacrylate (BMA)-co-EDMA] monoliths via both thermal-initiated and photo-initiated polymerization in 100 µm I.D. capillary columns. The monoliths showed slight differences in chromatographic performance for the separation of proteins. However, the monolith prepared by photo-initiated polymerization exhibited approximately twice the back pressure compared to a monolith prepared by themal-initiated polymerization, which indicates a different pore structure. Throckmorton et al.[52] prepared polymer monoliths in a microfabricated glass chip containing fluidic channels. Acrylate-based porous polymer monoliths were cast in channels by photopolymerization to serve as the stationary phase. The monoliths were cast *in situ* in less than 10 min with AIBN as initiator. Fast and efficient separation of peptides and amino acids were obtained. Acrylate-based monolithic capillary columns were also prepared using UV photopolymerization with AIBN as initiator by Augustin et al.[53] They investigated the effect of the dose of UV light used for the polymerization. They proved that irradiation energy is critical for monolith preparation. The minimum energy needed to obtain a suitable monolith was 3 J/m^2, and the maximum energy was around 12 J/m^2. A higher energy destroyed the monolith. This

group also prepared a hexyl acrylate-based monolith by *in situ* photopolymerization in both capillary and microchip format for online preconcentration and separation.[54]

Besides AIBN, other photo initiators, such as 2-methoxy-2-phenylacetophenone (MPA) and 2,2-dimethyl-2-phenylacetophenone (DMPA), were also used to prepare monoliths. Bernabé-zafón et al.[55] investigated the effects of four free-radical initiators [AIBN, DMPA, dibenzoyl peroxide (BPO), and lauroyl peroxide (LPO)] on the synthesis of lauryl methacrylate monoliths for capillary electrochromatography. They found that the type and variation of initiator content produced changes in the monolith structure, leading to variations in the final globule size and, therefore, variations in the electrochromatographic properties of the monoliths. Consequently, it is important to find an optimum concentration for each photo-initiator to obtain a monolith with high efficiency. Lee's research group at Brigham Young University (BYU) has also prepared numerous monoliths in capillary columns and microchips using photo-initiated polymerization with DMPA or AIBN as initiators.[56-67]

Radiation polymerization. Polymerization of a monolith can be induced by high energy radiation such as γ-rays and electron beams. Compared to free-radical polymerization, radiation polymerization needs no initiator. Polymerizations can be carried out at any temperature and in almost any container. Obviously, γ-rays are dangerous and significant safety requirements are required. γ-Rays were used to prepare monolithic material as early as 1989.[68] A monolithic hydrogel was prepared in an 18 mm I.D. glass tube using γ-rays from a ^{60}Co source. Unfortunately, the permeability of the resultant monolithic hydrogel was very low. Grasselli et al.[69] also used a ^{60}Co source to prepare a poly[diethylene glycol dimethacrylate (DEGDMA)-co-GMA] monolith in a 4 mm I.D. Teflon tube. The effects of the porogen solvents on the porous structure were investigated. Interestingly, monoliths prepared at higher polymerization

temperatures exhibited higher permeabilities, which is in contrast to those prepared from the more typical thermal-initiated polymerization. Sáfrány et al.[70] continued to use γ-rays from a ^{60}Co source to prepare monoliths using a single monomer, DEGDMA. Monoliths were easily obtained with the same chemical structure in various sizes and shapes. Monomer concentration, porogenic solvents, temperature, and irradiation dose affected the final polymer monolith. Using the same method, Beiler et al.[71] prepared a poly[2-hydroxyethyl-acrylate (HEA)-co-DEGDMA] monolith. An increase in HEA content in the monomer mixture increased the pore size and hydrophilicity of the resultant monolith. However, these monoliths were not successful for isocratic separation of amino acids.

An electron beam is another high energy alternative to γ-rays to initiate polymerization. Poly[hydroxyethyl methacrylate (HEMA)-co-EDMA] monoliths were prepared in 1 mm I.D. capillaries via electron beam-induced polymerization.[72] The influence of electron beam dose on flow properties was investigated. Monoliths prepared at high dose exhibited less permeability, which is in accord with the effects of polymerization kinetics for typical free radical polymerization.[42] Two other monoliths, poly(ethyl methacrylate-co-trimethylolpropane trimethacrylate) and poly(lauryl methacrylate-co-trimethylolpropane trimethacrylate), were prepared via electron beam-induced polymerization in Buchmeiser's group. The monoliths were used to separate proteins and amino acids.[73,74]

1.2.2.2 Monolith Preparation Methods

In order to fully utilize monoliths in separation science, the surfaces of the monoliths often must be modified or functionalized. For example, ionizable surface groups are required for separations by ion-exchange. Several methods have been developed to functionalize monolith surfaces.

Copolymerization. Copolymerization of functional monomers is the simplest approach to prepare monoliths. Many functional monomers have been used for the preparation of porous monoliths, including hydrophilic acrylamide[31] and HEMA,[72] ionizable 2-acrylamido-2-methyl-1-propanesulfonic acid (AMPS)[56] and (methacryloyloxy)ethyltrimethylammonium chloride (MEMAC),[75] reactive GMA[41] and 2-vinyl-4,4-dimethylazlactone,[76] and hydrophobic styrene[77] and butyl methacrylate.[78] Zwitterionic sulfobetains have also been used to prepare monoliths for separation of proteins. A monolith containing zwitterionic phases by incorporation of both acidic and basic methacrylic monomers was prepared to separate small molecules and peptides.[79]

Despite its simplicity, copolymerization has several limitations. First, the optimized conditions for one monolith preparation cannot be transferred directly to another system without further optimization. Due to changes in polarity, the new preparation must be modified in order to obtain the desired structure. Second, a major part of the functional monomer is located within the body of the monolith. Fortunately, by carefully selecting the porogenic solvents and fine-tuning other conditions, the concentration of functional groups on the surface can be maximized.

Post-modification of a reactive monolith. Another approach that can be used to introduce the desired functionality into the monolith while preserving the original porous structure is by chemical modification of reactive groups. By modification of a monolith containing reactive functionalities, a new monolith with various surface chemistries can be obtained for a variety of separation modes.

One of the most widely used approaches for post-modification functionalization is the use of GMA, because its epoxy groups can participate in a wide range of chemical reactions.[80,81] When the precursor monolith is completed, it can be flushed with reagent to add the desired functionality. If the monolith is simply hydrolyzed, a hydroxyl-functionalized monolith is

obtained.[82] The reaction of epoxy groups with diethylamine and trimethylamine led to the formation of weak and strong anion exchangers.[83] The resultant monolith was used for immobilized metal affinity chromatography after reacting with iminodiacetic acid.[84] Reaction with sodium sulfite yielded a sulfonate phase for cation exchange separation.[85,86] Latex coated porous monoliths have been introduced for separations of saccharides and inorganic anions based on poly(GMA-EDMA-AMPS).[87,88] A significant increase in surface area was reported with the coating of latex particles.

Introduction of specific ligands for bioaffinity chromatography is one of the most important modifications of monoliths based on GMA. Numerous methods have been proposed for affinity functionalization.[89] Platonova et al.[90] directly attached amino-bearing ligands such as proteins, peptides, or polyribonucleotides to the epoxy groups. However, the reaction of the amino group of the ligand and the epoxy groups was slow. Potter et al.[91] prepared boronate-functionalized poly(GMA-co-EDMA) monoliths for separations of 2-deoxycytidine and cytidine. The authors believed that this matrix was an ideal sorbent for isolation of glycoconjugates. Peptides are highly specific affinity ligands in addition to being more stable than proteins.[92] Korol'kov et al.[93] first prepared peptidylated methacrylate monoliths ready-to-use for affinity chromatography. They designed a method to introduce peptide ligands, which were nanopeptide bradykinin, on poly(GMA-co-EDMA) monolithic beads and disks. Monospecific antibodies against bradykinin were isolated from pre-purified rabbit serum. Similar approaches were also used by Pflegerl et al. to prepare peptidyl poly(GMA-co-EDMA) monoliths for affinity separation of blood coagulating factor and tissue plasminogen activator.[94,95]

GMA was also reacted with styrene to form a monolith, followed by modification with amines to give the corresponding functionalized supports,[96] or with 1,2-ethylene diamine and γ-

glucuronolactone, which yielded highly hydrophilic surfaces.[97] Friedel-Crafts alkylation reactions with α-chloroalkanes were reported to yield surface-alkylated stationary phases.[98]

Grafting. Grafting is an alternative approach to transform copolymerized monomers. It does not affect the pore size or morphology of the monoliths, similar to post-modification. However, grafting can provide multiple functionalities emanating from each surface, thus increasing the capacity significantly. In comparation, post-modification can only produce a single functionality from each surface site. A major advantage of this approach is that the parent monolithic system can be prepared from an optimized system.

Müller[99] used cerium (IV) to initially graft polymer chains containing hydroxyl groups onto the internal surface of porous beads. It was demonstrated that the hydroxyls were transformed into free radicals in the presence of cerium (IV). These free radicals were located in the pores, and initiated the polymerization reaction. The same method was used by Viklund et al. to graft AMPS onto the surface of a poly(GMA-co-EDMA) monolith.[100] The grafted monolith was used for fast ion exchange separation of proteins with an improved dynamic binding capacity of proteins.

Rånby et al.[101] were the first to introduce a mechanism for photografting onto polymer films using aromatic ketones as photoactive compounds. According to the mechanism, excitation of the photoinitiator by UV light at 200-300 nm leads to hydrogen abstraction and formation of free radicals on the polymer surface. These radicals then initiate propagation reactions, leading to grafting from the surface. Since the growing polymer chains grafted on the surface also contain hydrogen atoms, these new chains can be further grafted with polymer chains, leading to a branched polymer architecture. Based on this mechanism, several new monoliths were developed for various applications.[102-105] For example, Hilder et al.[104] applied photografting for construction

of shielded stationary phases for capillary electrochromatography (CEC). A poly(BMA-co-EDMA) monolith was first grafted with an ionizable monomer, AMPS, which allowed for establishing the electroosmotic flow (EOF). Then, a second layer of hydrophobic monomer butyl acrylate, was grafted onto the first layer. The second layer prevented the ionic analytes from interacting with the first ionic layer, allowing for fast separation.

One interesting characteristic of grafting is that more than one monomer can be grafted simultaneously. Eeltink et al.[106] grafted [2-(methacryloyloxy)ethyl]trimethyl ammonium and AMPS on the surface of a poly(BMA-co-EDMA) monolith for CEC. The study illustrated the possibility of controlled introduction of a number of groups on the surface of a monolithic matrix.

Zhang et al.[107] prepared (N-isopropylacrylamide)-grafted polymer monoliths using surface-initiated atom transfer radical polymerization (ATRP) within the pores of a poly(chloromethylstyrene-co-divinylbenzene) macroporous monolith. ATRP was first introduced by Wang and Matyjaszewski in the mid 1990s,[108] and is currently used in the preparation of well defined polymers and copolymers.[109] The grafted monolith was used for hydrophobic interaction chromatography (HIC) of proteins, which was influenced by temperature and salt concentration. Using ATRP, Sun et al.[110] grafted poly(ethylene glycol) methyl ether methacrylate on a poly(GMA-co-EDMA) monolith, for which the epoxy groups on the surface were activated by air plasma treatment. Polyethylene glycol layers grown on the surface were uniform, hydrophilic, stable, and resistant to protein adsorption. Excellent capillary electrophoresis (CE) separations of proteins and peptides were obtained.

For photografting, the molds and monomers must be UV transparent. Thus, polyimide coated capillaries and aromatic monomers such as styrene cannot be used. Due to UV absorption by the polymeric matrix, photografting is effective only for monoliths with short cross-section.

Ring-opening metathesis polymerization (ROMP). ROMP was introduced in the mid of 1970s[111] and scientists who developed it were awarded the 2005 Nobel Prize in chemistry. It has been used in the preparation of monoliths, enabling polymers with a variety of interesting properties.[112] ROMP is a transition-metal catalyzed polymerization technique. One of its major advantages is the use of functional monomers in the controlled "living" polymerization mechanism, allowing for flexible polymerization.

Buchmeiser and Sinner et al. have successfully prepared functionalized separation media[113-115] and catalytic supports[116-117] using this method alone or in combination with grafting and precipitation techniques. Later, this polymerization technique was applied to synthesize monoliths. For example, Gatschelhofer et al.[118] prepared functionalized monolithic columns via ROMP in silanized fused silica capillaries. The preparation procedure included two steps. The first step was the formation of the basic monolithic structure by polymerization of norborn-2-ene (NBE) and 1,4,4a,5,8,8a-hexahydro-1,4,5,8-exo,endo-dimethanonaphthalene (DMN-H6) using $RuCl_2(PCy_3)_2(CHpH)$ as initiator. In the second step, functional groups were attached onto the monolithic backbone by flushing the monolith with 7-oxanorborn-2-ene-5,6-carboxylic anhydride (ONDCA). Variation of the functionalization conditions was carefully studied to control the degree of functionalization and resulting ion-exchange capacity. Good separation of a standard peptide mixture in the cation-exchange mode was reported. Another example is the preparation of a monolith for anion-exchange chromatography.[119] The same procedure was applied, except that the monolith was flushed with 2-(N,N-dimethylaminoethyl)norborn-5-ene-2-

ylcarboxylic amide. The resulting functionalized monolith was successfully used in anion-exchange chromatography of oligodeoxynucleotides.

Polymerized high internal emulsions (polyHIPE). PolyHIPE is a new class of porous polymers, which was first described in detail by Small and Sherrington.[120] Polymers were prepared by emulsifying water containing a free radical initiator in an oil phase comprised of monomers as well as surfactant. The mixture formed a rigid mass after intensive stirring. The mixture was then filled in a mold and polymerized at an elevated temperature, forming a monolith with porous structure.

Cryogels. Cryogels are spongy hydrophilic materials with very large pores.[121] They are synthesized in semi-frozen aqueous media where ice crystals act as template porogen for continuous interconnected pores after melting. Various cryogels have been prepared with different monomers, including HEMA,[121] acrylamide,[122,123] dimethacrylamide,[124] N-isopropylacrylamide,[125] and N-vinylcaprolactam.[126] The porous structure of cryogels results from phase separation during freezing with one phase consisting of frozen crystals of water and the other a non-frozen liquid microphase. The water crystals form a continuous frozen framework, which is a porogenic structure that is interspersed with continuous monomer-rich liquid phase. Monomers in this phase polymerize, forming the pore walls. After completing polymerization, water within the pores can be thawed at ambient temperature and replaced by mobile phase. In this mechanism, many factors (e.g., temperature, percentage of monomers, and initiator) can affect the porous structure.

Besides the methods described above, other methods have been reported for preparation of monoliths for various applications. Polycondensation is a new method to prepare monoliths. It was first used to prepare chromatographic monoliths in 2002.[127] In this technique, the polymer

chain ends are repeatedly activated, allowing for growth of all polymer chains. This is in contrast to free radical polymerization, in which the polymer chain propagates during the entire polymerization process. Monoliths were reportedly prepared from soluble polymers.[128] Other methods, such as nitroxide mediated polymerization[129] and organotellurium initiator induced polymerization[130] have also been reported for synthesis of monoliths.

1.2.3 Applications of Monoliths in LC

1.2.3.1 Applications in IEC

IEC is one of the most frequently used techniques for separation of charged molecules. An important characteristic of IEC is its capacity. Recently, developments of monoliths for IEC were reviewed in detail.[131,132] Commercial monolithic materials available today include disks, columns, and tubes. The disk-shaped separation devices are, in fact, the first successful examples of monolithic ion exchangers. These devices, also called short columns, are produced by BIA Separations under the trade name CIM disks. BIA Separations also produces tube-shaped macro-scale monoliths. Dionex also produces monolithic columns for IEC under the trade name ProSwift. These columns allow a flow rate of up to 8 mL/min without loss in peak resolution for large biomolecules.[133] Excellent long-term stability has been confirmed by a large number of injections.

Monoliths can be used for IEC of small molecules. Although polymeric monoliths are mainly designed for separation of large molecules, they also can be used to separate small molecules. Hilder and Zakaria et al.[86-88] applied latex-coated monoliths for ion-exchange separation of small molecules. Excellent HPLC separation was demonstrated by Zakaria et al.[88] In their paper, a monolithic capillary column was obtained by *in situ* polymerization of BMA, EDMA, and AMPS, following coating with quaternary ammonium functionalized latex particles.

The column was used for separation of anionic analytes consisting of iodate, bromate, nitrite, benzoate, toluenesulfonate, and benzenesulfonate. Baseline separation of all analytes was obtained with an efficiency of 13,000 plates/m. Yang et al.[134,135] used weak ion-exchange monolithic columns for the determination of five postsynaptic α-1 adrenoreceptor antagonists and two antibiotics in human plasma. The authors demonstrated that these drugs can be easily enriched and detected in native human plasma without tedious sample pretreatment. A porous monolithic ion exchanger was used to develop a high-performance sensor.[136] The porous ion exchanger was formed using styrene and divinyl benzene, followed by functionalizing with chlorosulfuric acid. Trace amounts of inorganic ions as low as 10^{-7} M dissolved in aqueous solutions could be quantitatively determined. Ueki et al.[85] prepared strong cation-exchange monolithic capillary columns by radical polymerization of GMA and EDMA, and subsequent sulfonation based on ring opening of epoxides with Na_2SO_3. The resulting monolithic columns were evaluated for the separation of a model mixture of common cations including Na^+, NH_4^+, K^+, Mg^{2+}, and Ca^{2+} with an efficiency of 20,000 plates/m. Rey et al.[137] also used polymeric phases to separate hydrophobic and polyvalent amines.

Peptides and oligonucleotides can be separated in the IEC mode. Podgornik et al.[138] applied cation-exchange chromatography on short monolithic columns for the separation of a peptide mixture. Three peptides were separated on CIM SO_3 disks in both gradient and isocratic elution modes. They also used CIM DEAE disks for separation of four oligodeoxynucleotides differing by only 2 base units.[139] Vlakh et al.[140] also used CIM SO_3 disks to separate a peptide mixture containing three linear lysine homologs within 5 min in the gradient elution mode. Sykora et al.[141] used a poly(GMA-co-EDMA) monolith modified with diethylamine to separate two oligonucleotide mixtures consisting of oligodeoxyadenylic acids and oligodeoxythymydic

acids. Yamamoto et al.[142] investigated the retention mechanism of oligonucleotides of different sizes using anion exchange chromatography on monolithic disks. Two parameters, the numbers of binding sites and salt concentration were determined. Linear dependence of both parameters on the number of charges was established. Thayer et al.[143] prepared a methacrylate-based monolith for anion exchange chromatography of oligonucleotides. Predicted adjustment of oligonucleotide retention was demonstrated by programmed elution using pH and composition. Hydrophobic interactions between the monolith and analytes were suppressed by adding acetonitrile to the mobile phase. My group at BYU developed a series of polymeric monoliths for peptide separation.[56,58,60,61,75] The focus was on deducing the hydrophobicity, increasing the dynamic binding capacity, and improving the permeability of the monoliths. Excellent separations of peptides were obtained with these monoliths. For example, Gu et al.[56] prepared a poly(AMPS-co-PEGDA) monolith by photoinitiated copolymerization. Exceptionally high resolution resulting from extremely narrow peaks was obtained, resulting in a peak capacity of 179.

Separations of proteins are the main applications of monolithic IEC. Podgornik et al.[144] used ion-exchange CIM monolithic disks to separate manganese peroxidase (MnP) and lignin peroxidase (LiP) isoenzymes, which are extracellular enzymatic isoforms excreted by phanerochaete chrysosporium and involved in lignin degradation. Four main LiP fractions were easily separated from a crude culture filtrate on a CIM QA disk within 4 min with satisfactory resolution. Branovic et al.[145] used a poly(GMA-co-EDMA) monolith modified with DEAE for isolation of clotting factor IX from human plasma. The use of this monolithic column not only reduced the separation time, but also increased the specific activity of the product by almost one order of magnitude compared to product isolated using a DEAE-Sephadex column.

Du et al.[146] prepared monolithic columns modified with diethylamine using a solid-templating strategy for protein chromatography. To increase the permeability of monolithic columns, solid granules of Na_2SO_4 were introduced into the porogenic solvents. The obtained monoliths showed decreased back pressure compared to those prepared without the salt. The values of HETP for the monoliths decreased with an increase in flow rate within the range of 500-1500 cm/h and were nearly constant at a flow rate higher than 1500 cm/h. This demonstrated that an increase in flow rate led to the occurrence of convective flow in small channels, which resulted in an improvement in column efficiency.

Wang et al.[147] prepared a strong cation-exchange stationary phase by direct *in situ* polymerization of ethylene glycol methacrylate phosphate and bisacrylamide. A high dynamic binding capacity of 140 mg/mL peptide with fast kinetic adsorption was observed. The permeability of the resulting monolith was 10 times higher than a commercially available column containing 5 µm particles. The monolith was applied as a trap column in a nanoflow liquid chromatography-tandem mass spectrometry system for automated sample injection and online multidimensional separation of a tryptic digest of yeast proteins.

Dinh et al.[148] prepared strong and weak cation-exchange monoliths using ATRP with epoxy-based monoliths. Strong and weak cation-exchange groups were introduced onto the GMA-grafted monoliths by reactions with sodium hydrogen sulfite and iminodiacetic acid, respectively. Chromatographic assessments and problems associated with flow-through modification by ATRP were discussed.

Krenkove et al.[149] prepared strong and weak cation-exchange monoliths by photografting AMPS and acrylic acid on hydrolyzed poly(GMA-co-EDMA) monoliths. The resultant monoliths were used to separate proteins and peptides. The effects of surface hydrophilization,

grafting time, and mobile phase pH on the separation were studied. Lee's group at BYU also prepared several cation and anion-exchange monoliths, which provided excellent separations of proteins.[60,61,75]

1.2.3.2 Applications in RPLC

RPLC is based on interactions between the non-polar groups of analytes and hydrophobic ligands on the stationary phase. Monolithic RPLC applications are dominated by modified silica[150,151] and polystyrene.[152] The dominance of silica monoliths is associated with their pore structure. Silica monoliths have a bimodal pore size distribution with micrometer-sized throughpores and nanometer-sized mesopores, which leads to high surface area. Most of the surface area of silica monoliths is found within the networks of the mesopores. Silica monoliths are mainly for separation of small molecules, while polymer monoliths are more applicable to large molecules.

Lee et al.[153] prepared a poly(BMA-co-EDMA) monolith by *in situ* photo- and thermo-initiated polymerization for protein separation by RPLC. A protein mixture containing ribonuclease A, cytochrome C, myoglobin, and ovalbumin was separated using gradient elution. No significant effect of flow rate on peak resolution was observed, even at a flow rate of 85 mm/s, which is not possible for packed columns due to the high back pressure. Moravcová et al.[154] compared isocratic separations of nine benzene derivatives on the poly(BMA-co-EDMA) monolith and a column packed with Biosphere C18 beads. Both columns showed similar retention behavior, however the separation on the monolith was two times faster. Umemura et al.[155] prepared a poly(HMA-co-EDMA) monolith for fast separation of a protein mixture. The monolithic column was stable at least to 15 MPa, and allowed the separation at 15-20 times higher flow rates than normal. Separations of proteins were achieved on poly(BMA-co-glycerol

methacrylate) monoliths in RPLC.[156] The ratio of monomer to crosslinker for the synthesis of

one monolith was 30/70. When this ratio was reduced to 10/90, the separation resembled more a

HIC mechanism. Ueki et al.[157] prepared several alkyl methacrylate-based monoliths by *in situ*

polymerization inside 250 µm I.D. capillary columns. All columns were used to separate five

alkylbenzenes. A best efficiency of 30,000 plates/m was observed for the lauryl-bearing

monolith, while the octadecyl-bearing monolith gave the lowest flow resistance. The separation

time could be reduced 120-fold simply by increasing the flow rate and column temperature.

Jiang et al.[158] reported the *in situ* preparation of poly(stearyl methacrylate-co-EDMA)

monoliths inside 100 µm I.D. capillary columns. An optimized column was used to separate

several mixtures under RP chromatographic conditions. Baseline separations of mixtures of

thiourea, dimethyl phthalate, anisole, and naphthalene, as well as six phenols were obtained. A

separation of a mixture of 13 polycyclic aromatic hydrocarbons yielded baseline resolution of 10

compounds, whereas 6 out of 7 weakly basic anilines were baseline resolved. Ro et al.[159]

compared two types of monolithic columns, poly(octylstyrene-co-divinylbenzene) and

poly(lauryl methacrylate-co-EDMA), prepared in 100 µm I.D. capillary columns. These columns

were used to separate a peptide mixture obtained from BSA digestion. The authors concluded

that the poly(octylstyrene-co-divinylbenzene) monolith offered better chromatographic

performance and higher capacity than the poly(lauryl methacrylate-co-EDMA) monolith.

A poly(BMA-co-EDMA) monolith was also prepared for gradient separation of low

molecular mass alkylbenzenes as well as proteins.[160] The authors compared the performance of

the polymeric monolith with a silica-C18 monolithic column for the separation of proteins.

While both gave the same elution order, the polymeric monolith provided better separation.

Holdšvendová et al.[161] prepared poly(BMA-co-EDMA) monoliths using various initiators.

Isocratic separation of several benzene derivatives demonstrated that column efficiency and selectivity do not depend on the type of initiation. Eeltink et al.[162] studied the influence of polymer morphology on the efficiency of poly(BMA-co-EDMA) monoliths. Monoliths were prepared inside fused-silica capillaries by varying the polymerization mixture content. Unimodal and bimodal pore-size distributions were obtained. The monolith with biomodal pore structure provided better efficiency and much higher permeability. The column stability of the poly(BMA-co-EDMA) monolith was studied by Geiser et al.[51] Excellent intra-batch and inter-batch reproducibility was obtained. Coufal et al.[163] prepared poly(BMA-co-EDMA) monoliths in 320 µm I.D. capillary columns, and demonstrated that the 320 µm I.D. monolithic column exhibited separation performance similar to those observed for 100 and 150 µm monolithic columns,[164] however, the 320 µm I.D. monolithic column had higher sample loadability.

Lubbad et al.[165] prepared monoliths in 200 µm I.D. capillary columns via polymerization of tetrakis(4-vinylbenzyl)silane (TVBS) in the presence of 1-dodecanol and toluene. The resulting monoliths were optimized for separation of low, medium, and high molecular mass analytes. The porosity was adjusted by varying the amount of AIBN initiator. The monoliths were used for separation of a series of low molecular mass analytes, including alkylbenzenes, amines, carboxylic acids, phenols, and carbonyl compounds, as well as for medium molecular mass analytes such as peptides and high molecular mass analytes such as proteins. Due to the microporous structure, the monoliths displayed high efficiency and good performance for the separation of low molecular mass analytes. The authors then optimized the monoliths for fast separation of small molecules by investigating the polymerization mixture and polymerization temperature.[166] With optimized monolith structures, separation of a mixture of alkylbenzenes was accomplished in less than 2 min.

Trojer et al.[167] copolymerized methylstyrene and 1,2-bis(*p*-vinylphenyl)ethane (BVPE) in 200 I.D. capillary columns. The permeability and chromatographic efficiency of the monolithic column were highly influenced by the total monomer to porogen content as well as by the microporogen nature and its concentration. Monoliths with broad permeability were fabricated. A protein mixture was baseline separated in 35 s, and a homologous series of phosphorylated oligothymidylic acids was separated in less than 2 min. Greiderer et al.[168] used BVPE as single monomer to prepare monoliths in 200 µm I.D. capillary columns, obtaining a broad bimodal pore-size distribution from mesopores to small macropores in the range of 5-400 nm and flow channels in the µm range. Tremendous enhancement of surface area (101 m^2/g) was observed compared to typical organic monoliths (~ 20 m^2/g), indicating the presence of mesopores. The mesopores and macropores allowed rapid and high-resolution separation of low molecular mass analytes as well as biomolecules. The influence of polymerization time on the pore structure and chromatographic properties of poly(BVPE) has been studied.[169] Shortening the polymerization time resulted in enhanced total porosity due to enlarged flow-channel diameters and increased surface area because of the presence of a considerable number of mesopores. Trojer et al.[49] came to the same conclusion in preparation of a poly[*p*-methylstyrene-co-1,2-(*p*-vinylphenyl)ethane] monolith. The methodical reduction of polymerization time could be a simple tool to tailor the pore properties of organic monoliths for the rapid and high resolution chromatography of small organic molecules.

Fabrication of RP/ion-exchange mixed-mode monolithic materials for capillary LC was described by Jiang et al.[170] Monoliths were formed by copolymerization of pentaerythritol diacrylate monosterate (PEDAS), 2-sulfoethyl methacrylate (SEMA), and EDMA in 100 µm I.D. capillary columns. It was observed that a small amount of EDMA clearly improved the

mechanical stability of the monoliths. A range of neutral, acidic, and basic compounds was separated with the monoliths. Mobile phase pH clearly influenced the retention of basic compounds, which probably resulted from ion-exchange interaction between the positively charged analytes and the negatively charged sulfate groups. Other monolithic materials containing dual-functionality have also been reported.[171-174]

Bisjak et al.[175] studied the effect of total monomer to porogen ratio, nature of the pore forming agent, and polymerization temperature on the porous properties of poly(phenyl acrylate-co-1,4-phenylene diacrylate) monoliths. Monoliths with significantly different porosities were obtained. A correlation between porosity, retention behavior and efficiency was derived from the chromatographic separation of proteins and oligonucleotides. Mayr et al.[176] studied the influence of variations in polymerization of monoliths prepared by transition metal-catalyzed ring-opening metathesis. Chromatographic separation of oligodeoxynucleotides and eight model proteins were achieved. The role of additional phosphine on the polymerization and associated chromatographic separations was elucidated.

Gu et al.[177] prepared two monoliths in 320 µm fused capillary columns, namely poly(styrene-octadecene-divinylbenzene) (PS-OD-DVB) and poly(styrene-divinylbenzene) (PS-DVB). These monoliths were used to separate six standard proteins and human hemoglobin. It appeared that the two monoliths exhibited similar efficiencies for rapid separation of the six proteins. The PS-OD-DVB monolith showed higher loading capacity and higher resolution for the separation of the α and β chains of hemoglobin due to the presence of the C18 carbon chains.

Nordborg et al.[178] extended the variety of cross-linkers for the preparation of polymethacrylate-based monoliths. Several monoliths were prepared by *in situ* copolymerization of BMA with EDMA, diethylene glycol dimethacrylate, triethylene glycol dimethacrylate, and

pentaerythritol tetraacrylate in 250 µm I.D. capillary columns. Separations were achieved for a protein mixture using all of these columns.

1.2.3.3 Applications in HIC

HIC is a mild separation method mainly used for separation of proteins in their natural states. Compared to RPLC, the surface concentration of hydrophobic ligands is one order of magnitude lower. Ligands including methyl, ethyl, propyl, butyl, octyl, and dodecyl groups have been used for HIC separations. HIC is not as widely used as RPLC or IEC, because it is appropriate for proteins only, and the proteins should have significant hydrophobicities.

Tennikova and Svec et al. first used polymeric monoliths for the separation of a standard protein mixture in the HIC mode.[179,180] Štrancar et al.[181] prepared a propyl-modified poly(GMA-co-EDMA) monolith for the separation of a standard protein mixture by HIC. The separation of three proteins could be completed in 30 s without any loss in separation performance. Hemström et al.[156] prepared poly(BMA-co-HEMA-co-1,4-butanediol dimethacrylate) monoliths in 250 µm I.D. capillary columns for the separation of proteins in HIC. It was found that retention in this mode was not affected by the polarity of the porogens used for monolith preparation. Lee's group at BYU has developed several monoliths for HIC separation of proteins.[62,63] Poly(hydroxyethyl acrylate-co-polyethylene glycol diacrylate) monoliths were synthesized in 75 µm I.D. capillary columns by UV-initiated copolymerization. Six proteins were separated in 20 min with high resolution, resulting in a peak capacity of 54. Other monoliths were also prepared from single monomers, such as polyethylene glycol diacrylate or polyethylene glycol dimethacrylate. It was demonstrated that chromatographic performance was not affected by changing the porogens. Similar retention values and peak capacities were observed. Zhang et al.[107] grafted poly(N-isopropylacrylamide) on poly(chloromethylstyrene-co-divinylbenzene)

monoliths for HIC separation of proteins. The hydrophobicity of the grafted monolith was adjusted by adding different salts to the mobile phase in the order of sodium sulfate > ammonium sulfate > sodium chloride. Yao et al.[182] prepared poly(GMA-co-EDMA) monoliths by supramolecular self-assembly of high internal phase emulsions. A large dynamic binding capacity of 42.5 mg/mL for proteins was obtained. Separation of a protein mixture was achieved in 4 min at a velocity of 1440 cm/h.

1.2.3.4 Applications in Hydrophilic Interaction Chromatography (HILIC)

HILIC is an alternative to RPLC for separation of polar compounds. Carbohydrates, peptides, proteins, and polar pharmaceuticals have been separated using HILIC. HILIC is based on the combination of a hydrophilic stationary phase and a hydrophobic mobile phase. In HILIC, the mobile phase usually is more than 60% organic with low water content, leading to retention of polar compounds. Retention is caused by partitioning of the analytes between the bulk mobile phase and a water-rich layer immobilized on the stationary phase surface.

Jiang et al.[183] prepared porous zwitterionic monolithic columns for HILIC by thermal-initiated copolymerization of N,N-dimethyl-N-methacryloxyethyl-N-(3-sulfopropyl)ammonium betain (SPE) with EDMA in 100 µm I.D. capillary columns. Four neutral amides and seven benzoic acids were well separated. Retention times decreased dramatically with decreasing ACN concentration from 92 to 70%. The ion-exchange mechanism contributed significantly to retention if the pH of the mobile phase was above the pK_a of the charged analytes. Another monolith was prepared by copolymerization of methacryloyloxyethyl phosphorylcholine (MPC) and EDMA within a 100 µm I.D. capillary column.[184] A typical HILIC mechanism was observed with high organic solvent content (ACN > 60%). With low organic solvent content, baseline separation of several alkylphenones was observed by a reversed-phase separation mechanism.

Jiang et al.[185] also prepared another zwitterionic hydrophilic porous monolithic column by copolymerization of 1-(3-sulfopropyl)-4-vinylpyridinium betain and N,N'-methylenebisacrylamide. Higher hydrophilicity was achieved with this column compared to the two previously described phases. Fast separation of pyrimidines and purines was achieved in less than 1 min. Benzoic acid derivatives were also separated using either a pH or ACN gradient. Holdšvendová et al.[186] prepared a poly[N-(hydroxymethyl)methacrylamide-co-EDMA] monolith for separation of oligonucleotides in the HILIC mode. Baseline separation of analytes was achieved in 35 min. Good column-to-column reproducibility was obtained. Polymeric monoliths were prepared in capillaries using tris(2,3-epoxypropyl) isocyanurate (TEPIC) and 4-[(4-aminocyclohexyl)methyl]cyclohexylamine (BACM) or trans-1,2-cyclohexanediamine (CHD) in the presence of polyethylene glycol.[187] In 90% ACN, a poly(TEPIC-co-BACM) monolithic column separated nucleosides with an efficiency of over 70,000 plates/m. The optimum plate height reached 5 µm for separation of benzene within the linear velocity range of 1-2 mm/s.

A dual retention mechanism was demonstrated by Urban et al., who prepared monoliths in fused-silica capillaries by radical copolymerization of [2-(methacryloyloxy)ethyl]dimethyl-(3-sulfopropyl)ammonium hydroxide and EDMA.[173] The monolithic columns exhibited both a reversed-phase mechanism in a water-rich mobile phase and a HILIC mechanism for high concentration of ACN in an aqueous-organic mobile phase. A continuous change in retention was observed by increasing the concentration of water in ACN, giving rise to the characteristic U-turn plots of retention factor *verse* concentration of water in the mobile phase.

A mixed-mode hydrophilic interaction and anion-exchange polymeric monolith was prepared by copolymerization of 2-(methacryloyloxy)ethyltrimethylammonium methyl sulfate (META) and pentaerythritol triacrylate (PETA).[188] The hydrophilicity of the monolith increased

with an increasing content of META in the polymerization mixture. The monolith showed excellent selectivity for neutral, basic, and acidic polar analytes. A mixed-mode hydrophilic interaction and cation-exchange polymeric monolith was also prepared by copolymerization of 3-sulfopropyl methacrylate (SPMA) and PETA.[189]

In addition to the LC applications described above, polymeric monoliths have also been used in other fields, such as affinity chromatography,[190-192] sample preparation,[193-198] capillary electrochromatography,[199-202] and microfluidics.[203-204] Applications in enzyme immobilization,[205] chiral separations,[206] and isoelectric focusing[207] have also been reported. The unique properties of monolithic stationary phases, in particular the ease of preparation and low back pressure, make them superior to conventional packed columns for various applications. Thus, monolithic stationary phases have become an attractive alternative to packed columns since their introduction in 1990. Further efforts, however, are needed to improve the efficiency and reproducibility of monolithic columns for routine separations.

1.3 Dissertation Overview

My research focused on the preparation of polymeric monolithic capillaries for IEC of peptides and proteins. Chapter 2 reports the preparation of a strong cation-exchange (SCX) monolithic stationary phase in 75 μm I.D. capillaries by direct *in situ* polymerization of sulfopropyl methacrylate (SPMA) and polyethylene glycol diacrylate (PEGDA) in a ternary porogen system consisting of methanol, cyclohexanol, and water. The resulting monolith provided excellent ion exchange capillary LC of peptides using a simple salt gradient. Narrow peaks were obtained and a peak capacity of 28 was achieved. A dynamic binding capacity of 52 mg/mL of column volume for lysozyme was measured.

Chapter 3 describes the preparation of monoliths containing phosphoric acid functional groups. Monoliths containing phosphoric acid functional groups are assumed to swell less in aqueous buffer compared to those containing sulfonic acid functional groups. Two different monoliths, both containing phosphoric acid functional groups and polyethylene glycol (PEG) functionalities, were synthesized for cation-exchange chromatography of peptides and proteins. Phosphoric acid 2-hydroxyethyl methacrylate (PAHEMA) and bis[2-(methacryloyloxy)ethyl] phosphate (BMEP) were reacted with PEGDA and polyethylene glycol acrylate (PEGA), respectively, in 75 μm I.D. capillaries by photo-initiated polymerization. Dynamic binding capacities of 31.2 and 269 mg/mL were measured for the PAHEMA–PEGDA and BMEP–PEGA monoliths, respectively. Peak capacities of 50 and 31 were measured for peptides and proteins, respectively, using a PAHEMA–PEGDA monolith, and 31 for proteins using a BMEP-PEGA monolith. Good run-to-run [relative standard deviation (RSD) < 1.99%] and column-to-column (RSD < 5.64%) reproducibilities were achieved. Use of the new PEGDA biocompatible cross-linker over the conventional ethylene glycol dimethacrylate (EDMA) cross-linker for the preparation of polymer monoliths was found to be advantageous for the analysis of biological compounds.

Chapter 4 deals with improvement in reproducibility of monolith preparation. A single monomer was used to synthesize a phosphoric acid containing monolith to improve its stability and reproducibility. The monolith was synthesized from only BMEP in 75 μm I.D. UV transparent fused-silica capillaries by photo-initiated polymerization. The monolith exhibited low hydrophobicity and relatively low porosity due to the highly cross-linked structure. A dynamic binding capacity (lysozyme) of 73 mg/mL of column volume was measured. Efficiencies of 52,900 plates/m for peptides and 71,000 plates/m for proteins were obtained under isocratic

conditions. Good run-to-run reproducibility was achieved with an RSD less than 1.50% for retention times of proteins. The RSD for retention times of peptides from column-to-column was less than 3.50%. This monolithic column was used to monitor the deamidation variants of ribonuclease A. The kinetics of deamidation were found to be first order with a half life of 195 h.

In chapter 5, a stable poly[2-carboxyethyl acrylate-co-poly(ethylene glycol) diacrylate] monolith was synthesized inside a 75 µm I.D. capillary by direct in situ photo-initiated polymerization for weak cation-exchange capillary liquid chromatography of peptides and proteins. A high dynamic binding capacity of 72.7 mg lysozyme per cm^3 column volume was measured with fast mass transfer as demonstrated by steep breakthrough curves. The resulting monolith exhibited negligible hydrophobicity, leading to good separation of peptides and proteins. Peak capacities of 11 for peptides with a 10-min salt gradient and 39 for proteins with a 20-min salt gradient were measured. An efficiency of 37,000 plates/m for proteins was obtained under isocratic conditions. The effects of functional group concentration, porogenic solvent composition, mobile phase pH, salt gradient rate, and hydrophobicity on the retention of analytes were investigated. Good run-to-run [relative standard deviation (RSD) < 1.93%] and column-to-column (RSD < 4.63%) reproducibilities were achieved.

In chapter 6, zwitterionic monolithic columns based on photo-initiated copolymerization of N,N-dimethyl-N-methacryloxyethyl-N-(3-sulfopropyl)ammonium betain and poly(ethylene glycol) diacrylate were prepared in 75 μm I.D. fused silica capillaries for hydrophilic interaction chromatography. Inverse size exclusion chromatography was used to characterize the pore structure of the resulting monolith. A typical HILIC mechanism was observed when the organic content in the mobile phase was higher than 60%. Good separations of amides, phenols, and benzoic acids were achieved. An efficiency of 75,000 plates/m was obtained. The effects of

mobile phase pH, salt concentration, and organic modifier content on retention were investigated. For polar charged analytes, both hydrophilic interactions and electrostatic interactions contributed to the selectivity.

Chapter 7 outlines the future proposed research work on monolith for various applications.

1.4 References

1. Tswett, M. *Ber. D. deut. Botan. Ges.* **1906**, *24*, 384-393.

2. Mayer, H. *Planta* **1930**, *11*, 294-330.

3. Kuhn, R.; Winterstein, A.; Lederer, E. *The xanthophylls, Z. Physiol. Chem.* **1931**, *197*, 141-160.

4. Izmallov, N. A.; Shralber, S. M. *Pharmatsiya* **1938**, *3*, 1-7.

5. Martin, A. J. P.; Synge, R. L. M. *J. Biochem.* **1941**, *35*, 1358-1368.

6. Tyson, J. F. *Anal. Proc.* **1989**, *26*, 251-254.

7. Thompson, H. S. *J. Roy. Agr. Soc. Engl.* **1850**, *11*, 68-74.

8. Gans, R. *Jahrb. Preuss. Geol. Landesandstadt* **1905**, *26*, 179-211.

9. Adams, B. A.; Holmes, E. L. *J. Soc. Chem. Ind.* **1935**, *54*, 1-6T.

10. Taylor, T. I.; Urey, H. C. *J. Chem. Phys.* **1938**, *6*, 429-438.

11. Ketelle, B.; Boyd, G. *J. Am. Chem. Soc.* **1947**, *69*, 2800-2812.

12. Spedding, F. H.; Powell, E.; Svec, H. J. *J. Am. Chem. Soc.* **1955**, *77*, 6125-6132.

13. Nelson, F.; Rush, R. M.; Kraus, K. A. *J. Am. Chem. Soc.* **1960**, *82*, 339-348.

14. Samuelson, O. *Ion Exchange Separations in Analytical Chemistry*, Wiley, New York, **1963**.

15. Cohn, W. E. *J. Am. Chem. Soc.* **1949**, *71*, 2275-2276.

16. Sober, H. A.; Peterson, E. A. *J. Am. Chem. Soc.* **1954**, *76*, 1711-1712.

17. Chang, S. H.; Noel, R.; Regnier, F. E. *Anal Chem.* **1976**, *48*, 1839-1845.

18. Levison, R. P. *J. Chromatogr. B* **2003**, *790*, 17-33.

19. Jacob, L; Frech, C. *Biosep. Bioprocess.* **2007**, *1*, 125-143.

20. Lee, Y. C. *J. Chromatogr. A* **1996**, *720*, 137-149.

21. Wolters, D. A.; Washburn, M. P.; Yates, J. R. *Anal. Chem.* **2001**, *73*, 5683-5690.

22. Pohl, C. *LC GC N. Am.* **2006**, *24*, 32-37.

23. Jungbauer, A. *J. Chromatogr. A* **2005**, *1065*, 3-12.

24. Hashimoto, T. *J. Chromatogr.* **1991**, *544*, 257-265.

25. Gustavsson, P. E.; Larsson, P. O. *J. Chromatogr. A* **1996**, *734*, 231-240.

26. Colwell, L. F.; Hartwick, R. A. *J. Liq. Chromatogr.* **1987**, *10*, 2721-2744.

27. Afeyan, N. B.; Gordon, N. F.; Mazsaroff, I.; Varad, L.; Fulton, S. P.; Yang, Y. B.; Regnier, F. E. *J. Chromatogr.* **1990**, *519*, 1-29.

28. Kubin, M.; Spacek, P.; Chromecek, R. *Collect. Czech. Chem. Commun.* **1967**, *32*, 3881-3887.

29. Hileman, F. D.; Sievers, R. E.; Hess, G. G.; Ross, W. D. *Anal. Chem.* **1973**, *45,* 1126-1130.

30. Hjertén, S.; Liao, J.; Zhang, R. *J. Chromatogr.* **1989**, *473*, 273-275.

31. Svec, F.; Fréchet, J. M. J. *Anal. Chem.* **1992**, *64*, 820-822.

32. Svec, F.; Fréchet, J. M. J. *Science* **1996**, *273*, 205-211.

33. Minakuchi, H.; Nakanishi, K.; Soga, N.; Ishizuka, N.; Tanaka, N. *Anal. Chem.* **1996**, *68*, 3498-3501.

34. Jungbauer, A.; Hahn, R. *J. Sep. Sci.* **2004**, *27*, 767-778.

35. Yu, C.; Davey, M. H.; Svec, F.; Fréchet, J. M. J. *Anal. Chem.* **2001**, *73*, 5088-5096.

36. Oleschuk, R.; Shultz-Lockyear, L.; Ning, Y.; Harrison, D. J. *Anal. Chem.* **2000**, *72*, 585-590.

37. Gusev, I.; Huang, X.; Horva´th, C. *J. Chromatogr. A* **1999**, *855*, 273-290.

38. Palm, A.; Novotny, M. V. *Anal. Chem.* **1997**, *69*, 4499-4507.

39. Premstaller, A.; Oberacher, H.; Huber, C. G. *Anal. Chem.* **2000**, *72*, 4386-4393.

40. Fields, S. M. *Anal. Chem.* **1996**, *68*, 2709-2712.

41. Svec, F.; Fréchet, J. M. J. *Chem. Mater.* **1995**, *7*, 707-715.

42. Svec, F.; Fréchet, J. M. J. *Macromolecules* **1995**, *28*, 7580-7582.

43. Viklund, C.; Svec, F.; Fréchet, J. M. J.; Irgum, K. *Chem. Mater.* **1996**, *8*, 744-750.

44. Xie, S.; Svec, F.; Fréchet, J. M. J. *J. Chromatogr. A* **1997**, *775*, 65-72.

45. Peters, E. C.; Petro, M.; Svec, F.; Fréchet, J. M. J. *Anal. Chem.* **1997**, *69*, 3646-3649.

46. Yu, C.; Xu, M.; Svec, F.; Fréchet, J. M. J. *J. Polym. Sci. A Polym. Chem.* **2002**, *40*, 755-769.

47. Cooper, A. I.; Holmes, A. B. *Adv. Mater.* **1999**, *11*, 1270-1274.

48. Hebb, A. K.; Senoo, K.; Bhat, R.; Cooper, A. I. *Chem. Mater.* **2003**, *15*, 2061-2069.

49. Trojer, L.; Bisjak, C. P.; Wieder, W.; Bonn, G. K. *J. Chromatogr. A* **2009**, *1216*, 6303-6309.

50. Viklund, C.; Pontén, E.; Glad, B.; Irgum, K.; Horstedt, P.; Svec, F. *Chem. Mater.* **1997**, *9*, 463-471.

51. Geiser, L.; Eeltink, S.; Svec, F.; Fréchet, J. M. J. *J. Chromatogr. A* **2007**, *1140*, 140-146.

52. Throckmorton, D. J.; Shepodd, T. J.; Singh, A. K. *Anal. Chem.* **2002**, *74*, 784-789.

53. Augustin, V.; Jardy, A.; Gareil, P.; Hennion, M. *J. Chromatogr. A* **2006**, *1119*, 80-87.

54. Augustin, V.; Proczek, G.; Dugay, J.; Descroix, S.; Hennion, M. *J. Sep. Sci.* **2007**, *30*, 2858-2865.

55. Bernabé-zafón, V.; Beneito-Cambra, M.; Simó-Alfonso, E. F.; Herrero-Martínez, J. M. *J. Chromatogr. A* **2010**, *1217*, 3231-3237.

56. Gu, B.; Chen, Z.; Thulin, C. D.; Lee, M. L. *Anal. Chem.* **2006**, *78*, 3509-3518.

57. Gu, B.; Armenta, J. M.; Lee, M. L. *J. Chromatogr. A* **2005**, *1079*, 382-391.

58. Gu, B.; Li, Y.; Lee, M. L. *Anal. Chem.* **2007**, *79*, 5848-5855.

59. Li, Y.; Tolley, H. D.; Lee, M. L. *Anal. Chem.* **2009**, *81*, 4406-4413.

60. Chen, X.; Tolley, H. D.; Lee, M. L. *J. Chromatogr. A* **2010**, *1217*, 3844-3854.

61. Chen, X.; Tolley, H. D.; Lee, M. L. *J. Sep. Sci.* **2009**, *32*, 2565-2573.

62. Li, Y.; Tolley, H. D.; Lee, M. L. *Anal. Chem.* **2009**, *81*, 9416-9424.

63. Li, Y.; Tolley, H. D.; Lee, M. L. *J. Chromatogr. A* **2010**, *1217*, 4934-4945.

64. Sun, X.; Farnsworth, P. B.; Wooley, A. T.; Tolley, H. D.; Warnick, K. F.; Lee, M. L. *Anal. Chem.* **2008**, *80*, 451-460.

65. Sun, X.; Li, D.; Lee, M. L. *Anal. Chem.* **2009**, *81*, 6278-6284.

66. Liu, J.; Sun, X.; Lee, M. L. *Anal. Chem.* **2007**, *79*, 1926-1931.

67. Liu, J.; Sun, X.; Lee, M. L. *Anal. Chem.* **2005**, *77*, 6280-6287.

68. Kumakura, M.; Kaetsu, I.; Asami, K.; Suzuki, A. *J. Mater. Sci.* **1989**, *24*, 1809-1813.

69. Grasselli, M.; Smolko, E.; Hargittai, P.; Sáfrány, Á. *Nucl. Instrum. Meth. Phys. Res., Sect. B: Beam Interact. Mater. Atoms* **2001**, *185*, 254-261.

70. Sáfrány, Á.; Beiler, B.; László, K.; Svec, F. *Polymer* **2005**, *46*, 2862-2871.

71. Beiler, B.; Vincze, Á.; Svec, F.; Sáfrány, Á. *Polymer* **2007**, *48*, 3033-3040.

72. Chuda, K.; Jasik, J.; Carlier, J.; Tabourier, P.; Druon, C.; Coqueret, X. *Radiat. Phys. Chem.* **2006**, *75*, 26-33.

73. Bandari, R.; Knolle, W.; Prager-Duschke, A.; Gläsel, H.; Buchmeiser, M. R. *Macromol. Chem. Phys.* **2007**, *208*, 1428-1436.

74. Schlemmer, B.; Bandari, R.; Rosenkranz, L.; Buchmeiser, M. R. *J. Chromatogr. A* **2009**, *1216*, 2664-2670.

75. Li, Y.; Gu, B.; Tolley, H. D.; Lee, M. L. *J. Chromatogr. A* **2009**, *1216*, 5525-5532.

76. Xie, S.; Svec, F.; Fréchet, J. M. J. *Biotechnol. Bioeng.* **1999**, *62*, 30-35.

77. Xie, S.; Allington, R. W.; Svec, F.; Fréchet, J. M. J. *J. Chromatogr. A* **1999**, *865*, 169-174.

78. Viklund, C.; Irgum, K. *Macromolecules* **2000**, *33*, 2539-2544.

79. Fu, X.; Xie, C.; Dong, J.; Huang, X.; Zou, H. *Anal. Chem.* **2004**, *76*, 4866-4874.

80. Svec, F. *J. Sep. Sci.* **2004**, *27*, 1419-1430.

81. Buchmeiser, M. R. *Polymer* **2007**, *48*, 2187-2198.

82. Svec, F.; Fréchet, J. M. J. *J. Chromatogr. A* **1995**, *702*, 89-95.

83. Svec, F.; Fréchet, J. M. J. *Biotechnol. Bioeng.* **1995**, *48*, 476-480.

84. Luo, Q.; Zou, H.; Xiao, X.; Guo, Z.; Kong, L.; Mao, X. *J. Chromatogr. A* **2001**, *926*, 255-264.

85. Ueki, Y.; Umemura, T.; Li, J.; Odake, T.; Tsunoda, K. *Anal. Chem.* **2004**, *76*, 7007-7012.

86. Hutchinson, J. P.; Hilder, E. F.; Shellie, R. A.; Smith, J. A.; Haddad, P. R. *Analyst* **2006**, *131*, 215-221.

87. Hilder, E. F.; Svec, F.; Fréchet, J. M. J. *J. Chromatogr. A* **2004**, *1053*, 101-106.

88. Zakaria, P.; Hutchinson, J. P.; Advalovic, N.; Liu, Y.; Haddad, P. R. *Anal. Chem.* **2005**, *77*, 417-423.

89. Vlakh, E. G.; Tennikova, T. B. *J. Sep. Sci.* **2007**, *30*, 2801-2813.

90. Platonova, G. A.; Tennikova, T. B. *J. Chromatogr. A* **2005**, *1065*, 75-81.

91. Potter, O. G.; Breadmore, M. C.; Hilder, E. F. *Analyst* **2006**, *131*, 1094-1096.

92. Necia, R.; Amatschek, K.; Schallaun, E.; Schwinn, H.; Josic, D. J.; Jungbauer, A. *J. Chromatogr. B* **1998**, *715*, 191-201.

93. Korol'kov V. I.; Platonova, G. A.; Azanova, V. V.; Tennikova, T. B.; Vlasov, G. P. *Lett. Pept. Sci.* **2000**, *7*, 53-61.

94. Pflegerl. K.; Podgornik, A; Berger, E.; Jungbauer, A. *J. Comb. Chem.* **2002**, *4*, 33-37.

95. Pflegerl. K.; Podgornik, A; Berger, E.; Jungbauer, A. *Biotechnol. Bioeng.* **2002**, *79*, 733-740.

96. Gusev, I.; Huang, X.; Horváth, C. *J. Chromatogr. A* **1999**, *855*, 273-290.

97. Wang, Q.; Svec, F.; Fréchet, J. M. J. *Anal. Chem.* **1995**, *67*, 670-674.

98. Huang, X.; Zhang, S.; Schultz, G. A.; Henion, J. *Anal. Chem.* **2002**, *74*, 2336-2344.

99. Müller, W. *J. Chromatogr.* **1990**, *510*, 133-140.

100. Viklund, C.; Svec, F.; Fréchet, J. M. J. *Biotechnol. Prog.* **1997**, *13*, 597-600.

101. Rånby, B.; Yang, W. T.; Tretinnikov, O. *Nucl. Instrum. Meth. Phys. Res., Sect. B* **1999**, *151*, 301-305.

102. Krenkova, J.; Lacher, N. L.; Svec, F. *J. Chromatogr. A* **2009**, *1216*, 3252-3259.

103. Connolly, D.; O'Shea, V.; Clark, P.; O'Connor, B.; Paull, B. *J. Sep. Sci.* **2007**, *30*, 3060-3068.

104. Hilder, E. F.; Svec, F.; Fréchet, J. M. J. *Anal. Chem.* **2004**, *76*, 3887-3892.

105. Stachowiak, T. B.; Svec, F.; Fréchet, J. M. J. *Chem. Mater.* **2006**, *18*, 5950-5957.

106. Eeltink, S.; Hilder, E. F.; Geiser, L.; Svec, F.; Fréchet, J. M. J.; Rozing, G. P.; Schoenmakers, P. J.; Kok, W. T. *J. Sep. Sci.* **2007**, *30*, 407-413.

107. Zhang, R.; Yang, G.; Xin, P.; Qi, L.; Chen, Y. *J. Chromatogr. A* **2009**, *1216*, 2404-2411.

108. Wang, J.; Matyjaszewski, K. *J. Am. Chem. Soc.* **1995**, *117*, 5614-5615.

109. Tsarevsky, N. V.; Matyjaszewski, K. *Chem. Rev.* **2007**, *107*, 2270-2299.

110. Sun, X.; Liu, J.; Lee, M. L. *Anal. Chem.* **2008**, *80*, 856-863.

111. Novak, R. M.; Risse, W.; Grubbs, R. H. *Adv. Polym. Sci.* **1992**, *102*, 47-72.

112. Bielawski, C. W.; Grubbs, R. H. *Prog. Polym. Sci.* **2007**, *32*, 1-18.

113. Buchmeiser, M. R.; Atzl, N.; Bonn, G. K. *J. Am. Chem. Soc.* **1997**, *119*, 9166-9174.

114. Sinner, F.; Buchmeiser, M. R.; Tessadri, R.; Mupa, M.; Wurst, K.; Bonn, G. K. *J. Am. Chem. Soc.* **1998**, *120*, 2790-2797.

115. Buchmeiser, M. R.; Sinner, F.; Mupa, M.; Wurst, K. *Macromolecules* **2000**, *33*, 32-39.

116. Buchmeiser, M. R.; Wurst, K. *J. Am. Chem. Soc.* **1999**, *121*, 11101-11107.

117. Buchmeiser, M. R.; Schareina, T,; Kempe, R.; Wurst, K. *J. Organomet. Chem.* **2001**, *634*, 39-46.

118. Gatschelhofer, C.; Mautner, A.; Reiter, F.; Pieber, T. R.; Buchmeiser, M. R.; Sinner, F. M. *J. Chromatogr. A* **2009**, *1216*, 2651-2657.

119. Eder, K.; Huber, C. G.; Buchmeiser, M. R. *Macromol. Rapid Commun.* **2007**, *28*, 2029-2032.

120. Small, P. W.; Sherrington, D. C. *J. Chem. Soc., Chem. Commun.* **1989**, *21*, 1589-1591.

121. Plieva, F. M.; Galaev, I. Y.; Mattiasson, B. *J. Sep. Sci.* **2007**, *30*, 1657-1671.

122. Yao, K.; Yun, J.; Shen, S.; Wang, L.; He, X.; Yu, X. *J. Chromatogr. A* **2006**, *1109*, 103-110.

123. Yao, K.; Yun, J.; Shen, S.; Chen, F. *J. Chromatogr. A* **2007**, *1157*, 246-251.

124. Kumar, A.; Plieva, F. M.; Galaev, I. Y.; Mattiasson, B. *J. Immunol. Methods* **2003**, *283*, 185-194.

125. Galaev, I. Y.; Dainiak, M. B.; Plieva, F.; Mattiasson, B. *Langmuir* **2005**, *23*, 35-40.

126. Petrov, P.; Petrova, E.; Tsvetanov, C. B. *Polymer* **2009**, *23*, 1118-1123.

127. Sun, X.; Chai, Z. *J. Chromatogr. A* **2002**, *943*, 209-218.

128. Mai, N. A.; Duc, N. T.; Irgum, K. *Chem. Mater.* **2008**, *20*, 6244-6247.

129. Kanamori, K.; Nakanishi, K.; Hanada, T. *Adv. Mater.* **2006**, *18*, 2407-2411.

130. Goto, A.; Kwak, Y.; Fukuda, T.; Yamago, S.; Lida, K.; Nakajima, M.; Yoshida, J. *J. Am. Chem. Soc.* **2003**, *125*, 8720-8721.

131. Chambers, S. D.; Gleen, K. M.; Lucy, C. A. *J. Sep. Sci.* **2007**, *30*, 1628-1645.

132. Nordborg, A.; Hilder, E. F. *Anal. Bioanal. Chem.* **2009**, *394*, 71-84.

133. Vlakh, E. G.; Tennikova, T. B. J. Chromatogr. A 2009, 1216, 2637-2650.

134. Yang, G.; Liu, H.; Zhang, Y.; Wang, S.; Yin, J.; Yin, B.; Chen, Y. *J. Chromatogr. A* **2006**, *1129*, 231-235.

135. Yang, G.; Feng, S.; Liu, H.; Yin, J.; Zhang, L.; Cai, L. *J. Chromatogr. B* **2007**, 854, 85-90.

136. Aoki, H.; Miyano, K.; Yano, D.; Sano, K.; Yamanaka, K.; Kimura, C.; Sugino, T. *Polym. Eng. Sci.* **2007**, *47*, 1666-1670.

137. Rey, M.; Pohl, C. *J. Chromatogr. A* **2003**, *997*, 199-206.

138. Podgornik, A.; Barut, M.; Jančar, J.; Štrancar, A.; Tennikova, T. *Anal. Chem.* **1999**, *71*, 2986-2991.

139. Podgornik, A,; Barut, M.; Jančar, J.; Štrancar, A. *J. Chromatogr. A* **1999**, *848*, 51-60.

140. Vlakh, E. G.; Platonova, G. A.; Vlasov, G. P.; Kasper, C.; Tappe, A.; Kretzmer, G.; Tennikova, T. B. *J. Chromatogr. A* **2003**, *992*, 109-119.

141. Sykora, D.; Svec, F.; Fréchet, J. M. J. *J. Chromatogr. A* **1999**, *852*, 297-304.

142. Yamamoto, S.; Nakamura, M.; Tarmann, C.; Jungbauer, A. *J. Chromatogr. A* **2007**, *1144*, 155-160.

143. Thayer, J. R.; Barreto, V.; Rao, S.; Pohl, C. *Anal. Biochem.* **2005**, *338*, 39-47.

144. Podgornik, H.; Podgornik, A.; Perdih, A. *Anal. Biochem.* **1999**, *272*, 43-47.

145. Branovic, K.; Buchacher, A.; Barut, M.; Štrancar, A.; Josic, D. *J. Chromatogr. B* **2003**, *790*, 175-182.

146. Du, K.; Yang, D.; Sun, Y. *J. Chromatogr. A* **2007**, *1163*, 212-218.

147. Wang, F.; Dong, J.; Jiang, X.; Ye, M.; Zou H. *Anal. Chem.* **2007**, *79*, 6599-6606.

148. Dinh, N. P.; Cam, Q. M.; Nguyen, A. M.; Shchukarev, A.; Irgum, K. *J. Sep. Sci.* **2009**, *32*, 2556-2564.

149. Krenkove, J.; Gargano, A.; Lacher, N. A.; Schneiderheinze, J. M.; Svec, F. *J. Chromatogr. A* **2009**, *1216*, 6824-6830.

150. Bayer, M.; Hänsel, C.; Mosandl. A. *J. Sep. Sci.* **2006**, *29*, 1561-1570.

151. Altmaier, S.; Cabrera, K. *J. Sep. Sci.* **2008**, *31*, 2551-2559.

152. Kučerová, Z.; Szumskim, M.; Buszewski, B.; Jandera, P. *J. Sep. Sci.* **2007**, *30*, 3018-3026.

153. Lee, D.; Svec. F.; Fréchet, J. M. J. *J. Chromatogr. A* **2004**, *1051*, 53-60.

154. Moravcová, D.; Jandera, P.; Urban, J.; Planeta, J. *J. Sep. Sci.* **2003**, *26*, 1005-1016.

155. Umemura, T.; Ueki, Y.; Tsunoda, K.; Katakai, A.; Tamada, M.; Haraguchi, H. *Anal. Bioanal. Chem.* **2006**, *386*, 566-571.

156. Hemström, P.; Nordborg, A.; Irgum, K.; Svec, F.; Fréchet, J. M. J. *J. Sep. Sci.* **2006**, *29*, 25-32.

157. Ueki, Y.; Umemura, T.; Iwashita, Y.; Odake, T.; Haraguchi, H.; Tsunoda, K. *J. Chromatogr. A* **2006**, *1106*, 106-111.

158. Jiang, Z.; Smith, N. W.; Ferguson, P. D.; Taylor, M. R. *J. Biochem. Biophys. Methods* **2007**, *70*, 39-45.

159. Ro, K. W.; liu, J.; Busman, M.; Knapp, D. R. *J. Chromatogr. A* **2004**, *1047*, 49-57.

160. Jandera, P.; Urban, J.; Moravcová, D. *J. Chromatogr. A* **2006**, *1109*, 60-73.

161. Holdšvendová, P.; Coufal, P.; Suchánková, J.; Tesařová, E.; Bosáková, Z. *J. Sep. Sci.* **2003**, *26*, 1623-1628.

162. Eeltink, S.; Herrero-Martinez, J. M.; Rozing, G. P.; Schoenmakers. P. J.; Kok, W. T. *Anal. Chem.* **2005**, *77*, 7342-7347.

163. Coufal, P.; Čihák, M.; Suchánková, J.; Tesařová, E.; Bosáková, Z.; ŠtulíK, K. *J. Chromatogr. A* **2002**, *946*, 99-106.

164. Jiang, T.; Jiskra, J.; Claessens, H. A.; Cramers, C. A. *J. Chromatogr. A* **2001**, *923*, 215-217.

165. Lubbad, S. H.; Buchmeiser, M. R. *J. Sep. Sci.* **2009**, *32*, 2521-2529.

166. Lubbad, S. H.; Buchmeiser, M. R. *J. Chromatogr. A* **2010**, *1217*, 3223-3230.

167. Trojer, L; Lubbad, S. H.; Bisjak, C. P.; Bonn, G. K. *J. Chromatogr. A* **2006**, *1117*, 56-66.

168. Greiderer, A.; Ligon Jr., S. C.; Huck, C. W.; Bonn, G. K. *J. Sep. Sci.* **2009**, *32*, 2510-2520.

169. Greiderer, A.; Trojer, L.; Huck, C. W.; Bonn, G. K. *J. Chromatogr. A* **2009**, *1216*, 7747-7754.

170. Jiang, Z.; Smith, N. W.; Ferguson, P. D.; Taylor, M. R. *J. Sep. Sci.* **2008**, *31*, 2774-2783.

171. Guerrouache, M.; Pantazaki, A.; Millot, M-C.; Carbonnier, B. *J. Sep. Sci.* **2010**, *33*, 787-792.

172. Smigol, V.; Svec, F.; Fréchet, J. M. J. *Anal. Chem.* **1994**, *66*, 2129-2138.

173. Peterson, D. S.; Rohr, T.; Svec, F.; Fréchet, J. M. J. *Anal. Chem.* **2003**, *75*, 5328-5335.

174. Urban, J.; Škeříková, V.; Jandera, P.; Kubíčková, R.; Pospíšilová, M. *J. Sep. Sci.* **2009**, *32*, 2530-2543.

175. Bisjak, C. P.; Trojer, L.; Lubbad, S. H.; wieder, W.; Bonn, G. K. *J. Chromatogr. A* **2007**, *1154*, 269-276.

176. Mayr, B.; Tessadri, R.; Post, E.; Buchmeiser, M. R. *Anal. Chem.* **2001**, *73*, 4071-4078.

177. Gu, C.; Lin, L.; Chen, X.; Jia, J.; Ren, J.; Fang, N. *J. Sep. Sci.* **2007**, *30*, 1005-1012.

178. Nordborg, A.; Svec, F.; Fréchet, J. M. J.; Irgum, K. *J. Sep. Sci.* **2005**, *28*, 2401-2406.

179. Tennikova, T. B.; Bleha, M.; Svec, F.; Almazova, T. V.; Belenkii, B. G. *J. Chromatogr.* **1991**, *555*, 97-107.

180. Tennikova, T. B.; Svec, F. *J. Chromatogr.* **1993**, *646*, 279-288.

181. Štrancar, A.; Koselj, P.; Schwinn, H.; Josic, D. *Anal. Chem.* **1996**, *68*, 3483-3488.

182. Yao, C.; Qi, L.; Yang, G.; Wang, F. *J. Sep. Sci.* **2010**, *33*, 475-483.

183. Jiang, Z.; Smith, N. W.; Ferguson, P. D.; Taylor, M. R. *Anal. Chem.* **2007**, *79*, 1243-1250.

184. Jiang, Z.; Reilly, J.; Everatt, B.; Smith, N. W. *J. Chromatogr. A* **2009**, *1216*, 2439-2448.

185. Jiang, Z.; Smith, N. W.; Ferguson, P. D.; Taylor, M. R. *J. Sep. Sci.* **2009**, *32*, 2544-2555.

186. Holdšvendová, P.; Suchánková, J.; Bunček, M.; Bačkovská, V.; Coufal, P. *J. Biochem. Biophys. Methods* **2007**, *70*, 23-29.

187. Hosoya, K.; Hira, N.; Yamamoto, K.; Nishimura, M.; Tanaka, N. *Anal. Chem.* **2006**, *78*, 5729-5737.

188. Lin, J.; Lin, J.; Lin, X.; Xie, Z. *J. Chromatogr. A* **2009**, *1216*, 801-806.

189. Lin, J.; Huang, G.; Lin, X.; Xie, Z. *Electrophoresis* **2008**, *29*, 4055-4065.

190. Luo, Q.; Mao, X.; Kong, L.; Huang, X.; Zou, H. *J. Chromatogr. B* **2002**, *776*, 139-147.

191. Okanda, F. M.; El Rassi, Z. *Electrophoresis* **2006**, *27*, 1020-1030.

192. Armenta, J. M.; Gu, B.; Thulin, C. D.; Lee, M. L. *J. Chromatogr. A* **2007**, *1148*, 115-122.

193. Wen, Y.; Feng, Y. *J. Chromatogr. A* **2007**, *1160*, 90-98.

194. Wei, X.; Yin, J.; Yang, G.; He, C.; Chen, Y. *J. Sep. Sci.* **2007**, *30*, 2851-2857.

195. Huang, X.; Yuan, D. *J. Chromatogr. A* **2007**, *1154*, 152-157.

196. Courtois, J.; Fischer, G.; Sellergren, B.; Irgum, K. *J. Chromatogr. A* **2006**, *1109*, 92-99.

197. Tunc,Y.; Gölgelioğlu, C.; Hasirci, N.; Ulubayram, K.; Tuncel, A. *J. Chromatogr. A* **2010**, *1217*, 1654-1659.

198. Zheng, M.; Ruan, G.; Feng, Y. *J. Chromatogr. A* **2009**, *1216*, 7510-7519.

199. Huang, H.; Liu, Y.; Cheng, Y. *J. Chromatogr. A* **2008**, *1190*, 263-270.

200. Fu, H.; Xie, C.; Dong, J.; Huang, X.; Zou, H. *Anal. Chem.* **2004**, *76*, 4866-4874.

201. Lu, H.; Wang, J.; Wang, X.; Wu, X.; Lin, X.; Xie, Z. *J. Sep. Sci.* **2007**, *30*, 2993-2999.

202. Fu, H.; Xie, C.; Hua, X.; Dong, J.; Hu, J.; Zou, H. *J. Chromatogr. A* **2004**, *1044*, 237-244.

203. Levkin, P. A.; Eeltink, S.; Stratton, T. R.; Brennen, R.; Robotti, K.; Yin, H.; Killeen, K.; Svec, F.; Fréchet, J. M. J. *J. Chromatogr. A* **2008**, *1200*, 55-61.

204. Sun, X.; Yang, W.; Pan, T.; Woolley, A. T. *Anal. Chem.* **2008**, *80*, 5126-5130.

205. Benčina, K.; Podgornik, A.; Štrancar, A.; Benčina, M. *J. Sep. Sci.* **2004**, *27*, 811-818.

206. Huang, B.; Chen, Y.; Wang, G.; Liu, C. *J. Chromatogr. A* **2011**, *1218*, 849-855.

207. Han, B.; Wang, P.; Zhu, G.; Zhang, L.; Qu, F.; Deng, Y.; Zhang, Y. *J. Sep. Sci.* **2009**, *32*, 1211-1215.

CHAPTER 2 STRONG CATION-EXCHANGE MONOLITHIC COLUMNS CONTAINING SULFONIC ACID FUNCTIONAL GROUPS

2.1 Introduction

As discussed in Chapter 1, IEC is an important separation technique for analyzing large biomolecules, such as peptides and proteins, due to its high capacity and ability to perform separations under non-denaturing conditions.[1] It is highly orthogonal in separation selectivity to capillary electrophoresis and reversed-phase chromatography.[2-4]

The cross-linker plays an important role in monolith preparation. It has a significant effect on the rigidity, polarity and porosity of the resulting monolith. Ostuni et al. proved that surface coated with PEG resisted protein adsorption effectively.[5] A cross-linker, poly(ethylene glycol) diacrylate (PEGDA, Mn 258, Figure 2.1), which contains three ethylene glycol units, has been shown to be more biocompatible compared to conventional ethylene glycol dimethacrylate.[6-8] PEGDA is very useful for analysis of biological samples, such as peptides and proteins, due to low nonspecific interactions. Another advantageous feature of PEG is that it does not denature proteins, even if it is present at high concentration, which is in stark contrast to other organic solvents such as acetonitrile.[9]

Several approaches have been reported to synthesize strong cation exchange (SCX) polymer monoliths containing sulfonic acid groups, including adsorption,[10] postmodification,[11-13] and copolymerization.[14-19] Among these approaches, copolymerization is the simplest, only requiring one step. The concentration of functional groups in the monolith is controlled easily, although the ion exchange capacity of the monolith is lower than monoliths prepared by the other two approaches. Unfortunately, even though the copolymerization approach is simple, only a few monoliths containing a sulfonic acid-containing monomer have been synthesized.[20,21] Two

reasons may explain this. First, each individual monolith has its own optimized synthetic conditions, which cannot be easily transferred directly to another monolith. Second, sulfonic acid-containing monoliths swell in aqueous buffer. It is not easy to obtain a stable monolith from a sulfonic acid-containing monomer.

Sulfopropyl methacrylate (SPMA, Figure 2.1) was reported to copolymerize with pentaerythritol for capillary electrochromatography and capillary liquid chromatography of polar charged nucleotides and neutral phenols.[22] The separation of phenols exhibited a typical hydrophilic interaction mechanism. Electrostatic interaction as well as hydrophilic interaction was observed for separation of charged nucleotides. In this study, stable polymer monoliths containing sulfonic acid monomer concentrations as high as 40% (w/w) were prepared by direct copolymerization of SPMA and PEGDA. These monoliths were successfully used for SCX liquid chromatography of peptides and proteins at low pressure.

2.2 Experimental Section

2.2.1 Chemicals and Reagents

2,2-Dimethoxy-2-phenylacetophenone (DMPA, 99%), 3-(trimethoxysilyl)propyl methacrylate (98%), sulfopropyl methacrylate (SPMA), ethylene glycol dimethacrylate (EDMA), and poly(ethylene glycol) diacrylate (PEGDA, Mn ~ 258) were purchased from Sigma-Aldrich (Milwaukee, WI) and used without further purification. A synthetic peptide standard, CES-P0050, was obtained from Alberta Peptides Institute (Edmonton, Alberta, Canada). Peptide standard H2016, proteins (myoglobin from equine skeletal muscle, cytochrome *c* from bovine heart, α-chymotrypsinogen A from bovine pancreas, and lysozyme from chicken egg white) were also obtained from Sigma-Aldrich. Porogenic solvents for monolith synthesis and chemicals for mobile phase buffer preparation were HPLC or analytical reagent grade.
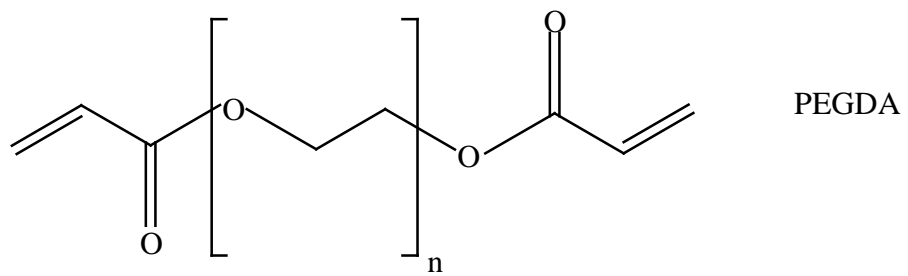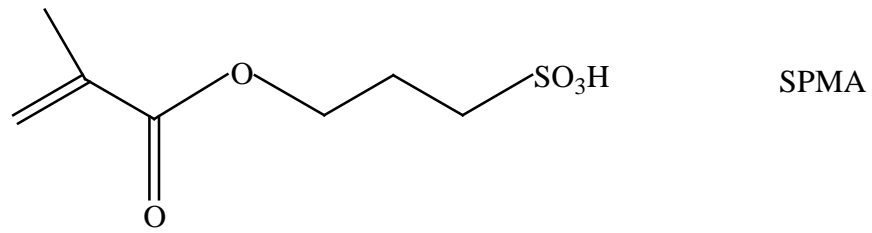
Figure 2.1. Chemical Structures of SPMA and PEGDA.

2.2.2 Polymer Monolith Preparation

A UV transparent fused-silica capillary (75 µm I.D. × 360 µm O.D., Polymicro Technologies, Phoenix, AZ) was treated with 3-(trimethoxysilyl)propyl methacrylate to provide pendant vinyl groups to ensure covalent bonding of the monolith to the capillary wall.[21] Polymer monoliths were prepared using the method introduced by Gu et al.[21] The polymerization mixture was prepared in a 4-mL glass vial by mixing 0.006 g of DMPA, 0.24 g of SPMA, 0.36 g of PEGDA, 0.6 g of cyclohexanol, 1.0 g of methanol and 0.1 g of water. The mixture was vortexed and ultrasonicated for 3 min to help dissolve SPMA and eliminate oxygen. The monomer solution was introduced into the capillary by capillary action. The capillary was placed directly under a PRX 1000-20 Exposure Unit UV lamp (TAMARACK Scientific, Corona, CA) for 3 min. The resulting monolith was then flushed with methanol and water sequentially to remove porogens and unreacted monomers using an LC pump. The capillary was stored in 10% methanol aqueous solution to avoid drying the monolith. Scanning electron microscopy (SEM) images were obtained as previous described.[21]

2.2.3 Capillary Liquid Chromatography (CLC)

CLC of peptides and proteins was performed using a system previously described, except the mobile-phase flow rate was set at 15 or 20 µL/min.[21] For CLC of peptides, mobile phase A was 5 mmol/L aqueous phosphate buffer (pH 2.7 or 6.0) with various amounts of acetonitrile. Mobile phase B was 0.5 M NaCl in mobile phase A. All mobile phases were filtered through a 0.2 µm Nylon membrane filter (Supelco, Bellefonte, PA). A Model UV3000 detector from Thermo Separations (Sunol, CA) was set at 214 nm. Data were acquired with ChromQuest 2.5.1 (ThermoQuest, Sunol, CA). Each chromatographic run was performed at least two times to ensure repeatability.

Cytochrome C and lysozyme were used to measure the dynamic binding capacity of the monolithic column. Lysozyme in 5 mmol/L phosphate buffer (15 mg/mL) at pH 6.0 was pumped under pressures of 800, 1000 and 1200 psi through the monolithic column (10 cm long). Cytochrome C (11.15 mg/mL) was also pumped through the column under the same conditions as lysozyme, except only at a pressure of 1000 psi. The procedure was previously described in detail.[21] The DBC was measured one time. The flow rate, measured using a calibration capillary (Eksigent, Livermore, CA), was 348, 426, and 522 nL/ min at 800, 1000 and 1200 psi. Different solvents such as methanol, acetonitrile and water were pumped through a 10-cm-long monolith to investigate the swelling/shrinking properties of the monolith.

2.3 Results and Discussion

2.3.1 Polymer Monolith Preparation

SPMA was selected as monomer to synthesize an SCX monolith because it contained a sulfonic acid group. PEGDA, which has an acrylate group at each end of the molecule and a three-unit ethylene glycol connecting chain, has shown its resistance to peptides and proteins. However, EDMA exhibits some adsorption.[23] Therefore, PEGDA was chosen as cross-linker.

While theories have been proposed for macroporous particle synthesis using suspension polymerization,[24,25] these theories are not suitable for monolith preparation. The best choice of porogens are still determined primarily by trial and error. Generally, the morphology of a monolith is controlled by porogen solvent, percentage of monomers and ratio between monomer and porogen solvents.[26,27] In this work, water was selected as one of the porogen components because SPMA dissolves in it well, in contrast to organic solvents. Methanol was also used as a porogen solvent because it can form macroporous through-pores.[23] Unfortunately, the combination of water and methanol resulted in no monolith, or a gel structure. Thus, ethyl ether

was selected as a third component because ethyl ether is a large pore forming solvent. However, the resulting monolith was not homogeneous. Finally, ethyl ether was replaced with cyclohexanol. The final recipe after simple optimization was 26% monomers composed of 40:60 wt% SPMA and PEGDA, and 74% porogens composed of 5.9:35.3:58.8 wt% water, cyclohexanol and methanol, respectively. The same components were also used to synthesize a poly(SPMA-co-EDMA) monolith in which PEGDA was substituted with EDMA.

Figures 2.2A and B show scanning electron micrographs of the final monolith. The morphology of the poly(SPMA-co-PEGDA) monolith is unique with fused microglobules and spherical units aggregated into large clusters. It displays both the characteristic particulate structure of a polymer monolith and the skeletal structure of a silica monolith.

To investigate the effect of cross-linker on the morphology of the monolith, EDMA was used instead of PEGDA to produce a poly(SPMA-co-PEGDA) monolith. SEM photographs are shown in Figures 2.2C and D. Cracks along the circumference of the monolith were caused by shrinkage of the monolith when it was dried before SEM analysis. This alone demonstrates that the poly(SPMA-co-EDMA) monolith is not as stable as the poly(SPMA-co-EDMA) monolith. The morphology of poly(SPMA-co-EDMA) exhibited the typical polymer monolithic morphology with discrete microglobules. As expected, the cross-linker plays an important role in the morphology of the monolith.

2.3.2 Stability, Permeability and Pore Size Distribution of the Poly(SPMA-co-PEGDA) Monolithic Column

Poly(SPMA-co-PEGDA) monoliths were synthesized in 75 μm I.D. fused silica capillaries. The hydrodynamic properties of the monoliths are important for chromatographic applications. To evaluate the mechanical stability of a synthesized monolith, the pressure drop
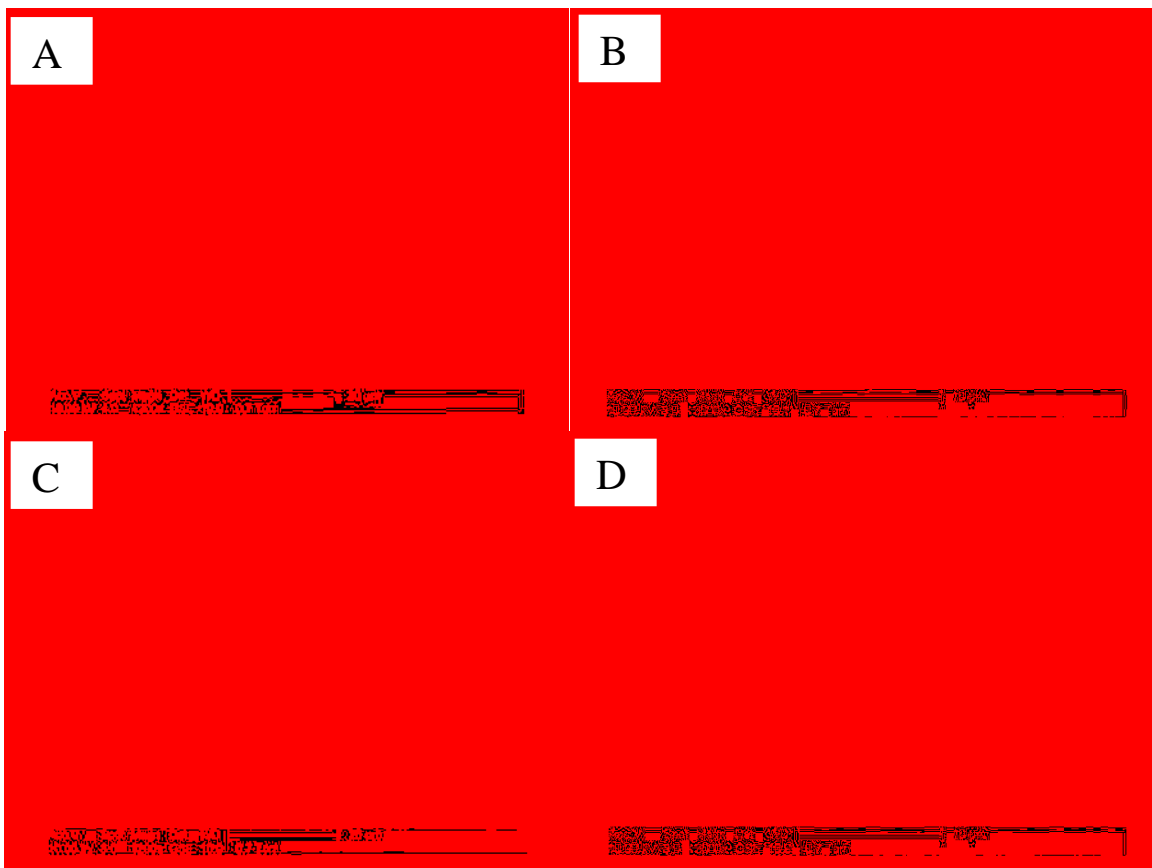
Figure 2.2. Scanning electron microphotographs of (A) optimized poly(SPMA-co-PEGDA) monolith (scale bar, 20 µm); (B) higher magnification of the monolith in (A) (scale bar, 10 µm); (C) poly(SPMA-co-EDMA) monolith (scale bar, 20 µm); (D) higher magnification of the monolith in (C) (scale bar, 10 µm).

across the column was measured using different solvents. The effect of flow rate on back pressure is shown in Figure 2.3. Clearly, there is a linear dependence of flow rate on back pressure for all solvents, indicating that the monolithic bed is stable even at 1500 psi. Permeability can be used to determine the swelling and shrinking of a monolith. An ideal monolith should show no excessive swelling or shrinking in mobile phases of different polarity. The permeability was calculated for a pressure of 1200 psi using Darcy's law. From Table 2.1, the permeability was of the same order of magnitude for both water and organic solvents. This indicates that the monolith did not shrink substantially in organic solvents or swell in more polar solvents. No detachment of the monolith from the capillary wall was observed under these conditions.

Inverse size exclusion chromatography (ISEC) was used to characterize the pore structure of the monolith. The total porosity was calculated to be 81.6%. The pore volumes corresponding to pores larger than 304 nm and for pores between 50 nm and 304 nm were 65.7% and 8.2%, respectively. The pore volume fractions for mesopores (2-50 nm) and for small pores (< 2 nm) were 17.2% and 8.9%, respectively. The pore volume fractions in the mesopore range and small pore range are relatively large, which suggests that this monolith may also be useful for size exclusion chromatography.

2.3.3 Separation of Peptides

SCX chromatography is probably the most useful mode of high-performance ion-exchange chromatography for peptide separation.[4,28] The utility of SCX chromatography lies in the ability to retain positively charged analytes in the acidic to neutral pH range. An ideal SCX column for LC of peptides should have specific properties, such as ability to retain weakly charged analytes and high binding capacity. Hodges et al. synthesized a series of undecapeptide
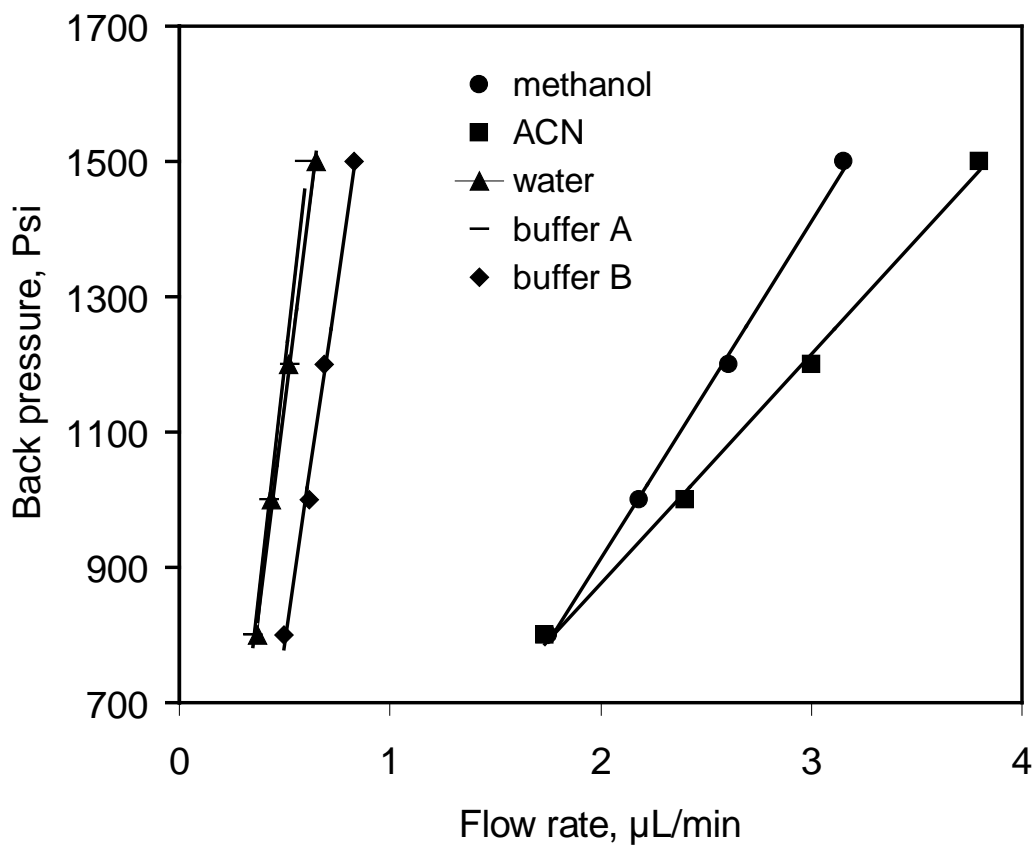
Figure 2.3. Effect of mobile phase flow rate on column back pressure. Conditions: 9.0 cm × 75 µm I.D. monolithic column; buffer A is 10 mmol/L phosphate buffer at pH 6.0 and buffer B is 0.5 M NaCl in buffer A. Flow rates were measured at pressures of 800 (5.52 MPa), 1000 (6.89 MPa), 1200 (8.27 MPa), and 1500 psi (10.3 MPa).

Table 2.1. Permeability of the poly(SPMA-co-PEGDA) monolith.

Solvent	Relative polarity[a]	Viscosity η (cp)[a]	Column back pressure Δp (psi)	Linear velocity u (mm/s)	Permeability k ($\times 10^{-15}$ m^2)
acetonitrile	0.460	0.369	1200	11.32	60.6
methanol	0.762	0.554	1200	9.85	79.1
water	1.00	0.890	1200	1.95	25.2
buffer A	/	0.890	1200	1.97	25.4
buffer B	/	0.936	1200	2.60	35.2

[a] Relative polarity data and viscosity data were from reference 21.

standards to evaluate particle packed SCX columns.[3] The peptide standards, CESP0050, were

selected for evaluation of the poly(SPMA-co-PEGDA) monolith. The structures and

characteristics of these peptide standards were previously described.[21] Figure 2.4 shows the

elution profiles of peptide standards under different buffer conditions using a poly(SPMA-co-

PEGDA) monolithic column. The mobile phases are identical except for the addition of various

amounts of acetonitrile. It is clear that with an increase in acetonitrile in the mobile phase from 0

to 40% (Figures 2.4 A-C), the elution times for peptides 1-4 decreased, particularly for peptide 4,

which is the most hydrophobic peptide. An increase in acetonitrile to 40% substantially

improved the peak shape and reduced the retention time of peptide 4 to almost 10 min, indicating

that addition of 40% acetonitrile was necessary to suppress hydrophobic interactions between the

monolith and the peptide. For the other three peptides, narrower peaks were obtained when

higher concentrations of acetonitrile were present in the mobile phase. Compared to two other

monoliths,[29] poly(AMPS-co-PEGDA) and poly(SEMA-co-PEGDA), the overall hydrophobicity

of poly(SPMA-co-PEGDA) is much less. Poly(SPMA-co-PEGDA) monolith can elute the most

hydrophobic peptide 4 in relatively short time without acetonitrile, making it useful as the first

dimension in 2-D chromatography.

From Figure 2.4C, when hydrophobic interactions were effectively suppressed, the

retention times of peptides 2-4 increased linearly with increasing net charge. Thus, the difference

in retention times for adjacent peptides was equal. We conclude that the greater difference in

retention between peptides 3 and 4 compared to peptides 2 and 3 (Figures 2.4A and B) indicates

the presence of hydrophobic interactions, although all four peptides can be eluted from the

column without any acetonitrile in the mobile phase. The hydrophobicity of the poly(SPMA-co-

PEGDA) monolith in the ion-exchange chromatography mode must come from SPMA itself,
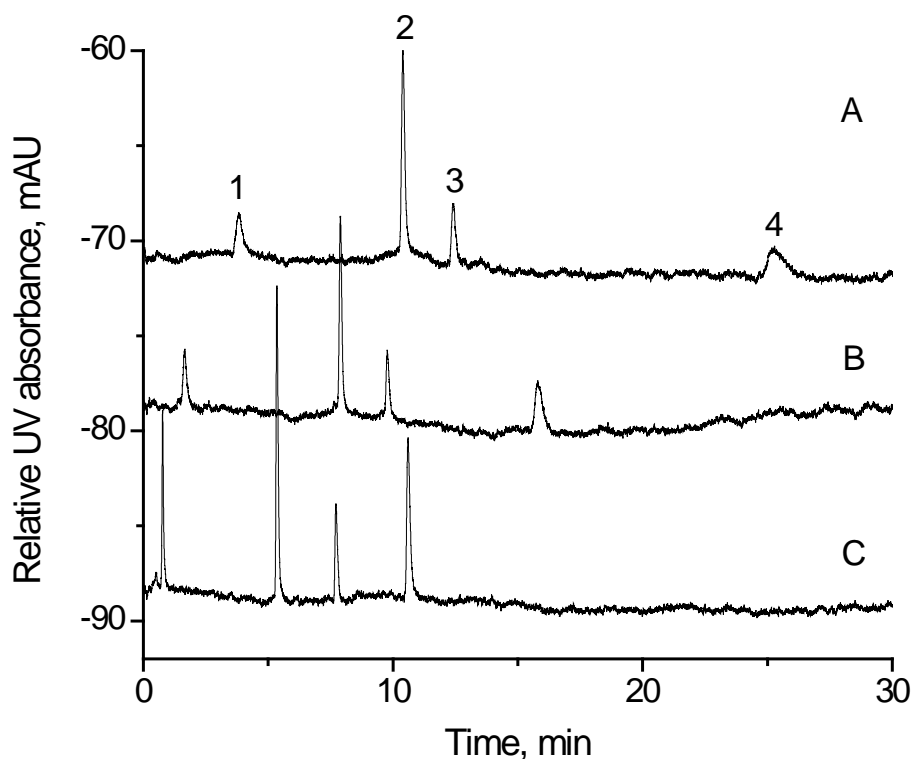
Figure 2.4. SCX chromatography of synthetic peptides. Conditions: 9.0 cm × 75 µm I.D. monolithic column; buffer A was 5 mmol/L NaH$_2$PO$_4$ (pH 2.5) and buffer B was buffer A plus 0.5 mol/L NaCl, both buffers containing 0, 20, or 40% (v/v) ACN (A–C, respectively); linear gradient from A to B in 10 min, followed by isocratic elution with 100% B; 20 µL/min flow rate; on-line UV detection at 214 nm. (1) Ac-Gly-Gly-Gly-Leu-Gly-Gly-Ala-Gly-Gly-Leu-Lys-amide, (2) Ac-Lys-Tyr-Gly-Leu-Gly-Gly-Ala-Gly-Gly-Leu-Lys-amide, (3) Ac-Gly-Gly-Ala-Leu-Lys-Ala-Leu-Lys-Gly-Leu-Lys-amide, and (4) Ac-Lys-Tyr-Ala-Leu-Lys-Ala-Leu-Lys-Gly-Leu-Lys-amide.

since the PEGDA cross-linker has been shown to exhibit negligible hydrophobicity. The hydrophobicity may result from the side chain of the SPMA molecule and the carbon-carbon backbone formed during the polymerization of the propyl groups in the SPMA molecule.

One of the most important metrics for the quality of a column under gradient conditions is the peak capacity, which is defined as the maxium number of peaks that can be separated with a given resolution. The four peptides eluted with an average peak width of 0.36 min when hydrophobic interactions were suppressed with 40% acetonitrile. According to the definition in gradient elution by Snyder et al.,[30] the peak capacity was calculated to be 28, which is almost the same as that of particulate based SCX columns,[3,4,31] and surpasses most polymer monolithic SCX columns.[16,32]

Buffer pH has a great effect on the separation of peptide standards (Figure 2.5). With an increase in buffer pH from 2.5 to 6.0, the retention times increased and the peaks became broader under the identical conditions as in Figure 2.4C. Ideally, there should be no difference in retention times of these peptides with a change in buffer pH, since the peptides bear the same charges in both buffers. Hodges et al. explained that the observed effects resulted from a reduction in column capacity to retain charged species as the pH became more acidic.[3]

2.3.4 SCX Separation of a Natural Peptide Mixture

The poly(SPMA-co-PEGDA) SCX monolith was applied to separate a natural peptide mixture, composed of 5 peptides (Table 2.2) using a buffer containing 20% acetonitrile for different gradient program rates (Figure 2.6). When a 5% B/min gradient was used, all five components eluted in 25 min (Figure 2.6D). The retention times decreased along with an increase in gradient rate. A further increase in the gradient rate to 50% B/min eluted all components in almost 12 min (Figure 2.6A). It is clear that the separation of natural peptides was
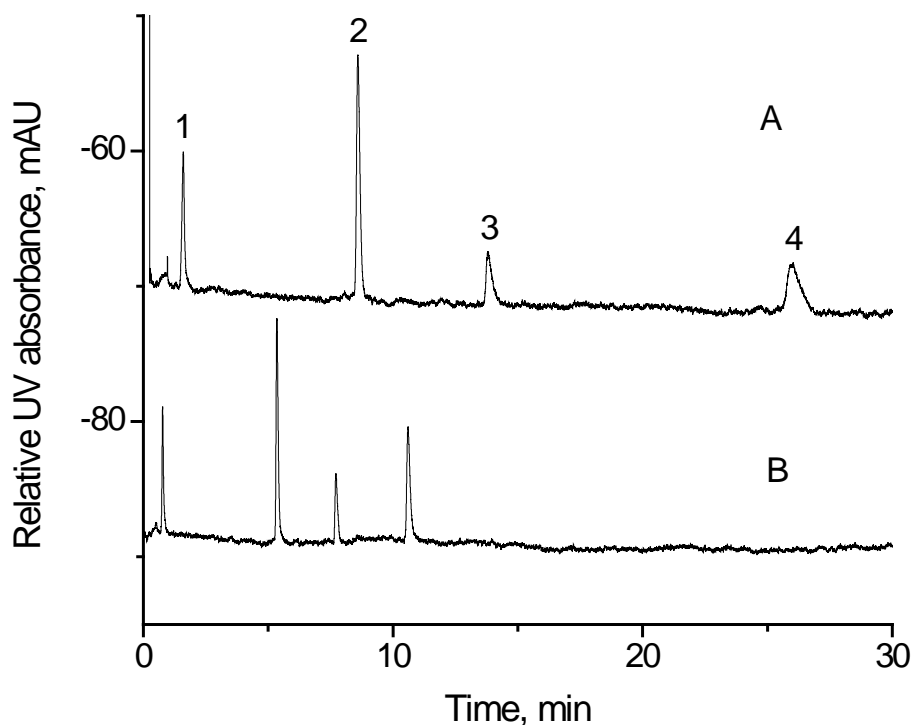
Figure 2.5. SCX chromatography of synthetic peptides. Conditions: 9.0 cm × 75 µm I.D. monolithic column; buffer A was 5 mmol/L Na_2HPO_4 (pH 6.0) for A and 5 mmol/L NaH_2PO_4 (pH 2.5) for B, and buffer B was buffer A plus 0.5 mol/L NaCl, both buffers containing 40% (v/v) ACN; linear gradient from A to B in 10 min, followed by isocratic elution with 100% B. 20 µL/min flow rate; on-line UV detection at 214 nm. (1) Ac-Gly-Gly-Gly-Leu-Gly-Gly-Ala-Gly-Gly-Leu-Lys-amide, (2) Ac-Lys-Tyr-Gly-Leu-Gly-Gly-Ala-Gly-Gly-Leu-Lys-amide, (3) Ac-Gly-Gly-Ala-Leu-Lys-Ala-Leu-Lys-Gly-Leu-Lys-amide, and (4) Ac-Lys-Tyr-Ala-Leu-Lys-Ala-Leu-Lys-Gly-Leu-Lys-amide.

Table 2.2. Peptide properties.

No.	Peptide	Mw	Amino acid sequence	No. of residues	Charge at pH 2.7
1	Methionine enkephalin	573	Tyr-Gly-Gly-Phe-Met	5	1
2	Leucine enkephalin	555	Tyr-Gly-Gly-Phe-Leu	5	1
3	Val-Tyr-Val	379	Val-Tyr-Val	3	1
4	Gly-Tyr	238	Gly-Tyr	2	1
5	Angiotensin II	1046	Asp-Arg-Val-Tyr-Ile-His-Pro-Phe	8	3

Figure 2.6. SCX chromatography of natural peptides. Conditions: 10.0×75 µm I.D. monolithic column; buffer A was 5 mmol/L NaH_2PO_4 (pH 2.5) and buffer B was buffer A plus 1.0 mol/L NaCl, both buffers containing 20% (v/v) ACN; linear gradient from A to B in (A) 2, (B) 5, (C) 10, and (D) 20 min, followed by isocratic elution with 100% B; 20 µL/min flow rate; on-line UV detection at 214 nm. (1) methionine enkephalin, (2) leucine enkephalin, (3) Val-Tyr-Val, (4) Gly-Tyr, and (5) angiotensin II.

governed by an ion-exchange mechanism, and a steeper gradient rate resulted in narrower peaks and reduced retention times.

It is interesting that the separation time in Figure 2.6A is less than 12 min, which is much less than observed in reversed phase liquid chromatography (RPLC).[33] Also, faster separation and narrower peaks were obtained in SCX chromatography. This indicates that the poly(SPMA-co-PEGDA) monolithic column is preferred over RPLC for this natural peptide sample. The average peak widths at baseline in Figures 2.6 A-D were 0.55, 0.55, 0.54, and 0.66 min, respectively, resulting in peak capacities of 4, 9, 18, and 30 for the gradient rates of 50, 20, 10 and 5% B/min, respectively. Thus, the peak capacity depends on the salt gradient rate, and a shallower gradient results in a greater peak capacity.

Noteworthy in Figure 2.6 is the excellent separation of methionine enkephalin and leucine enkephalin, which have the same charge and chain length, and similar molecular weights and hydrophobicities. This separation was based on ionic interactions due to 20% acetonitrile in the mobile phase, suppressing hydrophobic interactions. Since methionine enkephalin is a larger molecule than leucine enkephalin, ionic interaction is expected to be smaller, allowing it to elute earlier. The resolution values measured for methionine enkephalin and leucine enkephalin were 1.82, 1.40, 1.21, and 0.80 for gradient rates of 5, 10, 20 and 50% B/min, respectively. Only minor differences in ionic interactions resulted in the separations. The poly(SPAM-co-PEGDA) monolith is better than the poly(AMPS-co-PEGDA) monolith[21] for separation of methionine enkephalin and leucine enkephalin in terms of resolution, efficiency and retention time.

2.3.5 SCX Separation of Protein Standards

The poly(SPMA-co-PEGDA) monolith was used for the separation of a mixture of basic proteins containing ribonuclease A (pI 8.2), α-chymotrypsinogen A (pI 9.5), cytochrome C (pI

10.6) and lysozyme (pI 11.0). The effect of buffer concentration on protein retention and column efficiency was investigated. Baseline separation of the four proteins was achieved when 5, 10, and 20 mmol/L phosphate buffer at pH 6.0 were used. Clearly, both retention time and efficiency were reduced with an increase in buffer concentration (Table 2.3). The effect of pH on separation efficiency was probed over a pH range from 5.0 to 7.0 (Table 2.4). The retention time was lower and the efficiency was higher at lower pH. To realize fast separation, 20 mmol/L phosphate at pH 7.0 was selected as buffer. Similar to the previous observations that gradient rate has the greatest effect on peptide separation, it also affects protein separation. From Figure 2.7, a high gradient rate leads to reduced retention time and narrower peaks. All four proteins eluted in 7 min when a gradient rate of 50% B/min was used. The average peak widths at baseline in Figure 2.7 were 0.64, 0.78, and 0.94 min, resulting in peak capacities of 3, 6, and 10 for gradient rates of 50, 20, and 10% B/min, respectively. For proteins, a shallower gradient also leads to greater peak capacity. Since the poly(SPMA-co-PEGDA) monolith exhibited some hydrophobicity, 20% (v/v) acetonitrile was added to the buffer for protein separation. Sharper peaks were obtained for all four proteins (Figure 2.8). A peak capacity of 4 was obtained with an average peak width of 0.5 min. Although lower peak capacity was generated, better peak profiles for proteins were obtained. The acetonitrile suppressed hydrophobic interaction between proteins and monolith, resulting in all proteins being eluted in 4 min. The performance is better than for other monolithic SCX columns used for protein analysis.[21,34] This column was continuously used at ~ 1200 psi for almost 2 months, showing constant back pressure and no deterioration of column performance.

Table 2.3. Retention times (T_R, min) and column efficiencies (E_F, plates/m) for proteins.

Buffer concentration (mmol/L)	Ribonuclease A		α-Chymotrypsinogen A		Cytochrome C		Lysozyme	
	T_R	E_F	T_R	E_F	T_R	E_F	T_R	E_F
5	5.61	20723	5.093	15600	6.504	12923	13.972	8572
10	5.485	12155	5.932	18928	6.536	15655	13.416	6230
20	4.729	8742	5.422	8981	6.13	7565	13.056	8381

Table 2.4. Retention times (T_R, min) and column efficiencies (E_F, plates/m) for proteins.

| Buffer pH	Ribonuclease A		α-Chymotrypsinogen A		Cytochrome C		Lysozyme	
	T_R	E_F	T_R	E_F	T_R	E_F	T_R	E_F
5.0	4.838	12591	5.328	15875	6.024	8676	13.102	10002
6.0	4.486	3176	5.140	9682	5.827	11689	12.817	5630
7.0	3.168	2979	4.860	13742	5.349	5374	12.113	8032
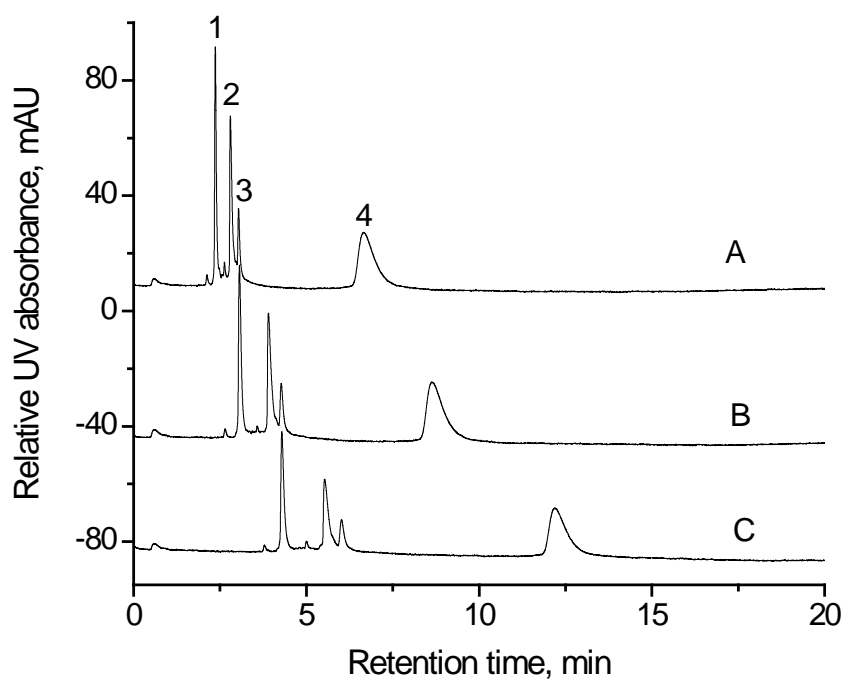
Figure 2.7. SCX chromatography of proteins. Conditions: 10.0×75 µm I.D. monolithic column; buffer A was 20 mmol/L Na_2HPO_4 (pH 7.0) and buffer B was buffer A plus 1.0 mol/L NaCl; linear gradient from A to B in (A) 2 min, (B) 5 min, and (C) 10 min, followed by isocratic elution with 100% B; 20 µL/min flow rate; on-line UV detection at 214 nm. (1) ribonuclease A, (2) α-chymotrypsinogen A, (3) cytochrome C and (4) lysozyme.
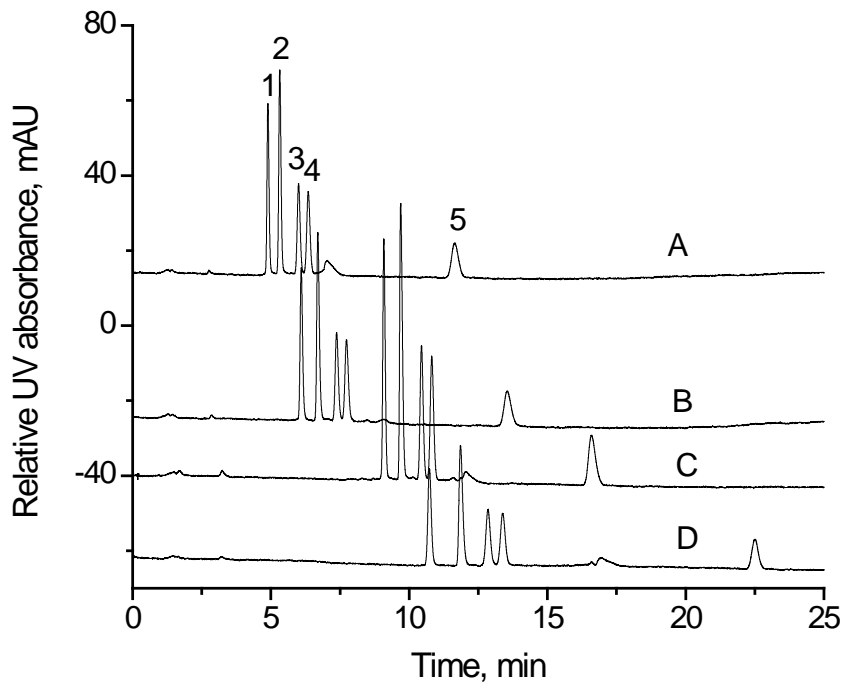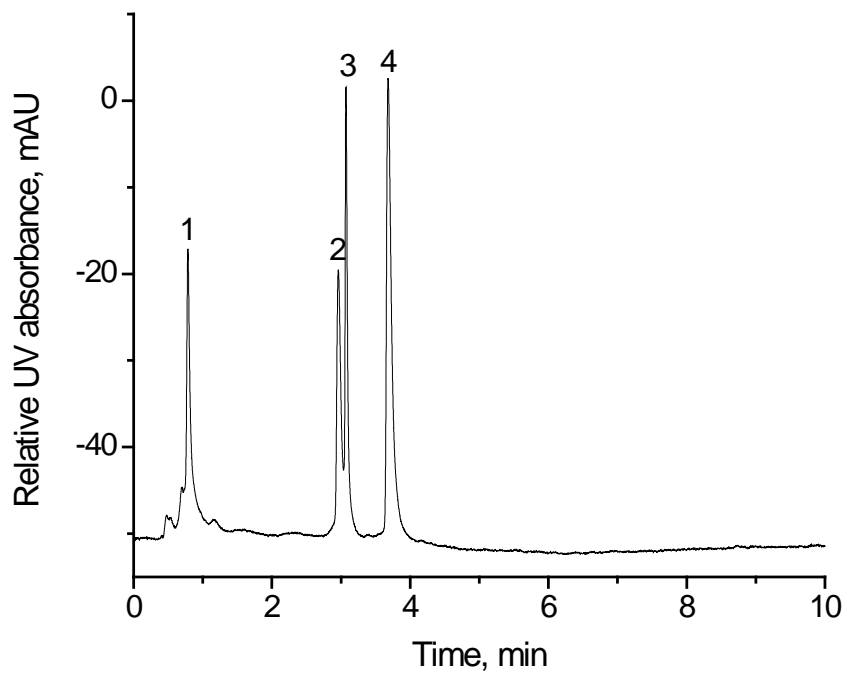
Figure 2.8. SCX chromatography of proteins. Conditions: 10.0×75 µm µm I.D. monolithic column; buffer A was 20 mmol/L Na_2HPO_4 (pH 7.0) and buffer B was buffer A plus 1.0 mol/L NaCl, both buffers containing 20% (v/v) ACN; linear gradient from A to B in 2 min, followed by isocratic elution with 100% B; 15 µL/min flow rate; on-line UV detection at 214 nm. (1) ribonuclease A, (2) α-chymotrypsinogen A, (3) cytochrome C, and (4) lysozyme.

2.3.6 Dynamic Binding Capacity

Binding capacity is one of the most important properties of an ion-exchange column, which determines the column resolution, column loadability, and gradient elution strength. Lysozyme and cytochrome C were used to measure the dynamic binding capacity of the poly(SPMA-co-PEGDA) monolithic column (10.0 cm $\times$ 75 μm I.D.). With the use of 15.0 mg/mL concentration of lysozyme and 11.2 mg/mL of cytochrome C, a sharp increase in the baseline was observed after column saturation, indicating fast kinetic binding of the proteins with the column. After the column was saturated, it was flushed with 20 mmol/L phosphate buffer (pH 7.0) containing 1 mol/L NaCl for 30 min and then equilibrated with 20 mmol/L phosphate buffer (pH 7.0) for 30 min before the next measurement. Measurements were made for pressures of 800, 1000, and 1200 psi for lysozyme and 1000 psi for cytochrome C. The dead volume of the column was measured by flushing toluene through the same column. Finally, the time for lysozyme saturation at 50% height was 5.39, 4.45, and 3.76 min at 800, 1000, and 1200 psi, respectively, and 5.72 min for cytochrome C saturation at 1000 psi. The dynamic binding capacity for lysozyme was 51.5, 52.2, and 53.7 mg/mL of column volume at 800, 1000, and 1200 psi, respectively, and 52.4 mg/mL of column volume at 1000 psi for cytochrome C. The binding capacity is comparable to the range of 30 to 100 mg/mL obtained by Staby et al. for commercial weak cation-exchange resins,[35,36] but is almost two times higher than that obtained for a tetrazole-functionalized ion exchanger.[37] This comparable dynamic binding capacity is presumably due to the high amount of SPMA used in the copolymerization.

2.4 Conclusions

A polymer-based strong cation-exchange monolithic stationary phase containing 40% SPMA in the monomers was synthesized in a capillary by UV-initiated copolymerization of

SPMA and PEGDA in a ternary porogen system. The resulting monolithic column had low flow resistance, good mechanical strength, high permeability, and comparable dynamic binding capacity to conventional cation exchange columns. The column was successfully applied for fast separation of synthetic peptides, natural peptides, and protein standards. With the advantages of easy preparation and excellent performance in chromatographic separations, this monolith should be applicable to various high throughput proteome analyses.

This work was published in the Journal of Separation Science, 2009, 32, 2565-2573.

2.5 References

1. Bonnerjea, J.; Oh, S.; Hoare, M.; Dunnill, P. *Bio-Technology* **1986**, *4*, 954-958.

2. Breadmore, M. C.; Macka, M.; Haddad, P. R. *Electrophoresis* **1999**, *20*, 1987-1992.

3. Burke, T. W. L.; Mant, C. T.; Balck, J. A.; Hodges, R.S. *J. Chromatogr.* **1989**, *476*, 377-389.

4. Alpert, A. J.; Andrews, P. C. *J. Chromatogr.* **1988,** *443*, 85-96.

5. Ostuni, E.; Chapman, R. G.; Holmlin, R.E.; Takayama, S.; Whitesides, G. M. *Langmuir* **2001**, *17*, 5605-5620.

6. Tan, H.; Yeung, E. S. *Electrophoresis* **1997**, *18*, 2893-2900.

7. Zhao, Z.; Malik, A.; Lee, M. L. *Anal. Chem.* **1993**, *65*, 2747-2752.

8. Zewert, T.; Harrington, M. *Electrophoresis* **1992**, *13*, 817-824.

9. Mondal, K.; Gupta, M. N.; Roy, I. *Anal. Chem.* **2006**, *78*, 3499-3504.

10. Liu, Z.; Wu, R.; Zou, H. *Electrophoresis* **2002**, *23*, 3954-3972.

11. Viklund, C.; Irgum, K. *Macromolecules* **2000**, *33*, 2539-2544.

12. Pucci, V.; Raggi, M. A.; Svec, F.; Fréchet, J. M. J. *J. Sep. Sci.* **2004**, *27*, 779-788.

13. Wieder, W.; Bisjak, C. P.; Huck, C. W.; Bakry, R.; Bonn, G. K. *J. Sep. Sci.* **2006**, *29*, 2478-2484.

14. Peters, E. C.; Petro, M.; Svec, F.; Fréchet, J. M. J. *Anal. Chem.* **1998**, *70*, 2288-2295.

15. Zakaria, P.; Hutchinson, J. P.; Avdalovic, N.; Liu, Y.; Haddad, P. R. *Anal. Chem.* **2005**, *77*, 417-423.

16. Hilder, E. F.; Svec, F.; Fréchet, J. M. J. *J. Chromatogr. A* **2004**, *1053*, 101-106.

17. Bedair, M.; El Rassi, Z. *J. Chromatogr. A* **2003**, *1013*, 35-45.

18. Bedair, M.; El Rassi, Z. *J. Chromatogr. A* **2003**, *1013*, 47-56.

19. Fu, H.; Xie, C.; Dong, J.; Huang, X.; Zou, H. *Anal. Chem.* **2004**, *76*, 4866-4874.

20. Wu, R.; Zou, H.; Fu, H.; Jin,W.; Ye, M. *Electrophoresis* **2002**, *23*, 1239-1245.

21. Gu, B.; Chen, Z.; Thulin, C. D.; Lee, M. L. *Anal. Chem.* **2006**, *78*, 3509-3518.

22. Lin, J.; Huang, G.; Lin, X.; Xie, Z. *Electrophoresis* **2008**, *29*, 4055-4065.

23. Gu, B.; Armenta, J. M.; Lee, M. L. *J. Chromatogr. A* **2005**, *1079*, 382-391.

24. Sederel, W. L.; Jong, G. J. *J. Appl. Polym. Sci.* **1973**, *17*, 2835-2846.

25. Guyot, A.; Bartholin, M. *Prog. Polym. Sci.* **1982**, *8*, 277-332.

26. Svec, F.; Fréchet, J. M. J. *Chem. Mater.* **1995**, *7*, 707-715.

27. Santora, B. P.; Gagne, M. R.; Moloy, K. G.; Radu, N. S. *Macromolecules* **2001**, *34*, 658-661.

28. Crimmins, D. L.; Gorka, J.; Thoma, R. S.; Schwartz, B. D. *J. Chromatogr.* **1988**, *443*, 63-71.

29. Gu, B.; Li, Y.; Lee, M. L. *Anal. Chem.* **2007**, *79*, 5848-5855.

30. Stadalius, A. A.; Quarry, M. A.; Snyder, L. R. *J. Chromatogr.* **1985**, *327*, 93-113.

31. Crimmins, D. L.; Thoma, R. S.; Mccourt, D. W.; Schwartz, B. D. *Anal. Biochem.* **1989**, *176*, 255-260.

32. Ueki, Y.; Umemure, T.; Li, J.; Odake, T.; Tsunoda, K. *Anal. Chem.* **2004**, *76*, 7007-7012.

33. http://www.sigmaaldrich.com/etc/medialib/docs/Fluka/Product_Information_Sheet/h2016pis. Par.0001.File.tmp/h2016pis.pdf. **2009**

34. Viklund, C.; Svec, F.; Fréchet, J. M. J. *Biotechnol. Prog.* **1997**, *13*, 597-660.

35. Staby, A.; Sand, M.; Hansen, R. G.; Jacobsen, J. H.; Andersen, L. A.; Gerstenberg, M.; Bruus, U. K.; Jensen, I. H. *J. Chromatogr. A* **2005**, *1069*, 65-77.

36. Staby, A.; Jacobsen, J. H.; Hansen, R. G.; Bruus, U. K.; Jensen, I. H. *J. Chromatogr. A* **2006**, *1118*, 168-179.

37. Lei, G.; Xiong, X.; Wei, Y.; Zheng, X.; Zhen, J. *J. Chromatogr. A* **2008**, *1187*, 197-204.

CHAPTER 3 STRONG CATION-EXCHANGE MONOLITHIC COLUMNS CONTAINING PHOSPHORIC ACID FUNCTIONAL GROUPS

3.1 Introduction

In Chapter 2, peptides and proteins were well separated using a poly(SPMA-co-PEGDA) monolithic stationary phase synthesized in a 75 µm I.D. fused-silica capillary. However, the monolith exhibited relatively high hydrophobicity, such that 20% (v/v) ACN had to be added in the aqueous mobile phase. Thus, effort was made to decrease the hydrophobicity and increase the performance of the stationary phase for the separation of proteins. In this chapter, monoliths with low hydrophobicities were designed and synthesized inside 75 µm I.D. fused-silica capillaries by photo-initiated copolymerization. Two monomers, phosphoric acid 2-hydroxyethyl methacrylate (PAHEMA) and bis[2-(methacryloyloxy)ethyl] phosphate (BMEP) (structures in Figure 3.1), were used to prepare new cation-exchange monolithic columns. The two monomers contain phosphoric acid functional groups that enable monoliths swell less in aqueous solution than monoliths containing sulfonic acid groups. Cation-exchange monoliths containing phosphoric acid groups were synthesized from PAHEMA and BMEP with selected PEG-containing co-monomers by *in situ* copolymerization. The synthesized monoliths were utilized in IEC to separate standard peptides and proteins. The effects of functional group concentration, salt gradient programming rate, and buffer pH on chromatographic performance were studied.

3.2 Experimental

3.2.1 Reagents and Chemicals

2,2-Dimethoxy-2-phenylacetophenone (DMPA, 99%), 3-(trimethoxysilyl) propyl methacrylate (TPM) (98%), uracil, poly(ethylene glycol) diacrylate (PEGDA, Mn ~ 258 and 570), poly(ethylene glycol) acrylate (PEGA, Mn ~ 375), PAHEMA, BMEP, and protein

PAHEMA
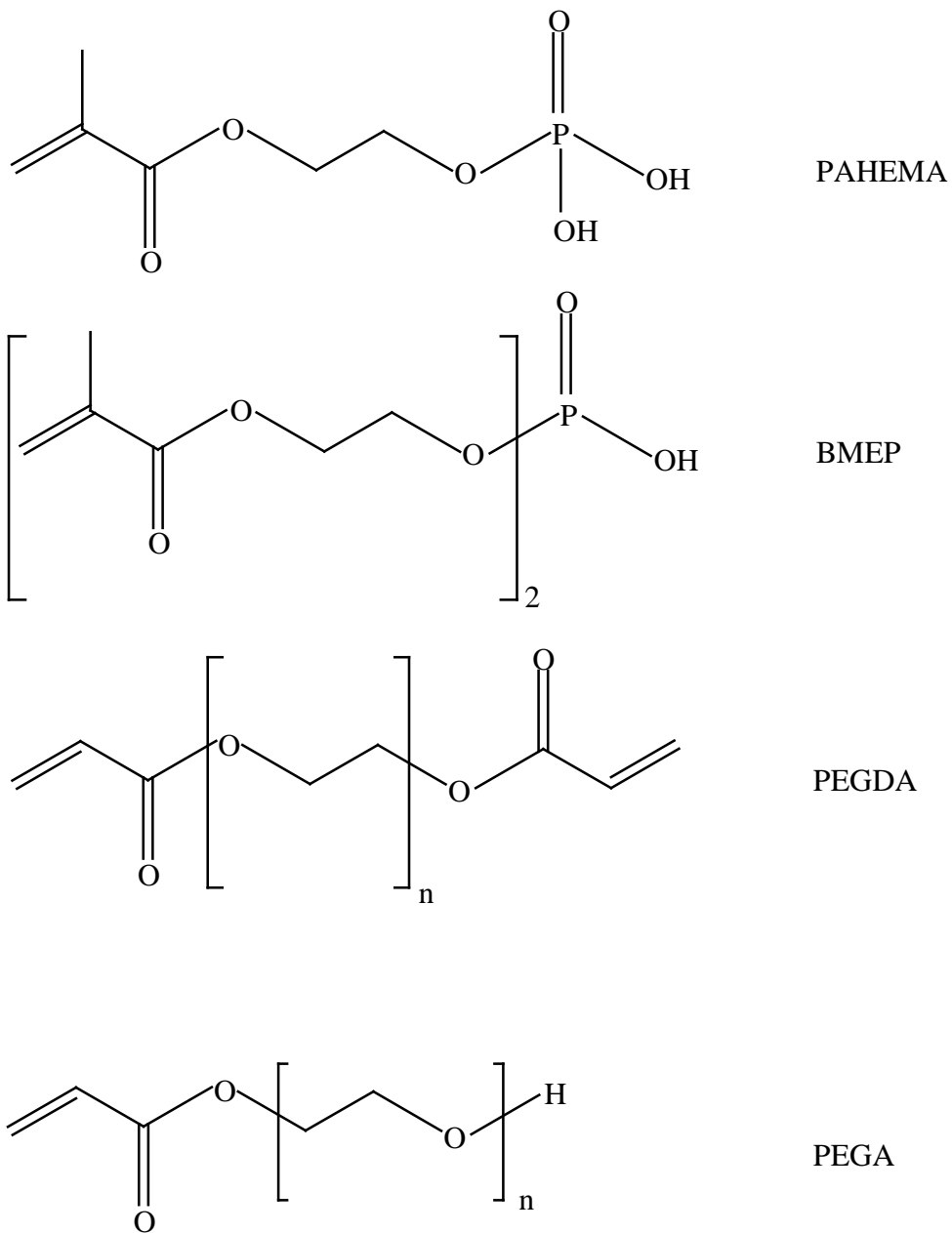
BMEP

PEGDA

PEGA

Figure 3.1. Chemical structures of PAHEMA, BMEP, PEGDA, and PEGA.

standards (i.e., trypsinogen from bovine pancrease, ribonuclease A from bovine pancrease, cytochrome C from bovine heart, α-chymotrypsinogen A from bovine pancreas, and lysozyme from chicken egg white) were purchased from Sigma-Aldrich (Milwaukee,WI). A synthetic peptide standard (CES-P0050) was obtained from Alberta Peptides Institute (Edmonton, Alberta, Canada). A natural peptide mixture (H2016) was also purchased from Sigma-Aldrich (Milwaukee, WI). Propyl paraben was purchased from Spectrum (Gardena, CA). Porogenic solvents for monolith synthesis and chemicals for mobile phase preparation were HPLC or analytical reagent grade.

3.2.2 Purification of PEGDA

Commercial PEGDA contains some impurities and inhibitors of Monomethyl Ether of Hydroquinone, which affect monolith preparation. Therefore, it was purified before use. The purification procedure was reported previously.[1,2] Briefly, PEGDA was washed with aqueous Na_2CO_3 to remove the acidic impurities and inhibitor. Then, excess water was used to remove the Na_2CO_3 residue. PEGDA was desiccated with anhydrous Na_2SO_4 after being extracted from the aqueous phase with dichloromethane. Finally, the dichloromethane solvent was removed using a rotary evaporator after filtering through 0.2 µm filter paper (Whatman, Hanover, PA).

3.2.3 Polymer Monolith Preparation

UV-transparent fused-silica capillaries (75 µm I.D. × 360 µm O.D., Polymicro Technologies, Phoenix, AZ) were first silanized with TPM to introduce pendant vinyl groups to anchor the polymer monolith to the capillary wall.[3,4] The monoliths were prepared as previously described.[5] Each polymerization mixture was prepared in a 4-mL glass vial by mixing initiator, monomer, cross-linker, and porogens (Table 3.1). The mixture was vortexed and ultrasonicated for 30 s to help form a homogeneous solution and eliminate oxygen. The monomer solution was

Table 3.1. Compositions of polymerization solutions used for the preparation of poly(PAHEMA-co-PEGDA) monoliths.

Column	Monomers		Porogens		Monomers (wt %)	Porogens (wt %)	N_{max} (plates/m)	Retention factor[a]
	PAHEMA (wt %)	PEGDA (wt %)	Methanol (wt %)	Ethyl ether (wt %)				
C1	40.0	60.0	45.0	55.0	33.3	66.7	4.05×10^3	5.35
C2	40.0	60.0	47.0	53.0	33.3	66.7	9.59×10^3	4.42
C3	40.0	60.0	48.0	52.0	33.3	66.7	2.73×10^3	4.30
C4	40.0	60.0	47.0	53.0	32.0	68.0	1.48×10^3	4.18
C5	40.0	60.0	47.0	53.0	35.0	65.0	15.6×10^3	5.41
C6	40.0	60.0	47.0	53.0	37.0	63.0	8.78×10^3	6.23
C7	30.0	70.0	47.0	53.0	35.0	65.0	High back pressure	
C8	35.0	65.0	47.0	53.0	35.0	65.0	8.75×10^3	3.36
C9	45.0	55.0	47.0	53.0	35.0	65.0	7.14×10^3	4.63
C10	50.0	50.0	47.0	53.0	35.0	65.0	2.99×10^3	3.87

[a] Retention factor of propyl paraben was measured in water

introduced into the capillary by capillary action. The capillary was placed directly under a PRX 1000-20 Exposure Unit UV lamp (TAMARACK Scientific, Corona, CA) for 3 min. A rigid monolith appeared in 1 min, indicating that polymerization was very rapid; 3-min exposure time completely converted the monomers. The resulting monolith was then flushed with methanol and water sequentially for 30 min each to remove porogens and unreacted monomers using a liquid chromatography (LC) pump. The capillaries were stored in 10% methanol aqueous solutions to prevent the monoliths from drying. Scanning electron microscopy (SEM) images of the monoliths were obtained as previously described.[5]

3.2.4 Capillary LC

Capillary LC of peptide and protein samples was performed using a system described previously.[6] The pump flow rate was 40 µL/min, which was split to provide a linear velocity of approximately 1-3 mm/s. Mobile phase A was 5 mmol/L aqueous phosphate buffer with various pH values. Mobile phase B was 1 mmol/L NaCl in mobile phase A. All mobile phases were filtered through a 0.2 µm Nylon membrane filter (Supelco, Bellefonte, PA). A Model UV3000 detector from Thermo Separations (San Jose, CA) was used at a wavelength of 214 nm. Data were acquired with ChromQuest 2.5.1 (ThermoQuest, San Jose, CA). The chromatographic conditions are given in the figure captions. For evaluation of the relative hydrophobicities of the monoliths, reversed-phase capillary LC elution measurements of propyl paraben and uracil were performed. The mobile phase was 20% aqueous acetonitrile, the pump flow rate was 30 µL/min, and the detection wavelength was 214 nm. Uracil was used as an unretained marker. The retention factor for propyl paraben was obtained from the equation, $k = (t_p - t_u)/t_u$, where k is the retention factor, and t_p and t_u are the retention times of propyl paraben and uracil, respectively.

3.2.5 Dynamic Binding Capacity (DBC) Measurements

DBC is an important property of an ion-exchange column. The DBC was examined via frontal analysis. The column was first equilibrated with buffer A at pH 6.0, and then a solution of lysozyme in buffer A was pumped through the column at a pressure of 10.34 MPa (1500 psi). The mobile phase flow rate was measured using a calibration capillary (Eksigent, Livermore, CA). The volume to saturate the column was calculated from the breakthrough curve. The DBC was measured one time for each column.

3.3 Results and Discussion

3.3.1 Polymer Monolith Preparation

PAHEMA and BMEP were selected as monomers to prepare cation-exchange monoliths because monoliths containing phosphoric acid groups would show less swelling/shrinking in aqueous buffer compared to sulfonic acid containing monoliths. PEGDA, which has an acrylate group at each end of the molecule and a three-unit ethylene glycol connecting chain, has been shown to be a biocompatible cross-linker.[5-9] The proper selection of porogens is important in the preparation of monoliths, because the porogens determine the resultant pore sizes and structures. For PEG monoliths, methanol is a common solvent, which offers good solubility. Therefore, methanol was chosen as the initial porogen solvent to prepare a poly(PAHEMA-co-PEGDA) monolith. With methanol as the only porogen, a white translucent gel structure was observed, which indicated that small pores occupied most of the column volume and confirmed that methanol was a small pore forming solvent. In order to increase the pore size, addition of a large pore forming solvent was required. Long chain aliphatic alcohols have been shown to function well as large pore forming solvents.[10] Therefore, decanol was selected as a second porogen. With an increase in weight percentage of decanol to total porogens from 40 to 60%, the back pressure

of the monolith decreased from 102 psi/cm to 17 psi/cm for a methanol flow rate of 0.2 µL/min. Unfortunately, the resulting monoliths were not macroscopically uniform. Therefore, decanol was replaced by ethyl ether, a non-polar large pore forming solvent. When 50.0 wt% ethyl ether was used, a high back pressure of 165 psi/cm was observed for a methanol flow rate of 0.2 µL/min, which reduced to 6.1 psi/cm when using 55 wt% ethyl ether and to 4.4 psi/cm when using 60.0 wt% ethyl ether. Finally, methanol and ethyl ether were chosen as porogen solvents for the poly(PAHEMA-co-PEGDA) monoliths.

Many factors, including monomer composition and properties, porogen composition and properties, and ratio of monomers to porogens affect the homogeneity of a monolith. In order to investigate the influence of porogen composition on the preparation of poly(PAHEMA-co-PEGDA) monoliths, the weight ratio of monomers to porogens (1:2) and the weight ratio of PAHEMA to PEGDA (1:2) were kept constant, while the porogenic solvent composition was varied (monoliths C1-C3 in Table 3.1). With an increase in ethyl ether in the porogen mixture, the back pressure decreased, confirming that ethyl ether was a macro-pore forming solvent. When the ethyl ether weight percentage in the porogen mixture decreased from 55.0 wt% to 53.0 wt%, the highest column efficiency of ~ 9590 plates/m among monoliths C1-C3 was obtained [column efficiency was measured using uracil in buffer A at pH 6.0 and a pressure of 10.34 MPa (1500 psi)]. A further decrease in ethyl ether to 52.0 wt% led to a dramatic decrease in efficiency to 2700 plates/m (Table 3.1). Obviously, the porogen composition and concentration of each component have a great effect on the morphology of the resulting monolith, including pore size, pore volume, and homogeneity. The morphology of C2 produced the best efficiency among monoliths C1-C3. The retention factors of propyl paraben on monoliths C1-C3 varied slightly.

The porogen composition of 47.0 wt% methanol and 53.0 wt% ethyl ether was selected for further optimization (monolith C2 in Table 3.1).

The influence of porogen concentration on the preparation of poly(PAHEMA-co-PEGDA) monoliths was investigated by keeping the weight ratios of PAHEMA to PEGDA (40:60) and methanol to ethyl ether (47:53) constant, while the porogen weight percent was varied from 68.0% (monolith C4, Table 3.1) to 63% (monolith C6). With a decrease in porogen weight percent from 68.0% (monolith C4) to 65.0% (monolith C5), the column efficiency increased dramatically to 15,600 plates/m, and the retention factor increased (Table 3.1). A further decrease in porogen weight fraction led to a decrease in column efficiency. Thus, a ratio of 35:65 of monomers to porogens (monolith C5) was selected for further optimization.

Monomer and cross-linker play important roles in monolith preparation. They have significant effects not only on the rigidity, polarity and porosity of the resulting monolith, but also on the composition of the monolith. To investigate the influence of cross-linker concentration, four additional monolithic columns (monoliths C7-C10) were prepared with various PEGDA weight percentages (from 50.0 to 70.0%), while the weight ratio of monomers to porogens (35:65) and the weight ratio of methanol to ethyl ether (47:53) were kept constant. With an increase in monomer or decrease in cross-linker, the column efficiency decreased, while the retention factor increased. When the monomer concentration was 30.0 wt%, methanol could not flow through the column at a pressure of 13.8 MPa (2000 psi). Based on efficiency measurements, monolith C5, which was composed of 35.0 wt% monomers (PAHEMA/PEGDA, 40:60, w/w) and 65.0 wt% porogens (methanol/ethyl ether, 47:53, w/w), was selected for further experiments. A porosity of 81.4% for monolith C5 was obtained using uracil as dead volume marker in buffer A.

Table 3.2. Compositions and physical properties of BMEP monoliths.

Column	Monomers				Porogens			Monomers (wt %)	Porogens (wt %)	Porosity (%)	Retention factor	DBC (mg/mL)
	BMEP (wt %)	PEGA (wt %) (375)[a]	PEGDA (wt %) (258)[a]	PEGDA (wt %) (570)[a]	Methanol (wt %)	Decanol (wt %)	Ethyl ether (wt %)					
M1	30.0	70.0			28.6	57.1	14.3	38.6	61.4	84.4	0.0872	269
M2	35.0	65.0			28.6	57.1	14.3	38.6	61.4	80.2	0.111	199
M3	40.0	60.0			28.6	57.1	14.3	38.6	61.4	78.3	0.127	85.1
M4	54.5	45.5			28.6	57.1	14.3	38.6	61.4	73.6	0.130	44.3
M5	70.0	30.0			28.6	57.1	14.3	38.6	61.4	68.4	0.131	28.3
M6	40.0		60.0		28.6	57.1	14.3	38.6	61.4	62.6	0.339	15.2
M7	40.0			60.0	28.6	57.1	14.3	38.6	61.4	75.2	0.719	17.5

[a] average molecular weight

Using the same strategy as described for preparing poly(PAHEMA-co-PEGDA) monoliths, several poly(BMEP-co-PEGA) monoliths were prepared with weight percentages of BMEP from 30.0 to 70.0% in the monomer mixture (Table 3.2). With a BMEP weight percentage lower than 30.0%, the resultant monolith was not rigid, and when higher than 70.0%, the back pressure was very high. For comparison, the same porogens were used to synthesize poly(BMEP-co-PEGDA) monoliths (Table 3.2).

SEM provides direct images of the PAHEMA and BMEP monoliths (Figure 3.2). These monoliths are uniform and firmly bonded to the capillary wall. Spherical units are aggregated into large clusters in poly(PAHEMA-co-PEGDA) monoliths (Figure 3.2B). Conventional polymer monolithic morphology with discrete microglobules and a few fused microglobules are observed in Figure 3.2D. The through pores of the monoliths are obvious. In Figure 3.2F, spherical units are aggregated into larger clusters.

3.3.2 Stability of PAHEMA and BMEP Monoliths

All of the PAHEMA and BMEP monoliths were synthesized in 75 µm I.D. fused-silica capillaries. Column pressure drops were measured using different solvents [i.e., water, methanol, and acetonitrile (ACN)] to evaluate the mechanical stabilities of the synthesized monoliths. A linear dependence of flow rate on column back pressure was observed (data not shown), indicating that these monoliths were not compressed at least up to 3 mm/s (back pressure < 1500 psi).

Permeability measurements can be used to study the swelling and shrinking of a monolith. If a monolith swells, its through pores decrease in size, resulting in lower permeability, and vice versa. The permeability was calculated using Darcy's law, $K = \eta u L/\Delta P$, where η is the
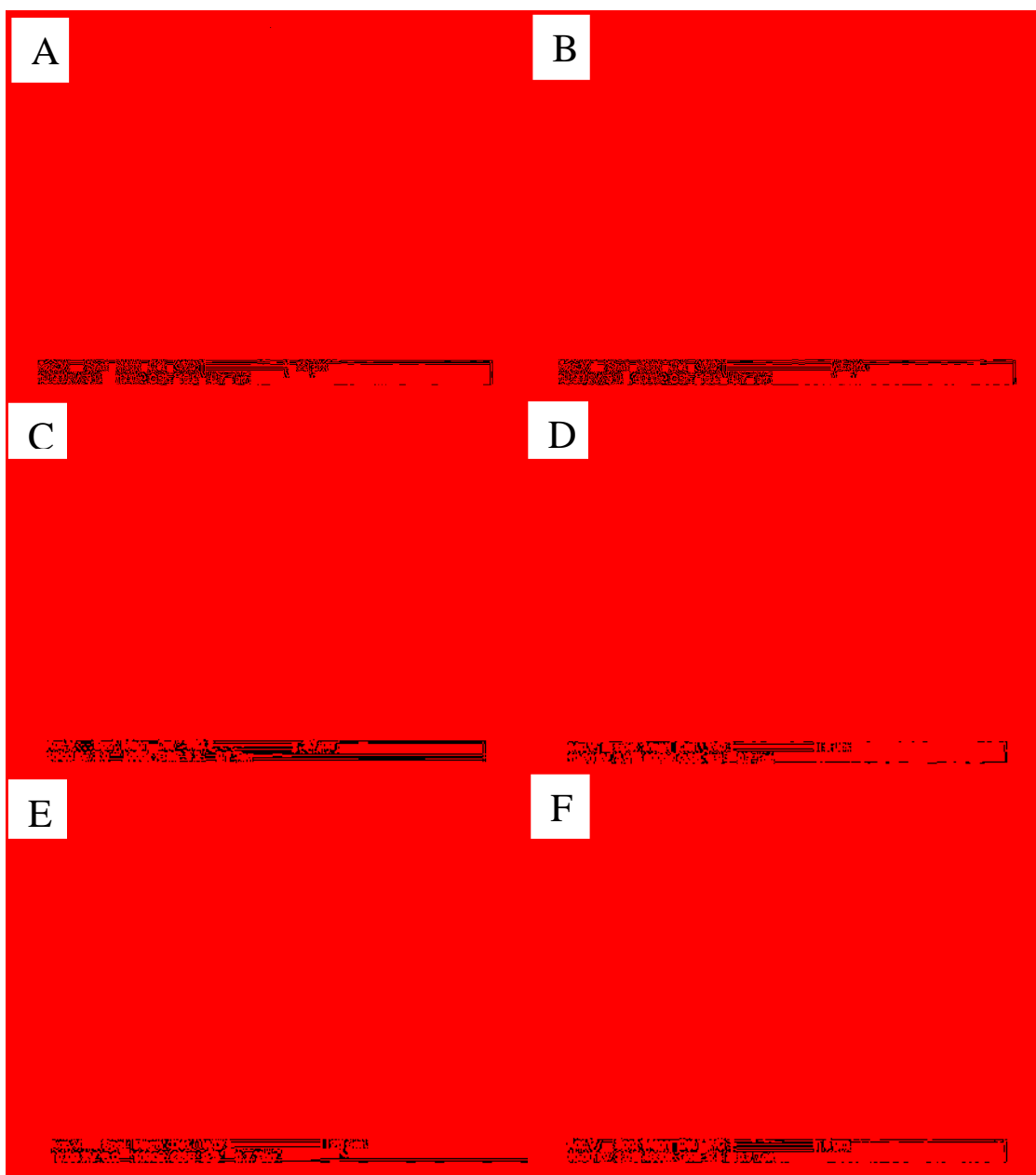
Figure 3.2. Scanning electron micrographs of (A) poly(PAHEMA-co-PEGDA monolith (scale bar, 20 µm), (B) poly(PAHEMA-co-PEGDA) monolith (scale bar, 5 µm), (C) poly(BMEP-co-PEGA) monolith (M3) (scale bar, 20 µm), (D) poly(BMEP-co-PEGA) monolith (M3) (scale bar, 5 µm), (E) poly(BMEP-co-PEGDA) monolith (M6) (scale bar, 20 µm), and (F) poly(BMEP-co-PEGDA) monolith (M6) (scale bar, 5 µm).

dynamic viscosity of the mobile phase, L is the column length, u is the linear velocity of the mobile phase, and ΔP is the column pressure drop. As seen in Table 3.3, the permeability of the poly(PAHEMA-co-PEGDA) monolith was 2.5 times higher in methanol and 3.8 times higher in ACN than in water. These results indicate that the PAHEMA monoliths swelled in aqueous solution. However, they swelled less than previously reported sulfonic acid cation-exchange monoliths.[5,6] During tests with different solvents, no detachment of the monolith from the capillary wall was observed. The solvent flow rate reached a constant value rapidly, indicating that swelling and shrinking was reversible.[5] The permeability of poly(BMEP-co-PEGA) monolith M3 was 1.38 and 1.82 times higher in water than in methanol and ACN, respectively. The monolith showed slight swelling in methanol and ACN, which is in contrast to shrinking of sulfonic acid monoliths in the same solvents.[5,6] With increasing concentration of BMEP in the monoliths, the permeabilities decreased (M1-M5), which was most likely due to the reduced porosity. The permeability of M3 was 1.48 times higher than that of M6. Since M6 was synthesized from BMEP and PEGDA, it was highly cross-linked, which led to low porosity and low permeability.

The poly(PAHEMA-co-PEGDA) monoliths gave higher retention factors than the poly(BMEP-co-PEGA) monoliths. It is worth pointing out that retention factors of propyl paraben on the PAHEMA monoliths were less than those for poly(AMPS-co-PEGDA), poly[sulfoethyl methacrylate (SEMA)-co-PEGDA], and poly[vinylsulfonic acid (VS)-co-PEGDA] monoliths synthesized previously.[3,5] The low retention factors may be due to the biocompatible structure of PAHEMA in addition to the cross-linkers. With increasing content of BMEP in the monoliths (M1-M5), retention factors increased, which demonstrated that BMEP was less hydrophilic than PEGA. Comparing the retention factors of M3, M6, and M7, It was

Table 3.3. Permeabilities, capacity factors and DBC values for monoliths in this study.

Column	Mobile phase	Relative polarity[a]	Viscosity η (cP)[b]	Permeability K ($\times 10^{-15}$ m^2)	Retention factor	DBC (mg/mL)
PAHEMA-PEGDA monolith (9.0 cm $\times$ 75 µm I.D.)	Water	1.00	0.890	20.5		
	Methanol	0.762	0.544	51.2	0.150	31.2
	Acetonitrile	0.460	0.369	78.8		
BMEP-PEGA monolith M3 (7.2 cm $\times$ 75 µm I.D.)	Water	1.00	0.890	28.7		
	Methanol	0.762	0.544	20.8	0.127	85.1
	Acetonitrile	0.460	0.369	15.8		
BMEP-PEGA monolith M1 (7.2 cm $\times$ 75 µm I.D.)	Water	1.00	0.890	42.1	0.0872	269
BMEP-PEGA monolith M2 (7.2 cm $\times$ 75 µm I.D.)	Water	1.00	0.890	31.4	0.111	199
BMEP-PEGA monolith M4 (7.2 cm $\times$ 75 µm I.D.)	Water	1.00	0.890	11.2	0.130	44.3
BMEP-PEGA monolith M5 (7.2 cm $\times$ 75 µm I.D.)	Water	1.00	0.890	6.87	0.131	28.3
BMEP-PEGDA monolith M6 (7.2 cm $\times$ 75 µm I.D.)	Water	1.00	0.890	19.4	0.339	15.2

[a] Relative polarity data were from http://virtual.yosemite.cc.ca.us/smurov/orgsoltab.htm. [b] Viscosity data were from online CRC Handbook of Chemistry and Physics, 85th ed.; CRC: Boca Raton, FL, 2004-2005.

concluded that PEGA is more hydrophilic than PEGDA (Mn 285), which is more hydrophilic than PEGDA (Mn 570). The retention factor of propyl paraben on poly(BMEP-co-PEGDA) monolith M6 was much higher than for the poly(PAHEMA-co-PEGDA) monolith with the same concentration of PEGDA in the monomers, indicating higher hydrophobicity for the poly(BMEP-co-PEGDA) monolith. The hydrophobicity may come primarily from the BMEP monomer because it contains two 2-carbon linkages, while PAHEMA contains only one 2-carbon linkage (see structures of BMEP and PAHEMA, Figure 3.1).

3.3.3 DBC of PAHEMA and BMEP Monoliths

DBC is an important property of ion-exchange columns, which affects column resolution and loadability. Using frontal analysis, the DBC was measured as reported previously.[6] Since the columns were designed for ion exchange chromatography of large biomolecules, lysozyme was used to measure the DBC of the columns. Obviously, the DBC values measured using proteins would be less than measured using small peptides, since part of the surface area of the monolith is not accessible to proteins. Using a 1.00 mg/mL lysozyme solution, a DBC of 31.2 mg/mL of column volume was measured for the poly(PAHEMA-co-PEGDA) monolith. The DBC value is approximately equal to, or higher than, various synthesized and commercial columns.[11,12] By comparing theoretical binding capacities of 447 µequiv/mL for the poly(PAHEMA-co-PEGDA) monolith, only 0.49 wt% of the PAHEMA in the monolith was accessible for ionic interaction with proteins. Most of phosphoric acid functional groups were buried in the monolith structure and not available at the surface for interaction. The sharp frontal analysis curves indicated rapid adsorption of lysozyme on these monoliths. Only one plateau was observed in the frontal analysis curves, indicating a strong cation-exchange mechanism.

A 3.00 mg/mL lysozyme solution was used to determine the DBC of the BMEP monolithic columns. Using frontal analysis, the DBC values were measured to be 268, 199, 85.1, 44.3, 28.3, 15.2, and 17.5 mg/mL column volume for monoliths M1-M7, respectively. The DBC values for column M1 showed good batch-to-batch reproducibility (3 batches) with a relative standard deviation (RSD) of 5.6%. Interestingly, with increases in concentration of BMEP, the DBC values decreased. Two factors may explain the decrease in DBC values. First, the porosity of the monolith decreased with an increase in BMEP. It was reported that a higher proportion of cross-linker in the monomer mixture led to a decrease in the average pore size.[13] Reduced porosity may cause lower surface area and fewer interacting sites, which would result in reduced DBC. The second reason is related to the accessibility of the phosphoric acid groups for interaction. Since a higher DBC was measured for the poly(BMEP-co-PEGDA) (Mn 570) monolith than for the poly(BMEP-co-PEGDA) (Mn 258) monolith, the rigidity of the structure could inhibit solute interaction with the functional groups. Obviously, the DBC value cannot be increased solely by increasing the concentration of functional monomer.

3.4 Chromatographic Performance

3.4.1 Ion-exchange Separation of Synthetic Peptides

The performances of the PAHEMA and BMEP monoliths were investigated by IEC separation of undecapeptides, as recommended by Mant and Hodges[14] to evaluate particle-based ion-exchange columns in the salt gradient mode. Peptide mixture CES P0050 contains four peptides having the same chain length and no acidic residues, which causes them to exhibit the same charge in acidic, neutral, and even basic buffers. Their structures and properties were described previously.[14]

Figure 3.3 shows typical elution profiles of the four undecapeptides using the PAHEMA and BMEP monolithic columns. Four peaks were eluted without ACN in the mobile phase within 15 min with good peak shapes, demonstrating the low hydrophobicities of the PAHEMA and BMEP monoliths. In Figure 3.3, the BMEP-PEGA monolith showed better peak profiles compared to the poly(PAHEMA-co-PEGDA) monolith, most likely due to a higher DBC value and lower column hydrophobicity.

The effect of BMEP concentration in the monoliths on the separation of peptides was investigated. As seen, retention decreased with an increase in BMEP concentration (Table 3.4). This trend was not followed for column M5 due to its lower permeability. Furthermore, the peptides were retained less than expected on M1 because M1 had high permeability and low hydrophobicity. Good separation of peptides was achieved with excellent peak profiles without addition of ACN in the mobile phase. The synthetic peptides were eluted as sharp peaks with average peak widths of 0.53, 0.38, 0.42, 0.43, and 0.56 min, respectively, for columns M1-M5. According to the definition of peak capacity in gradient elution (i.e., peak capacity = gradient time/peak width),[15] the peak capacities were calculated to be 19, 26, 24, 23, and 18, respectively, for columns M1-M5. Column M2 provided the best separation for peptides, although the DBC value for M2 was lower than for M1. This is a result of the less homogeneous morphology of M1 due to a lower amount of BMEP in the monolith. Obviously, BMEP monolith M2 provided better separation of peptides than PAHEMA monoliths. A higher DBC value, homogeneous morphology, and lower hydrophobicity of M2 contributed to its better performance.
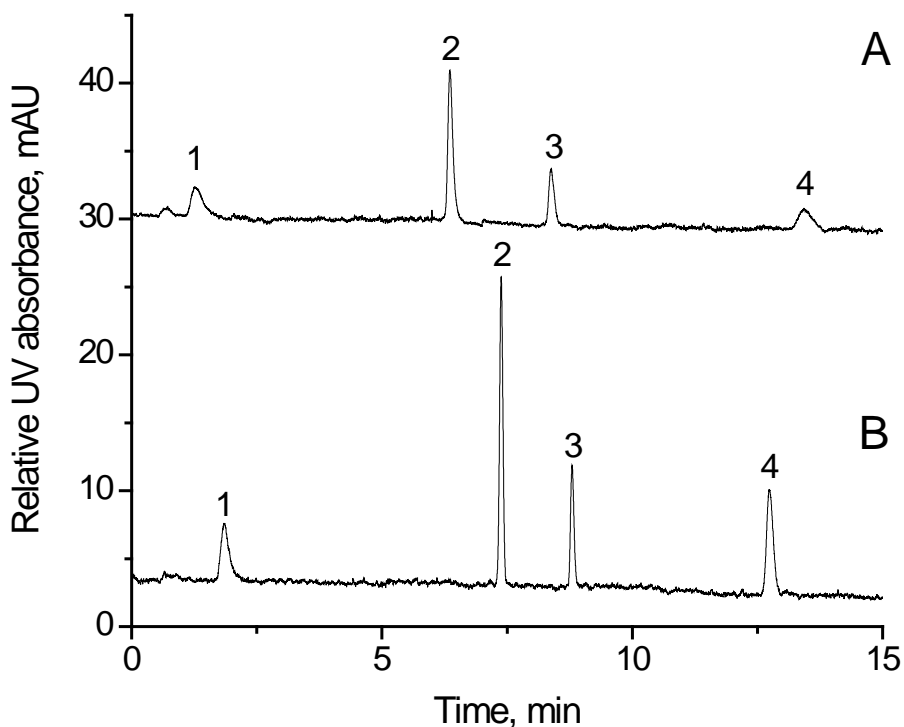
Figure 3.3. Separations of synthetic peptides. Conditions: (A) 8.7 cm × 75 µm I.D. poly(PAHEMA-co-PEGDA) monolith, and (B) 9.0 cm × 75 µm I.D. poly(BMEP-co-PEGA) monolith M3; buffer A was 5 mmol/L phosphate at pH 8.0 (A) and 6.0 (B), buffer B was 1 mol/L NaCl in buffer A; linear gradient from 100% A to 100% B in 10 min, followed by 100% B; 40 µL/min pump flow rate; on-line UV detection at 214 nm. Peak identifications: (1) Ac-Gly-Gly-Gly-Leu-Gly-Gly-Ala-Gly-Gly-Leu-Lys-amide, (2) Ac-Lys-Tyr-Gly-Leu-Gly-Gly-Ala-Gly-Gly-Leu-Lys-amide, (3)Ac-Gly-Gly-Ala-Leu-Lys-Ala-Leu-Lys-Gly-Leu-Lys-amide, and (4) Ac-Lys-Tyr-Ala-Leu-Lys-Ala-Leu-Lys-Gly-Leu-Lys-amide.

Table 3.4. Effect of BMEP concentration on the separation of peptides.[a]

Column	Length (cm)	Peak 1		Peak 2		Peak 3		Peak 4		Peak capacity[d]
		t_R[b]	w_d[c]	t_R	w_d	t_R	w_d	t_R	w_d	
M1	9.0	3.04	0.69	10.5	0.34	11.8	0.38	16.4	0.66	19 ± 6.8
M2	9.0	3.05	0.38	8.60	0.30	9.85	0.38	13.9	0.45	26 ± 4.3
M3	9.0	1.84	0.61	7.38	0.35	8.80	0.29	12.7	0.42	24 ± 8.0
M4	10	1.32	0.48	5.55	0.33	7.13	0.29	11.0	0.63	23 ± 8.3
M5	9.0	1.85	0.57	5.83	0.35	7.93	0.48	12.5	0.76	18 ± 5.9

[a] Conditions: 100% A to 100% B in 10 min, followed by 100% B, where A was 5 mmol/L phosphate buffer at pH 6.0 and B was 1 mol/L NaCl in A, 40 µL/min pump flow rate, on-line detection at 214 nm. [b] retention time in min. [c] peak width in min. [d] calculated from gradient time/peak width. Peaks 1-4 represent Ac-Gly-Gly-Gly-Leu-Gly-Gly-Ala-Gly-Gly-Leu-Lys-amide, Ac-Lys-Tyr-Gly-Leu-Gly-Gly-Ala-Gly-Gly-Leu-Lys-amide, Ac-Gly-Gly-Ala-Leu-Lys-Ala-Leu-Lys-Gly-Leu-Lys-amide, and Ac-Lys-Tyr-Ala-Leu-Lys-Ala-Leu-Lys-Gly-Leu-Lys-amide, respectively.

The pH of the mobile phase has an important effect on the separation of peptides and proteins in the ion-exchange mode by determining the extent of ionization of the ion-exchange functional groups and the analytes. Since phosphoric acid is a medium acid, pH has a negligible effect on its ionization. The standard peptides were all undecapeptides that do not have any acidic residues, so they have the same charge in acidic to neutral buffers. Thus, in theory, pH should have no appreciable effect on the separation of the peptides. The pH effect on separation of synthetic peptides using PAHEMA monoliths was investigated using salt gradient elution (Table 3.5). The peak capacity varied slightly from pH 6.0 to 9.0 for the PAHEMA monolith (Table 3.5). The retention times and peak capacities varied slightly at pH 3.0 compared to pH 6.0. This pH effect was reported earlier.[5,6] Hodges[14] explained that these effects were due to a reduction in the column capacity to retain charged species as the pH became more acidic, which is not desirable. The slight differences in peak capacities at different pH values demonstrated that the poly(PAHEMA-co-PEGDA) monolith was stable.

Since a poly(BMEP-co-PEGA) M3 monolith demonstrated high efficiency in peptide and protein separations, it was selected to study the effect of pH on BMEP monolith chromatographic performance. Retention times at pH 6.0 (Figure 3.4B) were less than at pH 3.0 (Figure 3.4A) with peak capacity values increasing slightly from 24 to 25. This is in contrast to sulfonic acid ion-exchange monolithic columns[5,6] and the PAHEMA monoliths, for which the retention times of peptides decreased with a decrease in buffer pH. The increase in retention was caused by an increase in column capacity to further retain the charged species when the pH became more acidic.[14] When the mobile phase pH increased from 6.0 to 8.0 (Figures 3.4B and C), the retention times and peak capacities varied only slightly. Compared to sulfonic acid ion-exchange monolithic columns, the poly(BMEP-co-PEGA) monoliths were less affected by buffer

Table 3.5. Effect of pH on the separation of synthetic peptides.[a]

pH	Peak 1		Peak 2		Peak 3		Peak 4		Peak capacity[d]
	t_R[b]	w_d[c]	t_R	w_d	t_R	w_d	t_R	w_d	
3.0	1.80	0.35	7.30	0.47	9.46	0.36	16.7	0.79	20 ± 8.5
6.0	1.59	0.36	8.51	0.46	11.3	0.47	20.4	0.78	19 ± 6.8
7.0	1.75	0.56	6.91	0.45	8.57	0.38	18.2	0.70	19 ± 5.1
8.0	1.38	0.72	6.68	0.42	8.50	0.36	13.5	0.61	19 ± 6.0
9.0	1.26	0.56	6.35	0.59	8.38	0.35	13.4	0.66	18 ± 4.6

[a] Conditions: 8.7 cm × 75 µm I.D. poly(PAHEMA-co-PEGDA) monolith, 100% A to 100% B in 10 min, followed by 100% B, where A was 5 mmol/L phosphate buffer and B was 1 mol/L NaCl in A, 40 µL/min pump flow rate, on-line detection at 214 nm. [b] retention time in min. [c] peak width in min. [d] calculated from gradient time/peak width. Peaks 1-4 are as listed in Table 3.4.
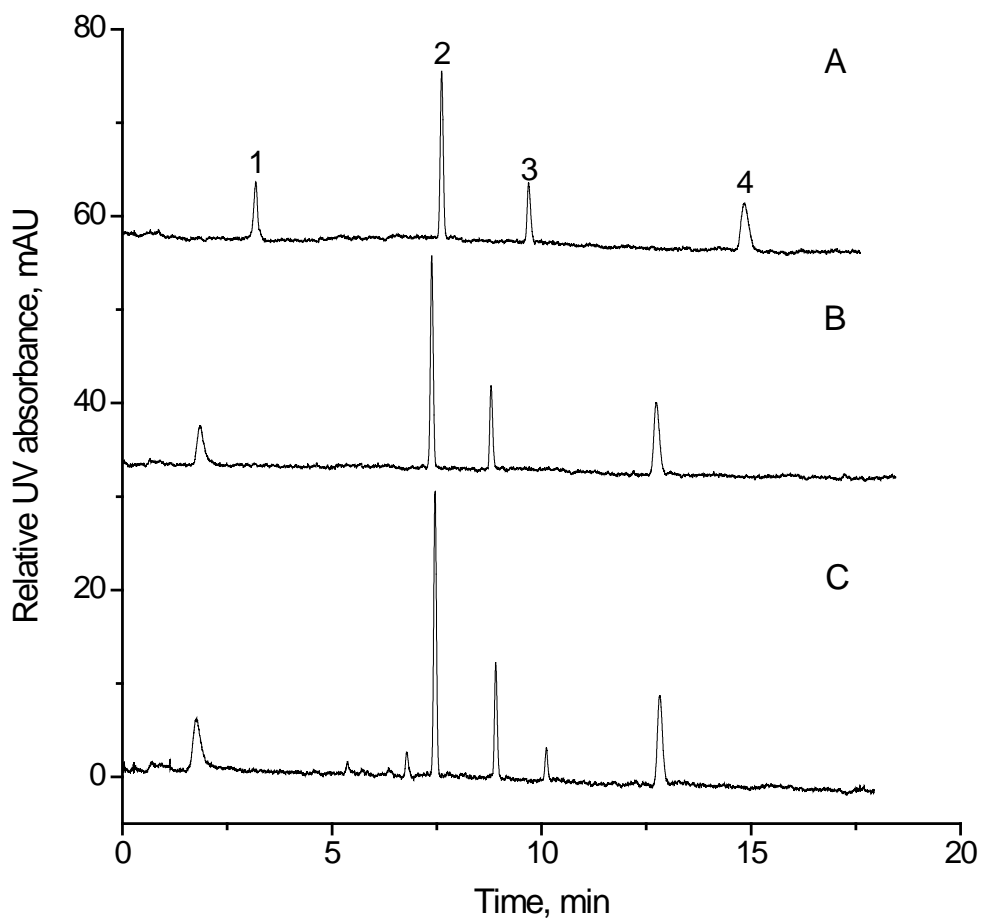
Figure 3.4. Separations of synthetic peptides at different pH values. Conditions: poly(BMEP-co-PEGA) M3 monolith (9.0 cm × 75 µm I.D.); other conditions are the same as in Figure 3.3B, except that buffers A and B were adjusted to (A) pH 3.0, (B) 6.0, and (C) 8.0. Peak identifications are the same as in Figure 3.3.

pH. Poly(BMEP-co-PEGA) monolithic columns showed good run-to-run reproducibility. For three consecutive runs using column M3 (conditions as in Figure 3.3B), the RSD of retention times for peptides 1-4 were 1.02, 0.68, 0.59, and 0.87%, respectively. The low RSD values indicate that shrinkage that occurred in the aqueous buffer solutions was reversible.

Since the PAHEMA monoliths showed higher hydrophobicity than the BMEP monoliths, effect of ACN concentration in the mobile phase on the separation of synthetic peptides using the PAHEMA monolith was investigated. Table 3.6 provides elution data for the four synthetic peptides as a result of variation in ACN concentration. Peptide 4, which is the most hydrophobic among the four peptides, was eluted from both monoliths in 20 min without ACN. With 10% (v/v) ACN in the mobile phase, hydrophobic interactions were partially suppressed in the poly(PAHEMA-co-PEGDA) monolith. A further increase of ACN to 20% narrowed the peak for peptide 4 slightly more. The peak capacity increased 25% (from 20 to 25) with the addition of 20% ACN. For three consecutive runs using the same conditions as specified in Table 3.6 with 20% (v/v) ACN in the mobile phase, the RSD of retention times for peptides 1-4 were 1.22, 1.92, 1.99 and 1.93%, respectively, for the poly(PAHEMA-co-PEGDA) monolith. These data indicate that good reproducibility was achieved after column equilibration with starting buffer, despite swelling of the monoliths in aqueous buffer.

3.4.2 Ion-exchange Separation of Natural Peptides

Separation of a natural peptide mixture (H2016) was achieved using the PAHEMA monoliths, while no separation was observed using BMEP monoliths. The structures and characteristics of these natural peptides were described previously.[6] As seen in Figure 3.5, five peaks were separated with 20% (v/v) ACN in the mobile phase. It was noticed that with the addition of ACN in the mobile phase, better peak shapes and narrower peak widths were

observed. With an increase of ACN from 0 to 20% in the mobile phase, the peak capacity was increased from 13 to 16 for the poly(PAHEMA-co-PEGDA) monolith.

Accepted resolution of methionine enkephalin (peak 1 in Figure 3.5) and leucine enkephalin (peak 2 in Figure 3.5) was obtained. Methionine enkephalin (Mw 573) and leucine enkephalin (Mw 555) have the same charge and chain length, and similar molecular weights and hydrophobicities. Ionic interaction is less for methionine enkephalin than for leucine enkephalin, due to its greater molecular weight, thus, leading to earlier elution. Resolution between methionine enkephalin and leucine enkephalin was 1.10, 1.28, and 0.84 using the poly(PAHEMA-co-PEGDA) monolith with 0, 10, and 20% ACN concentrations, respectively, in the mobile phase. Comparing the resolution with and without ACN in the mobile phase, it is clear that hydrophobic interactions also contributed to the separation of methionine enkephalin and leucine enkephalin. Although somewhat hydrophobic, the monolith provides better resolution of methionine enkephalin and leucine enkephalin than the poly(AMPS-co-PEGDA) monolith.[5]

3.4.3 Ion-exchange Separation of Proteins

The PAHEMA monoliths were also evaluated for the separation of a mixture of trypsinogen, ribonuclease A, α-chymotrypsinogen A, cytochrome C, and lysozyme (Figure 3.6). Column-to-column reproducibility measurements of a poly(PAHEMA-co-PEGDA) monolith gave retention RSD values (n = 3) of 2.49%, 3.66%, 2.36%, 2.71%, and 2.42% for trypsinogen, ribonuclease A, α-chymotrypsinogen A, cytochrome C, and lysozyme, respectively. These data demonstrate that good column-to-column reproducibility was achieved. Separations of proteins were also performed using a poly(PAHEMA-co-PEGDA) monolith under isocratic conditions with various

Table 3.6. Effect of ACN on the separation of synthetic peptides.[a]

ACN (%, v/v)	Peak 1		Peak 2		Peak 3		Peak 4		Peak capacity[d]
	t_R[b]	w_d[c]	t_R	w_d	t_R	w_d	t_R	w_d	
0	1.80	0.35	7.30	0.47	9.46	0.36	16.7	0.79	20 ± 8.5
10	1.22	0.40	4.14	0.36	6.01	0.41	9.40	0.66	22 ± 6.5
20	0.859	0.37	3.65	0.39	4.73	0.39	8.33	0.45	25 ± 2.2

[a] Conditions: 8.7 cm $\times$ 75 µm I.D. poly(PAHEMA-co-PEGDA) monolith, 100% A to 100% B in 10 min, followed by 100% B, where A was 5 mmol/L phosphate buffer at pH 3.0 and B was 1 mol/L NaCl in A, both buffers containing 0, 10, and 20% (v/v) ACN, 40 µL/min pump flow rate, on-line detection at 214 nm. [b] retention time in min. [c] peak width in min. [d] calculated from gradient time/peak width. Peaks 1-4 represent are as listed in Table 3.4.
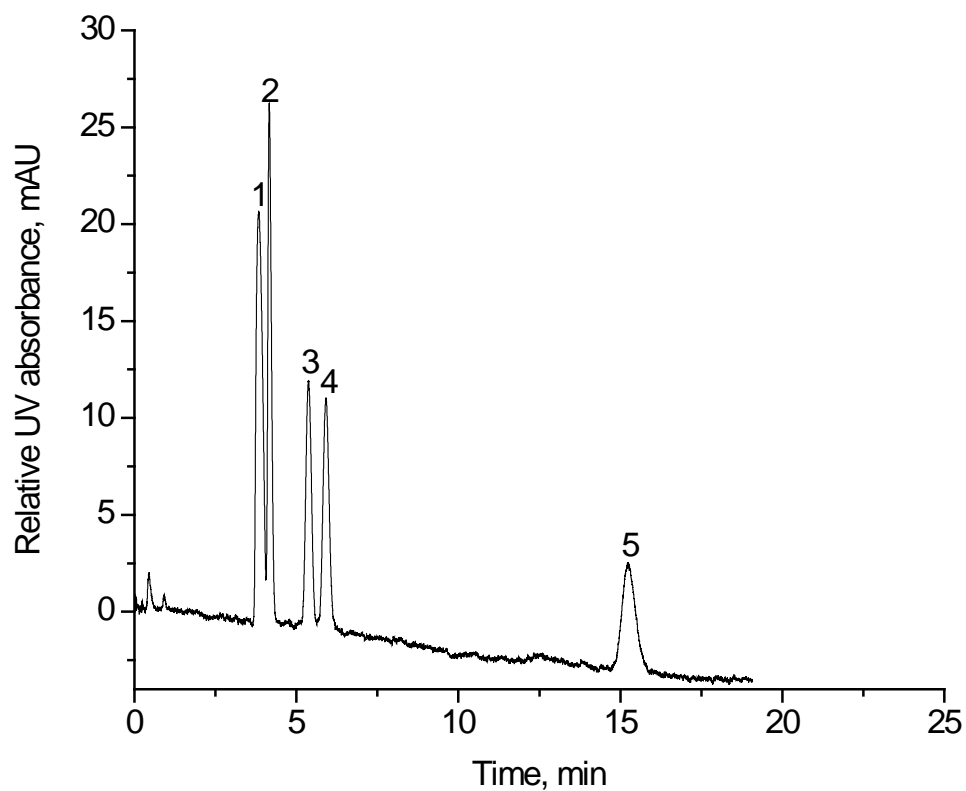
Figure 3.5. Separation of natural peptides. Conditions: 8.7 cm × 75 µm I.D. poly(PAHEMA-co-PEGDA) monolith; buffer A was 5 mmol/L phosphate at pH 3.0, buffer B was 1 mol/L NaCl in buffer A, both buffers containing 20% (v/v) ACN; linear gradient from 100% A to 100% B in 10 min, followed by 100% B; 40 µL/min pump flow rate; on-line UV detection at 214 nm. Peak identifications: (1) methionine enkephalin, (2) leucine enkephalin, (3) Val-Tyr-Val, (4) Gly-Tyr, and (5) angiotensin II.

buffer salt concentrations. The linear retention behavior confirmed that the retention was governed by cation-exchange (Figure 3.7).

Poly(BMEP-co-PEGA) monoliths M1-M5 were used to separate a protein mixture containing ribonuclease A, α-chymotrypsinogen A, cytochrome C, and lysozyme. Sharp peaks were obtained with average peak widths of 0.49, 0.53, 0.37, 0.48, and 0.48 min for columns M1-M5, respectively, resulting in corresponding peak capacities of 20, 19, 27, 21, and 21 (Table 3.7). Column M3 provided the highest efficiency for protein separation, which is ascribed to its high DBC value and homogeneous morphology. The measured peak capacities are comparable or superior to other reported polymer monolithic cation- exchange columns.[16-18] The resolution values for α-chymotrypsinogen A and cytochrome C were determined to be 1.14, 1.25, 0.97, 1.29, and 0.74 for columns M1-M5, respectively. The superior resolution obtained using column 4 was due to the longer M4 column.

The run-to-run reproducibility of the poly(BMEP-co-PEGA) monolithic column was good. For three consecutive runs using column M3 (conditions as in Figure 4B), the RSD values of retention times for proteins 1-4 were 0.90, 0.85, 1.12, and 1.45%, respectively.

Buffer pH has a major effect on the separation of proteins because it determines the extent of ionization of both ion exchanger and analytes. Since PAHEMA and BMEP are strong cation-exchangers, pH has a negligible effect on the ionization of the ion exchanger. However, pH significantly affects the ionization of proteins. Table 3.8 shows the effects of pH on retention time, peak capacity, and resolution between α-chymotrypsinogen A and cytochrome C using the poly(PAHEMA-co-PEGDA) monolith. With an increase in pH, the retention time of each protein decreased. Ribonuclease A eluted before α-chymotrypsinogen A and cytochrome C when the pH was 7.0 or higher, while it eluted later at pH 6.0. The peak capacity varied slightly from pH 6.0
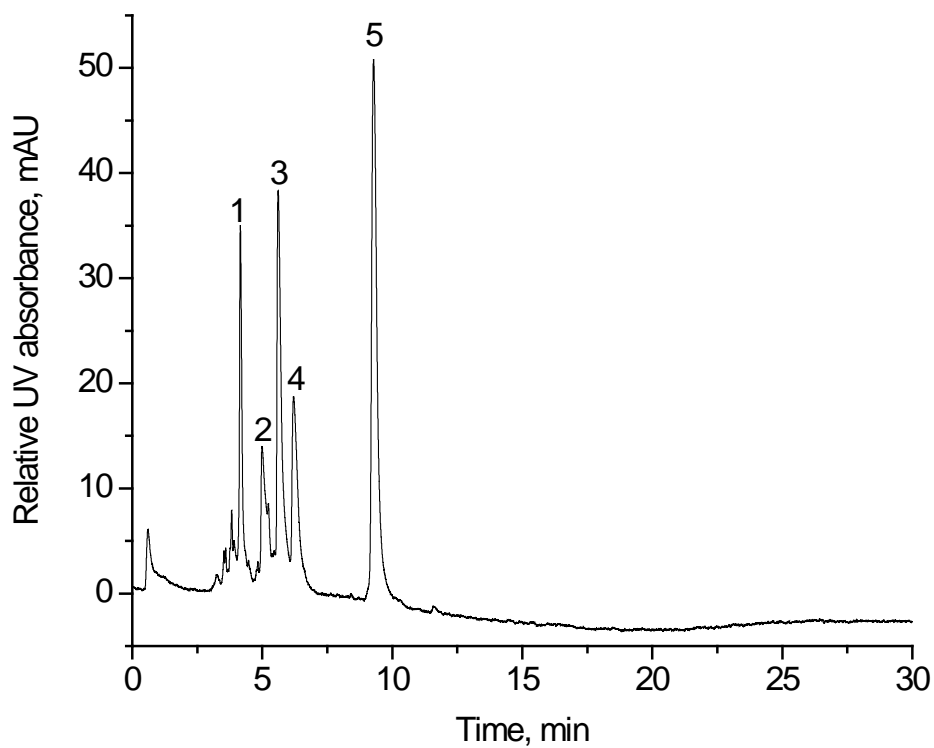
Figure 3.6. Separation of proteins. Conditions: 8.7 cm × 75 µm I.D. poly(PAHEMA-co-PEGDA) monolith; buffer A was 5 mmol/L phosphate at pH 8.0, buffer B was 1 mol/L NaCl in buffer A; linear gradient from 100% A to 100% B in 10 min, followed by 100% B for A; 40 µL/min pump flow rate; on-line UV detection at 214 nm. Peak identifications: (1) trypsinogen, (2) ribonuclease A, (3) α-chymotrypsinogen A, (4) cytochrome C, and (5) lysozyme.
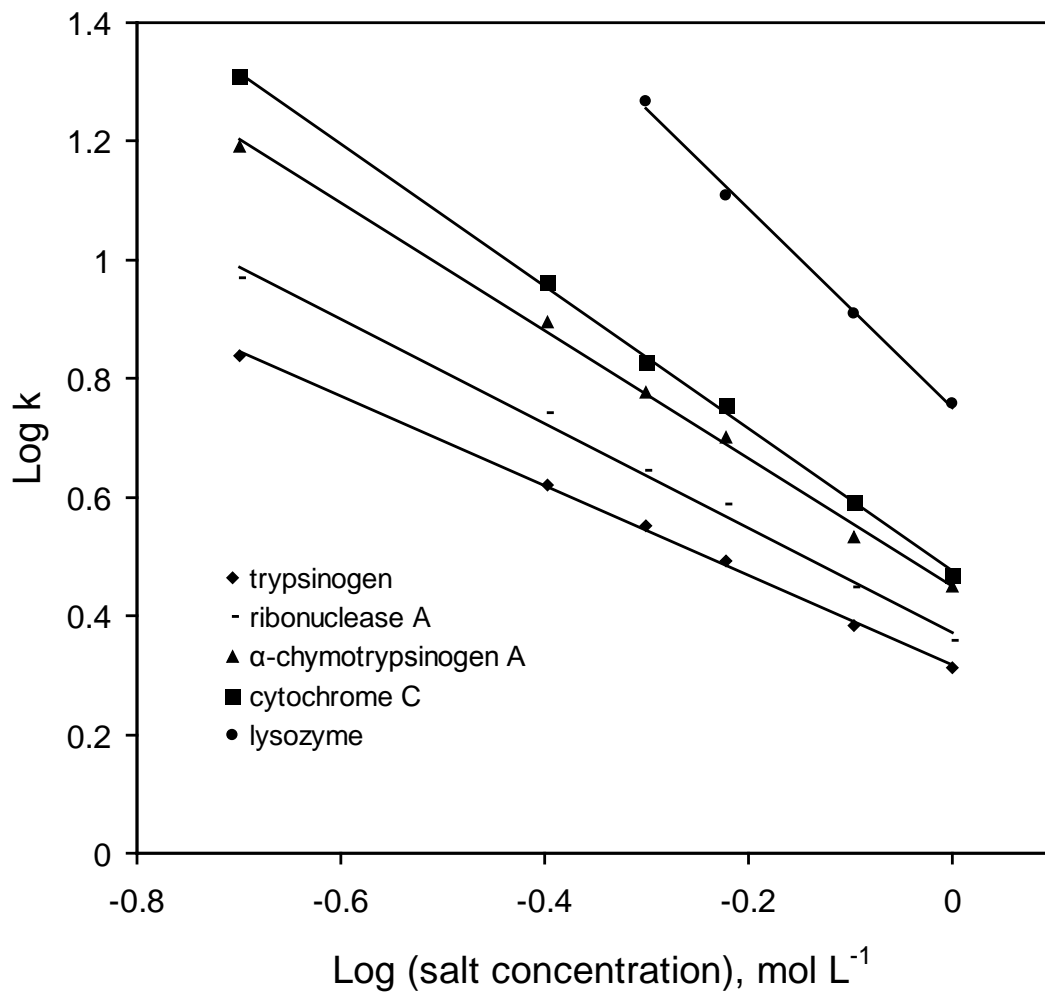
Figure 3.7. Relationship between retention factor (K) and salt concentration for proteins. Conditions: 10 cm × 75 µm I.D. PAHEMA–PEGDA monolith; buffer was 5 mmol/L phosphate with various salt concentrations at pH 8.0; 40 µL/min pump flow rate; on-line UV detection at 214 nm.

to 9.0, indicating that the column efficiency was stable at different pH values. The resolution between α-chymotrypsinogen A and cytochrome C decreased from 4.18 to 0.1 at pH 6.0 and 9.0, respectively. For poly(BMEP-co-PEGA) monolith M3, an increase in pH from 6.0 to 8.0 (Figures 3.8A and B) led to a decrease in retention times of proteins as a result of less positive ionization of the proteins, and a reduction in peak capacity from 27 to 19. Resolution between α-chymotrypsinogen A and cytochrome C (peaks 1 and 2 in Figures 3.8A and B) was also reduced from 0.97 to 0.47. Mobile phase pH also affected the separation selectivity. Ribonuclease A eluted before α-chymotrypsinogen A at pH 8.0, and eluted after α-chymotrypsinogen A at pH 6.0. This effect can be used to optimize various separations.

The effects of salt gradient rate on protein retention times, resolution, and peak capacity were examined using the poly(PAHEMA-co-PEGDA) monolith. Retention times and peak widths of proteins were reduced for steep salt gradient rates, showing typical ion-exchange behavior again. With a shallow gradient rate of 5% B/min, a resolution of 1.23 was obtained for α-chymotrypsinogen A and cytochrome C, while only 0.68 was obtained for a steep gradient of 20% B/min. The shallow salt gradient rate resulted in a peak capacity of 31 compared to 11 for a steep gradient rate. Obviously, a shallow salt gradient afforded better resolution and higher peak capacity at the expense of elution time. The effect of salt gradient rate on protein retention, resolution, and peak capacity was examined using column M3 (Figure 3.9). For all gradient rates, proteins eluted with sharp peaks, indicating that there were low or no non-specific interactions between the proteins and the monolithic column. Baseline separation was achieved with either steep (20% B/min) or shallow (5% B/min) salt gradient rates. With a salt gradient rate of 20% B/min, a peak capacity of 18 and resolution of 0.65 between α-chymotrypsinogen A and cytochrome C were measured. When the gradient rate was reduced to 10% B/min, the peak

Table 3.7. Effect of BMEP concentration on the separation of proteins.[a]

Column	Length (cm)	Peak 1		Peak 2		Peak 3		Peak 4		Resolution[d]	Peak capacity[e]
		t_R[b]	w_d[c]	t_R	w_d	t_R	w_d	t_R	w_d		
M1	9.0	8.23	0.36	8.76	0.57	10.1	0.59	13.9	0.45	1.1	20 ± 4.4
M2	9.0	7.18	0.42	7.71	0.42	8.94	0.62	12.2	0.67	1.2	19 ± 4.6
M3	9.0	6.43	0.29	6.74	0.34	7.94	0.34	11.5	0.51	0.97	27 ± 7.0
M4	10	5.17	0.31	5.59	0.46	6.70	0.53	9.88	0.57	1.3	21 ± 5.2
M5	9.0	5.84	0.24	6.08	0.43	7.34	0.58	11.2	0.62	0.74	21 ± 7.9

[a] Conditions: 100% A to 100% B in 10 min, followed by 100% B, where A was 5 mmol/L phosphate buffer at pH 6.0 and B was 1 mol/L NaCl in A, 40 µL/min pump flow rate, on-line detection at 214 nm. [b] retention time in min. [c] peak width in min. [d] Resolution between peaks 1 and 2. [e] calculated from gradient time/peak width. Peaks 1-4 represent α-chymotrpsinogen A, cytochrome C, ribonuclease A, and lysozyme, respectively.

Table 3.8. Effect of pH on the separation of proteins.[a]

pH	Peak 1		Peak 2		Peak 3		Peak 4		Peak 5		Resolution[d]	Peak capacity[e]
	t_R[b]	w_d[c]	t_R	w_d	t_R	w_d	t_R	w_d	t_R	w_d		
6.0	4.78	0.31	8.46	0.82	4.95	0.25	6.45	0.47	12.5	2.20	4.2	12 ± 7.8
7.0	4.43	0.36	5.99	0.32	6.22	0.36	6.64	0.68	10.4	1.26	0.83	16 ± 8.2
8.0	4.16	0.40	4.99	0.31	5.61	0.58	6.21	0.88	9.28	1.14	0.82	15 ± 7.9
9.0	0.715	0.28	3.74	0.67	5.31	0.93	5.24	0.81	8.95	1.18	0.10	13 ± 5.6

[a] Conditions: 8.7 cm × 75 µm I.D. poly(PAHEMA-co-PEGDA) monolith, 100% A to 100% B in 10 min, followed by 100% B, where A was 5 mmol/L phosphate buffer and B was 1 mol/L NaCl in A, 40 µL/min pump flow rate, on-line detection at 214 nm. [b] retention time in min. [c] peak width in min. [d] Resolution between peaks 3 and 4. [e] calculated from gradient time/peak width. Peaks 1-5 represent trypsinogen, ribonuclease A, α-chymotrypsinogen A, cytochrome C, and lysozyme, respectively.
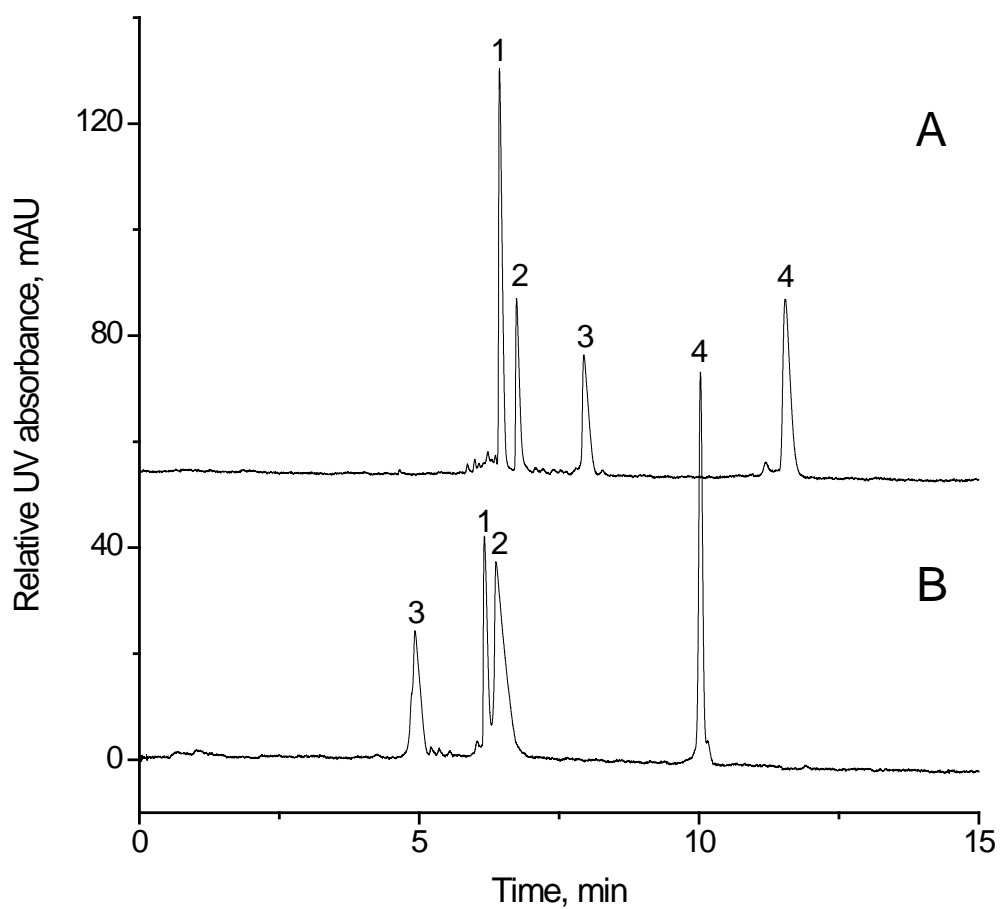
Figure 3.8. Separations of proteins at different pH values. Conditions: column M3 (9.0 cm × 75 µm I.D.); other conditions are the same as in Figure 3.4, except that buffers A and B were adjusted to (A) pH 6.0, and (B) 8.0. Peak identifications: (1) α-chymotrypsinogen A, (2) cytochrome C, (3) ribonuclease A, and (4) lysozyme.
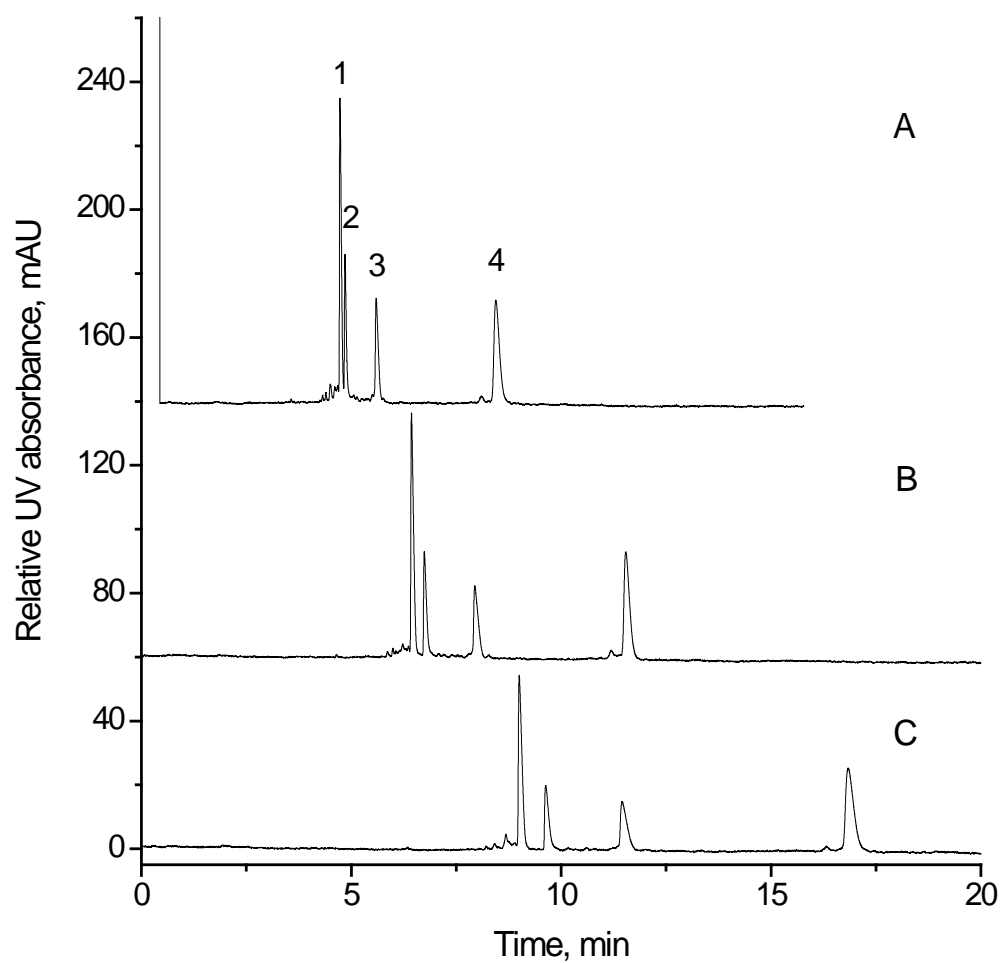
Figure 3.9. Separations of proteins using different salt gradient rates. Conditions: column M3 (9.0 cm ×
75 µm I.D.); other conditions are the same as in Figure 3.4, except linear gradient from 100% A to 100%
B in (A) 5 min, (B) 10 min, and (C) 20 min. Peak identifications: (1) α-chymotrypsinogen A, (2)
cytochrome C, (3) ribonuclease A, and (4) lysozyme.

capacity increased to 27 and the resolution increased to 0.97. A further decrease in gradient rate to 5% B/min led to a peak capacity of 31 and resolution of 1.35. These results show the expected trend that a shallow salt gradient rate yields better resolution and higher peak capacity.

3.5 Conclusions

In this study, two monomers, PAHEMA and BMEP containing phosphoric acid functional groups were used to prepare stable cation-exchange monoliths by photo-initiated copolymerization in 75 µm I.D. capillaries. The resulting monoliths provided relatively high dynamic binding capacities and permeabilities, and low back pressures. These monolithic columns were used for IEC of peptides and proteins. Good stability and reproducibility were observed, and high peak capacity was measured. The biocompatible structures of BMEP and PEGA made the hydrophobicity of the poly(BMEP-co-PEGA) monolith negligible. Compared to poly(PAHEMA-co-PEGDA) monoliths, the poly(BMEP-co-PEGA) monoliths have higher DBC values and lower hydrophobicities, leading to excellent performance for peptide and protein separations.

This work was published in the Journal of Chromatography A, 2010, 1217, 3844-3854.

3.6 References

1. Liu, J.; Sun, X.; Lee, M. L. *Anal. Chem.* **2007**, *79*, 1926-1931.

2. Sun, X.; Li, D.; Lee, M. L. *Anal. Chem.* **2009**, *81*, 6278-6284.

3. Gu, B.; Li, Y.; Lee, M. L. *Anal. Chem.* **2007**, *79*, 5848-5855.

4. Vidic, J.; Podgornik, A.; Štrancar, A. *J. Chromatogr. A* **2005**, *1065*, 51-58.

5. Gu, B.; Chen, Z.; Thulin, C. D.; Lee, M. L. *Anal. Chem.* **2006**, *78*, 3509-3518.

6. Chen, X.; Tolley, H. D.; Lee, M. L. *J. Sep. Sci.* **2009**, *32*, 2565-2573.

7. Li, Y.; Gu, B.; Tolley, H. D.; Lee, M. L. *J. Chromatogr. A* **2009**, *1216*, 5525-5532.

8. Unsal, E.; Elmas, B.; Cağlayan, B.; Tuncel, M.; Patir, S.; Tuncel, A. *Anal. Chem.* **2006**, *78*, 5868-5875.

9. Gatschelhofer, C.; Mautner, A.; Reiter, F.; Pieber, T. R.; Buchmeiser, M. R.; Sinner, F. M. *J. Chromatogr. A* **2009**, *1216*, 2651-2657.

10. Li, Y.; Tolley, H. D.; Lee, M. L. *Anal. Chem.* **2009**, *81*, 9416-9424.

11. Weitzhandler, M.; Farnan, D.; Horvath, J.; Rohrer, J. S.; Slingsby, R. W.; Avdalovic, N.; Pohl, C. *J. Chromatogr. A* **1998**, *828*, 365-372.

12. Krenkova, J.; Gargano, A.; Lacher, N. L.; Schneiderheinze, J. M.; Svec, F. *J. Chromatogr. A* **2009**, *1216*, 6824-6830.

13. Viklund, C.; Svec, F.; Fréchet, J. M. J.; Irgum, K. *Chem. Mater.* **1996**, *8*, 744-750.

14. Mant, C. T.; Hodges, R. S. *J. Chromatogr.* **1985**, *327*, 147-155.

15. Stadalius, A. A.; Quarry, M. A.; Snyder, L. R. *J. Chromatogr.* **1985**, *327*, 93-113.

16. Viklund, C.; Svec, F.; Fréchet, J. M. J. *Biotechnol. Prog.* **1997**, *13*, 597-600.

17. Ueki, Y.; Umemura, T.; Li, J.; Odake, T.; Tsunoda, K. *Anal. Chem.* **2004**, *76*, 7007-7012.

18. Zakaria, P.; Hutchinson, J. P.; Advalovic, N.; Liu, Y,; Haddad, P. R. *Anal. Chem.* **2005**, *77*, 417-423.

CHAPTER 4 STRONG CATION-EXCHANGE MONOLITHIC COLUMNS SYNTHESIZED FROM A SINGLE PHOSPHATE-CONTAINING DIMETHACRYLATE

4.1 Introduction

One problem that limits the widespread adoption of monoliths for LC is reproducibility. Many factors, such as temperature, ratio between monomers and porogens, and ratios of the porogen solvents affect the synthesis of monoliths. A minor change in these factors may lead to dramatic alteration of the resulting monolith. Normally, a monomer and cross-linker are the major components to prepare a monolith. In this chapter, only a cross-linker is used to prepare a cation-exchange polymeric monolith. With only one monomer, the reproducibility of the synthesized monolith is improved, and the resulting highly cross-linked structure ensures long-term stability. However, only a few studies of monoliths synthesized from only one monomer have been reported. Lubbad et al.[1] used tetrakis(4-vinylbenzyl)silane (TVBS) to prepare a highly cross-linked polymer to separate both low, medium, and high-molecular-weight analytes. The monolith showed low swelling propensity due to the highly cross-linked structure. Greiderer et al.[2] used 1,2-bis(p-vinylphenyl)ethane (BVPE) to obtain a monolith for simultaneous separation of low and high-molecular-weight compounds. Good reproducibility and low swelling propensity were also achieved. The limited numbers of reports on monoliths synthesized from one monomer mainly result from the limited availability of suitable monomers.

In this chapter, bis[2-(methacryloyloxy)ethyl] phosphate (BMEP) (structure in Figure 4.1) was used as a single monomer to prepare polymeric cation exchange monolithic columns for LC by *in situ* photo-initiated copolymerization. The performance of these columns for separation of peptides and proteins under both isocratic and gradient ion-exchange conditions are presented.
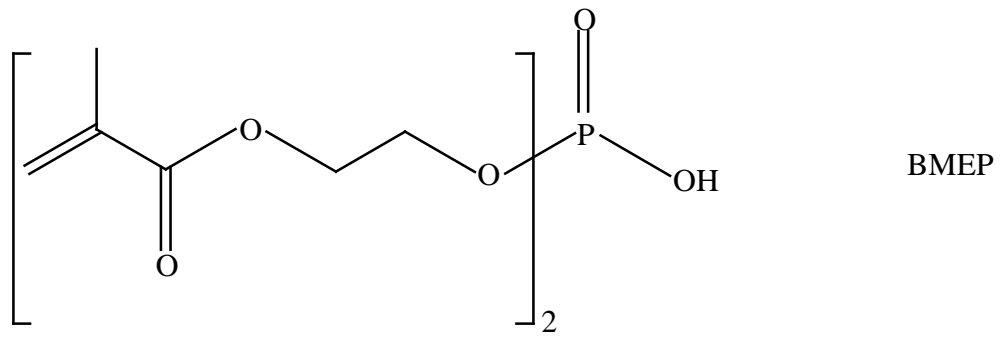
Figure 4.1. Chemical structure of BMEP.

4.2 Experimental Section

4.2.1 Materials

Uracil, 2,2-dimethoxy-2-phenylacetophenone (DMPA, 99%), 3-(trimethoxysilyl)propyl methacrylate (TPM, 98%), BMEP, a natural peptide mixture (H2016), peptides (i.e, D-Leu-Gly, Gly-Gly-Tyr-Arg, Gly-Tyr, angiotensin II, and leucine enkephalin), proteins (i.e., trypsinogen from bovine pancrease, ribonuclease A from bovine pancrease, cytochrome C from bovine heart, α-chymotrypsinogen A from bovine pancreas, and lysozyme from chicken egg white) were purchased from Sigma-Aldrich (Milwaukee, WI) and used without further purification. Propyl paraben was purchased from Spectrum (Gardena, CA). A synthetic peptide standard (CES-P0050) was obtained from Alberta Peptides Institute (Edmonton, Alberta, Canada). Porogenic solvents for monolith synthesis and chemicals for mobile phase buffer preparation were HPLC or analytical reagent grade. Fused-silica capillaries (75 µm I.D. × 360 µm O.D.) were purchased from Polymicro technologies (Phoenix, AZ, USA).

4.2.2 Preparation of Polymeric Monolithic Columns

UV-transparent fused-silica capillaries were first silanized with TPM to introduce pendant vinyl groups to anchor the polymer monolith to the capillary wall.[3,4] Polymeric monoliths were prepared as previously described.[5] The polymerization mixture was prepared in a 4-mL glass vial by mixing initiator, monomers, and porogens. The mixture was vortexed and ultrasonicated for 1 min to form a homogeneous solution and eliminate oxygen. The monomer solution was introduced into the capillary by capillary action. The capillary was placed directly under a PRX 1000-20 Exposure Unit UV lamp (TAMARACK Scientific, Corona, CA) for various times. The resulting monoliths were then flushed with methanol and water sequentially for 30 min each to remove porogens and unreacted monomers using an LC pump. The capillaries

were stored in 10% methanol aqueous solutions to prevent the monoliths from drying. Scanning electron microscopy (SEM) images of the monoliths were obtained as previously described.[6]

4.2.3 Capillary LC

Capillary LC of peptides and proteins was performed using a system described previously.[6] Two ISCO 100 DM syringe pumps with a flow controller were used to generate the salt gradient. A Valco splitting tee (Houston, TX) was positioned between the static mixer of the syringe pumps and the 60-nL Valco internal loop sample injector. A 40-cm-long capillary (30 µm I.D.) was used as the splitting capillary and a 10-cm-long capillary (30 µm I.D.) was connected between the splitting tee and the injector. The mobile phase flow rate was set at 40 µL/min, and the linear velocity in the monolithic capillary column was 1-3 mm/s. The mobile phase was 5 mmol/L aqueous phosphate buffer at various pH values. All mobile phases were filtered through a 0.2 µm Nylon membrane filter (Supelco, Bellefonte, PA). A Model UV3000 detector from Thermo Separations (San Jose, CA) was used at a wavelength of 214 nm. Data were acquired with ChromQuest 2.5.1 software (ThermoQuest, San Jose, CA). The detailed chromatographic conditions are given in the figure captions.

For evaluation of the relative hydrophobicities of the monoliths, reversed-phase capillary LC elution measurements of propyl paraben and uracil were performed. The mobile phase was 20% (v/v) acetonitrile in water. The pump flow rate was 40 µL/min, and the detection wavelength was 254 nm. Uracil was used as an unretained marker. The retention factor for propyl paraben was obtained from the equation, $k = (t_p - t_u)/t_u$, where k is the retention factor, and t_p and t_u are the retention times of propyl paraben and uracil, respectively.

4.2.4 DBC Measurements

DBC is an important property of an ion exchange column. The DBC was examined via frontal analysis with a procedure described previously.[5] The column was first equilibrated with 5 mmol/L sodium phosphate buffer at pH 6.0, and then a solution of 3.15 mg/mL lysozyme in buffer was pumped through the column at a pump flow rate of 40 µL/min. The mobile phase flow rate in the monolithic capillary column was measured using a calibration capillary (Eksigent, Livermore, CA). The binding capacity was calculated at 50% of the final absorbance value of the breakthrough curve and expressed in mg/mL of column volume.

4.2.5 Separation of Protein Digest

A cytochrome C digest was prepared according to a published procedure.[7] Cytochrome C (2.67 mg/mL) was diluted with 100 mmol/L ammonium bicarbonate solution. Trypsin was added at a substrate-to-enzyme ratio of 50:1 (w/w) and the solution was incubated at 37 °C for 20 h. Proteolysis was terminated by decreasing the pH below 2 by addition of formic acid to the solution. The digest was then desalted using a Sep-Pak Vac 3 cc C18 Cartridge (Waters, Milford, MA) following the protocol suggested by the manufacturer. The peptide solutions in microvials were vacuum-dried to pellets that were redissolved in 5 mmol/L sodium phosphate buffer at pH 3.0 for separation.

4.2.6 Separation of Deamidation Variants of Ribonuclease A

The deamidation variants of ribonuclease A were prepared according to a protocol provided by Dionex.[8] A 334 µL volume of 15 mg/mL ribonuclease A, 100 µL 10 wt% ammonium bicarbonate, and 566 µL water were combined in a microvial and incubated at 37 ℃. Then, 50 µL aliquots were withdrawn periodically and frozen for further tests.

4.3 Results and Discussion

4.3.1 Single Monomer Monolith Preparation

BMEP, which is a commercial cross-linker, was chosen as a monomer to prepare a cation-exchange monolith because it contains phosphate functional group. This cross-linker was previously used to synthesize cation-exchange monolithic columns with a second monomer, polyethylene glycol acrylate (PEGA).[9] The poly(BMEP-co-PEGA) monoliths demonstrated excellent separation of peptides and proteins in the cation-exchange mode. However, PEGA is no longer commercially available, probably due to the reactivity of the acrylate group. Since BMEP has two reactive methacrylate end groups, it can be used as a single monomer to synthesize a cation-exchange monolith. From preliminary work, it was observed that monoliths synthesized using only BMEP were highly cross-linked and, thus, more stable than monoliths obtained using two monomers. The single monomer synthesis should also increase batch-to-batch reproducibility.

Methanol, dodecanol, and ethyl ether were used as porogen solvents in previous work to synthesize poly(BMEP-co-PEGA) monoliths.[9] We initially started with these three solvents for the synthesis of BMEP-only monoliths. However, the resulting monolith morphologies were not uniform when observed under the microscope, even after trying various ratios of the solvents. With methanol and ethyl ether as porogen solvents, the resulting monoliths demonstrated low efficiency for separations of peptide and protein standards. Methanol and dodecanol were finally chosen as the best porogen solvents, since the morphologies of the monoliths appeared uniform under the microscope. Several monoliths were prepared as listed in Table 4.1. These monolithic columns exhibited low hydrophobicities (see Table 4.1).

Table 4.1. Compositions and physical properties of monoliths.

Column	BMEP (g)	Methanol (g)	Dodecanol (g)	DMPA (g)	UV time (min)	Porosity (%)	Hydrophobicity[a]
1	0.60	1.15	0.35	0.006	3	64	0.489
2	0.60	1.18	0.32	0.006	3	62	0.451
3	0.60	1.20	0.30	0.006	3	57	0.454
4	0.55	1.18	0.32	0.006	3	64	0.484
5	0.58	1.18	0.32	0.006	3	63	0.420
6	0.65	1.18	0.32	0.006	3	55	0.439
7	0.60	1.18	0.32	0.006	2	68	0.447
8	0.60	1.18	0.32	0.006	5	61	0.479
9	0.60	1.18	0.32	0.006	10	58	0.488

[a] Procedure is described in 4.2.3

4.3.2 Effect of Porogen Solvents on the Separation of Peptides and Proteins

Selection of the porogen solvents has a great effect on the morphology of the resultant monolith, thus, affecting significantly the separation. Methanol is a "good" solvent, which leads to late phase separation during polymerization and results in small pores.[10] With more methanol in the porogens, the back pressure of the monolith increases, while the total porosity decreases (columns 1-3 in Table 4.1). These three columns were used to separate peptide and protein standards. CES P0050 is a mixture of four undecapeptides designed for evaluation of particle packed strong cation-exhange columns.[5,11] The protein standard mixture contained five proteins including trypsinogen, ribonuclease A, cytochrome C, α-chymotrypsinogen A, and lysozyme. Longer times were required to elute peptides and proteins from monoliths prepared with more methanol in the porogens (Tables 4.2 and 4.3). Peak capacities (time of gradient/peak width) of 16 and 15 were obtained for peptides and proteins using column 2. These peak capacities are greater than those obtained using column 3 and similar to column 1. However, the peak shapes of peptides and proteins were better with column 2 than with column 1.

4.3.3 Effect of BMEP Concentration on the Separation of Peptides and Proteins

Considering the trade-off between retention time and resolution, the porogen system of column 2 was selected for further experiments. The monomer concentration in the monolith alters both the monolith morphology and the monolith composition. With a higher concentration of monomer in the preparation of the monolith, the back pressure of the monolith increased and the porosity decreased (columns 2 and 4-6 in Table 4.1). When the BMEP concentration in the solution was lower than 26.8 wt% (column 4), the monolith was not rigid. When it was higher than 31.8 wt%, mobile phase could not flow through the monolith at a pressure of 3000 psi. With an increase in concentration of BMEP in the monolith, the elution times for both peptides and

Table 4.2. Effect of porogen solvents on the separation of peptides.[a]

| | Peptides | | | | | | | | Peak capacity[d] |
| | Peak 1 | | Peak 2 | | Peak 3 | | Peak 4 | | |
Column	t_R[b]	w_d[c]	t_R	w_d	t_R	w_d	t_R	w_d	
1	0.958	0.50	7.09	0.51	8.95	0.52	13.9	0.83	17 ± 4.6
2	2.68	0.68	13.5	0.44	16.2	0.44	26.4	0.95	16 ± 6.2
3	6.13	1.20	26.3	1.22	37.3	0.77	79.0	2.80	7 ± 4.0

[a] Conditions: 100% A to 100% B in 10 min, followed by 100% B, where A was 5 mmol/L phosphate buffer at pH 3.0, and B was 1 mol/L NaCl in A, 40 µL/min pump flow rate, on-line detection at 214 nm. [b] retention time in min. [c] peak width in min. [d] calculated from gradient time/peak width for peptides. Peptides 1-4 represent Ac-Gly-Gly-Gly-Leu-Gly-Gly-Ala-Gly-Gly-Leu-Lys-amide, Ac-Lys-Tyr-Gly-Leu-Gly-Gly-Ala-Gly-Gly-Leu-Lys-amide, Ac-Gly-Gly-Ala-Leu-Lys-Ala-Leu-Lys-Gly-Leu-Lys-amide, and Ac-Lys-Tyr-Ala-Leu-Lys-Ala-Leu-Lys-Gly-Leu-Lys-amide, respectively.

Table 4.3. Effect of porogen solvents on the separation of proteins.[a]

| | Proteins | | | | | | | | | | R_s[d] |
| | Peak 1 | | Peak 2 | | Peak 3 | | Peak 4 | | Peak 5 | | |
Column	t_R	w_d	t_R	w_d	t_R	w_d	t_R	w_d	t_R	w_d	
1	5.89	0.36	7.05	0.39	8.26	0.49	9.26	0.66	12.0	0.95	3.56
2	9.57	0.53	11.7	0.50	13.6	0.57	15.4	0.71	20.8	1.10	3.55
3	22.8	1.16	29.6	1.05	30.8	0.63	33.7	1.46	38.6	1.84	1.43

[a] Conditions: 10.0 cm columns 1, 2, and 3. 100% A to 100% B in 10 min, followed by 100% B, where A was 5 mmol/L phosphate buffer at pH 6.0, and B was 1 mol/L NaCl in A, 40 µL/min pump flow rate, on-line detection at 214 nm. [b] retention time in min. [c] peak width in min. [d] resolution between protein peaks 2 and 3. Proteins 1-5 represent trypsingen, α-chymotrpsinogen A, cytochrome C, ribonuclease A, and lysozyme, respectively.

proteins increased. It is reasonable to conclude that more phosphate groups were exposed on the surface of the monolith, thus leading to higher DBC. When a higher BMEP pencentage was used in the monolith preparation, a higher surface area was generated. A combination of low porosity led to increased retention of peptides and proteins. When 30.2 wt% BMEP was used (monolith 6), it took approximately 100 min for the last peptide to elute. The resolution of peptides and proteins also increased with an increase in concentration of BMEP in the monolith. Good peak profiles were obtained using these monoliths for both peptides and proteins. For the separation of CES P0050, peak capacities of 28, 23, and 16 were obtained using columns 4, 5, and 2, respectively, and peak capacities of 25, 18, and 15 were obtained for separation of proteins. Although peak capacities are higher for columns 4 and 5, peak resolution, especially the resolution between cytochrome C and α-chymotrypsinogen A, was lower than with column 2 (Tables 4.4 and 4.5). Considering retention time, resolution, and peak capacity, the conditions for column 2 were selected for further studies.

4.3.4 Effect of UV Exposure Time on the Separation of Peptides and Proteins

The polymerization time affects the conversion of functional groups, and the properties and morphologies of the resulting monoliths. From Table 4.1, the porosity decreased with an increase in polymerization time. To evaluate the dependence of BMEP conversion on polymerization time, DBC was measured for columns 2, 7, 8, and 9. Using frontal analysis, the DBC was measured as reported previously.[12] Since the columns were designed for ion exchange chromatography of large biomolecules, a 3.15 mg/mL lysozyme solution was used to measure the DBC of the columns. DBC values of 53.5, 51.1, 54.7, and 72.7 mg/mL of column volume were measured for columns 2, 7, 8, and 9, respectively (Figure 4.2). These DBC values are approximately equal to, or higher than, various synthesized and commercial columns.[7,13] The

Table 4.4. Effect of BMEP concentration on the separation of peptides.[a]

| Column | Length (cm) | Peptides | | | | | | | | Peak capacity[d] |
| | | Peak 1 | | Peak 2 | | Peak 3 | | Peak 4 | | |
		t_R[b]	w_d[c]	t_R	w_d	t_R	w_d	t_R	w_d	
2	10.5	2.68	0.68	13.5	0.44	16.2	0.44	26.4	0.95	16 ± 6.2
4	10.0	1.07	0.52	5.80	0.56	6.85	0.52	9.91	0.49	25 ± 1.1
5	10.0	3.40	0.48	9.04	0.40	10.5	0.48	5.05	0.56	20 ± 2.8
6	10.0	6.86	1.22	28.7	1.67	42.4	1.29	97.1	3.59	5 ± 2.9

[a] Conditions: 100% A to 100% B in 10 min, followed by 100% B, where A was 5 mmol/L phosphate buffer at pH 3.0, and B was 1 mol/L NaCl in A, 40 µL/min pump flow rate, on-line detection at 214 nm. [b] retention time in min. [c] peak width in min. [d] calculated from gradient time/peak width for peptides. Peptides 1-4 represent Ac-Gly-Gly-Gly-Leu-Gly-Gly-Ala-Gly-Gly-Leu-Lys-amide, Ac-Lys-Tyr-Gly-Leu-Gly-Gly-Ala-Gly-Gly-Leu-Lys-amide, Ac-Gly-Gly-Ala-Leu-Lys-Ala-Leu-Lys-Gly-Leu-Lys-amide, and Ac-Lys-Tyr-Ala-Leu-Lys-Ala-Leu-Lys-Gly-Leu-Lys-amide, respectively.

Table 4.5. Effect of BMEP concentration on the separation of peptides and proteins.[a]

| Column | Length (cm) | Proteins | | | | | | | | | | R_s[d] |
| | | Peak 1 | | Peak 2 | | Peak 3 | | Peak 4 | | Peak 5 | | |
		t_R[b]	w_d[c]	t_R	w_d	t_R	w_d	t_R	w_d	t_R	w_d	
2	10.5	9.57	0.53	11.7	0.50	13.6	0.57	15.4	0.71	20.8	1.10	2.82
4	10.0	5.05	0.18	5.62	0.22	7.25	0.38	7.69	0.30	9.99	0.72	1.29
5	10.0	6.96	0.45	8.07	0.41	10.3	0.50	10.9	0.43	14.9	1.04	1.29
6	10.0	21.2	1.85	35.8	0.96	38.2	0.74	42.5	0.99	48.9	1.32	4.97

[a] Conditions: 100% A to 100% B in 10 min, followed by 100% B, where A was 5 mmol/L phosphate buffer at pH 6.0, and B was 1 mol/L NaCl in A, 40 µL/min pump flow rate, on-line detection at 214 nm. [b] retention time in min. [c] peak width in min. [d] resolution between protein peaks 3 and 4. [e] calculated from gradient time/peak width for peptides. Proteins 1-5 represent trypsingen, α-chymotrpsinogen A, cytochrome C, ribonuclease A, and lysozyme, respectively.
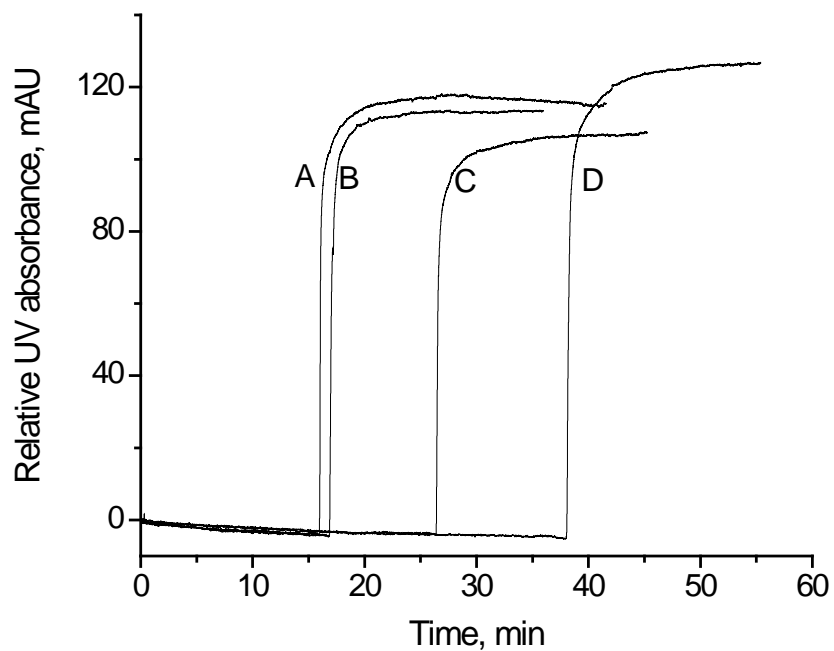
Figure 4.2. Breakthrough curves for lysozyme on monoliths polymerized for various times. Conditions: 9.2, 9.2, 8.1, and 7.0 cm × 75 µm I.D. for columns (A) 7, (B) 8, (C) 2, and (D) 9, respectively; 5 mmol/L phosphate at pH 6.0 mobile phase; 3.15 mg/mL lysozyme in the mobile phase; 40 µL/min pump flow rate; on-line UV detection at 214 nm.

sharp frontal analysis curves indicated rapid adsorption of lysozyme on these monoliths. Only one plateau was observed in the frontal analysis curves, indicating a strong cation-exchange mechanism. Obviously, an increase in the polymerization time from 2 to 5 min had no significant effect on the conversion of BMEP on the surface of the monolith. With a further increase to 10 min, the conversion increased, as indicated by the approximately 33% increase in DBC value. Figure 4.3 shows SEM images of columns 1, 2, 7, 8, and 9. As can be easily seen, the morphologies are different. However, the back pressures of these monolithic columns varied only slightly. It was reported previously that the polymerization time did not affect the pore-size-distribution of monoliths significantly.[14] A similar pore-size-distribution led to a similar back pressure. The increased polymerization time also increased the rigidity of the resulting monolith. The monolith prepared with 2 min polymerization time was separated under vacuum during SEM (Figure 4.3A); the other monoliths were stable under the same conditions. Although the monolith in column 7 separated, there were no gaps observed between the monolith and the column inner wall, which indicates that the monolith was covalently bonded to the capillary.

Monolithic columns 2, 7, 8, and 9 were used to separate peptides and proteins for evaluation of their performances (Figure 4.4). As shown, the elution times increased using monoliths with longer polymerization times. The longer elution time for column 2 compared to column 8 was due to the longer length of column 2. The longer elution times for peptides and proteins on monoliths prepared with longer polymerization times resulted from higher dynamic binding capacity and lower porosity. The peak capacities on columns 2, 7, 8, and 9 were 20, 16, 15, and 11 for peptides, and 14, 15, 19, and 13 for proteins, respectively. Since column 8 exhibited the highest peak capacity for proteins, it was selected for additional testing.
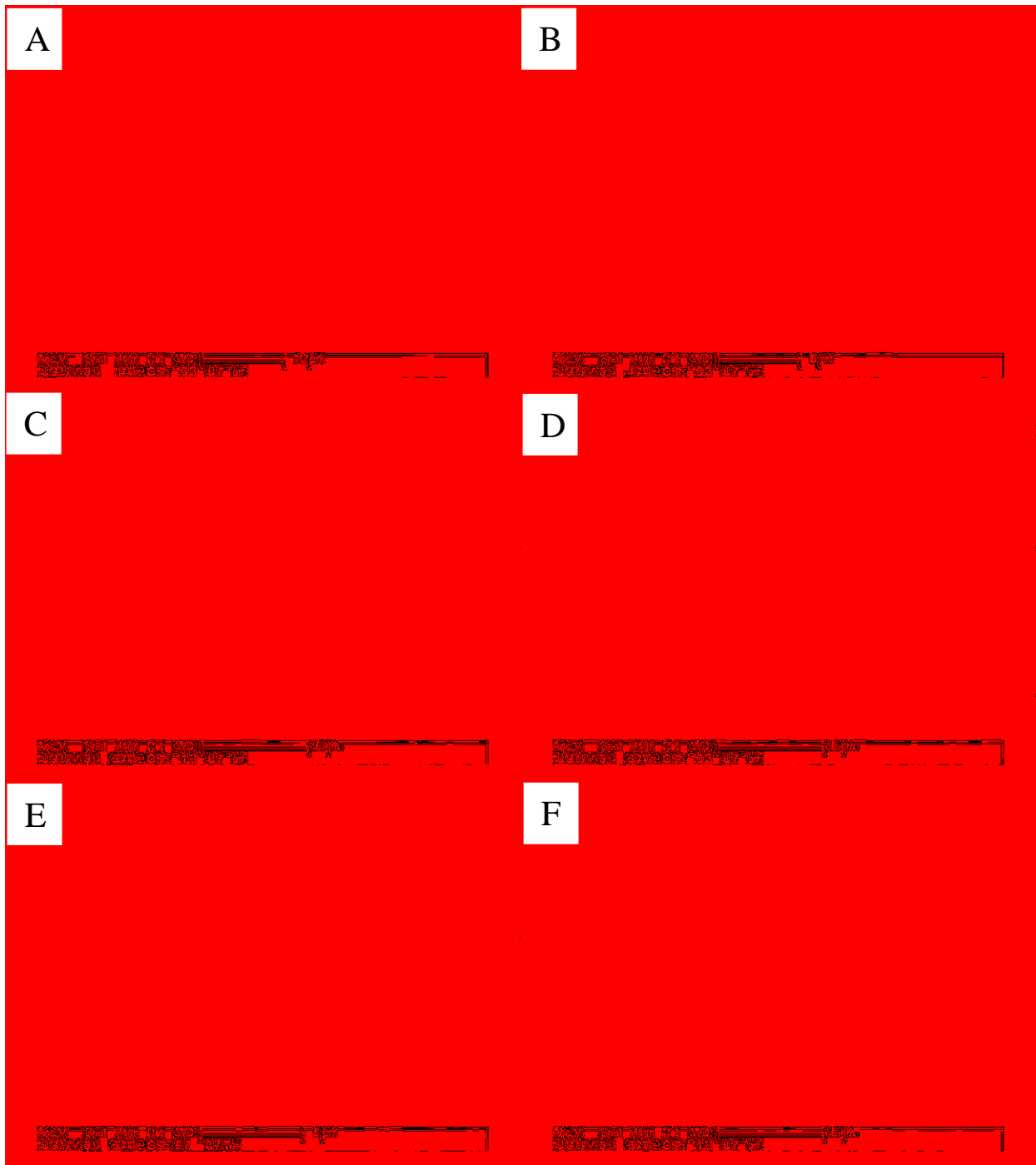
Figure 4.3. Scanning electron micrographs of (A) column 7 (scale bar, 20 µm), (B) column 7 (scale bar, 5 µm), (C) column 2 (scale bar, 5 µm), (D) column 8 (scale bar, 5 µm), (E) column 9 (scale bar, 5 µm), and (F) column 1 (scale bar, 5 µm).
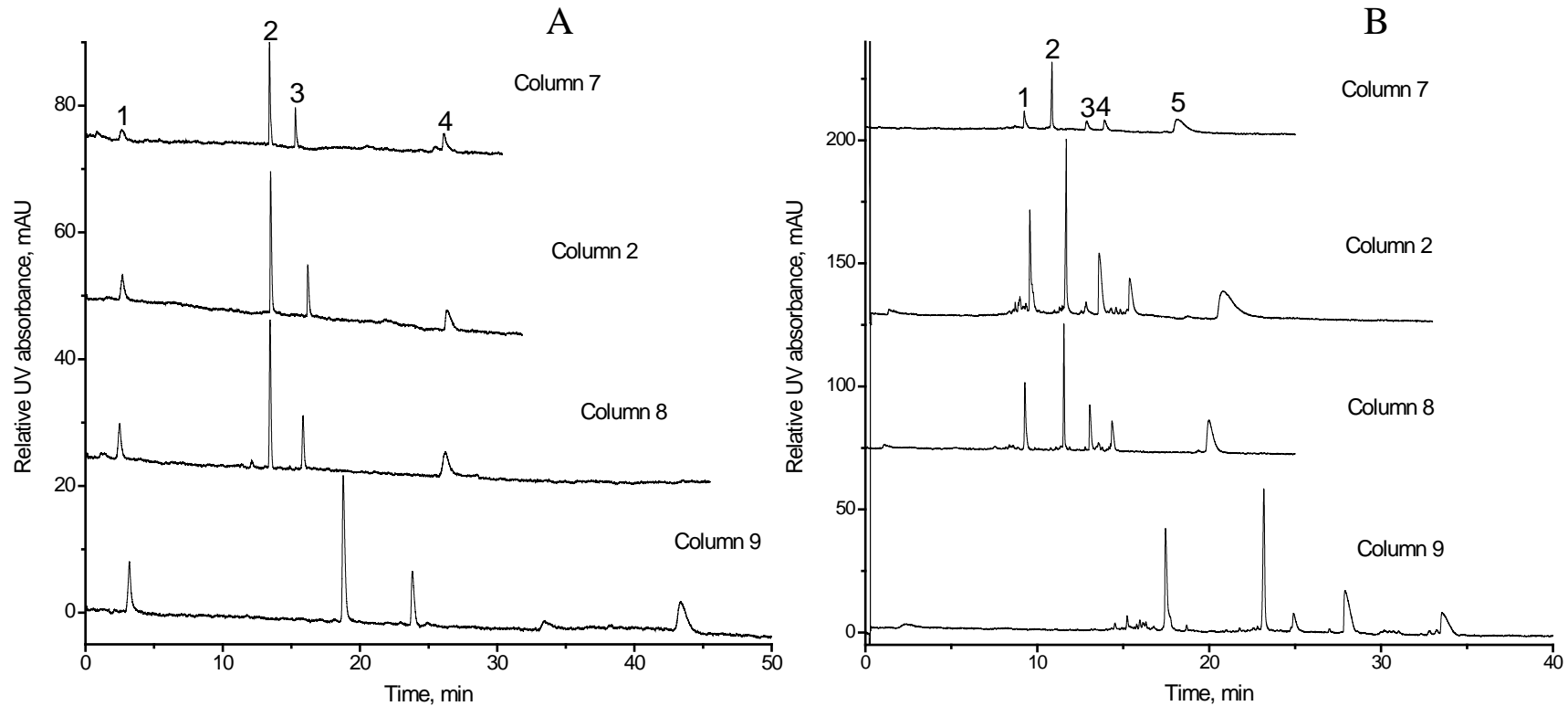
Figure 4.4. Effect of polymerization time on the separation of peptides and proteins. Conditions: 10.5, 9.0, 10.0, and 10.0 cm × 75 µm I.D. for columns 2, 7, 8, and 9, respectively; buffer A was 5 mmol/L phosphate at pH 6.0, buffer B was 1 mol/L NaCl in buffer A; 2-min isocratic elution of buffer A, followed by linear gradient from buffer A to buffer B in 10 min; 40 µL/min pump flow rate; on-line UV detection at 214 nm. Peak identifications: (A): (1) Ac-Gly-Gly-Gly-Leu-Gly-Gly-Ala-Gly-Gly-Leu-Lys-amide, (2) Ac-Lys-Tyr-Gly-Leu-Gly-Gly-Ala-Gly-Gly-Leu-Lys-amide, (3) Ac-Gly-Gly-Ala-Leu-Lys-Ala-Leu-Lys-Gly-Leu-Lys-amide, (4) Ac-Lys-Tyr-Ala-Leu-Lys-Ala-Leu-Lys-Gly-Leu-Lys-amide; (B): (1) trypsinogen, (2) α-chymotrypsinogen A, (3) cytochrome C, (4) ribonuclease A, and (5) lysozyme.

4.3.5 Hydrophobic Interactions

Hydrophobic interactions between analytes and the column are detrimental for ion exchange chromatography. Analyte retention when using a high concentration of salt in the mobile phase is strongly affected by hydrophobic interactions. A pure ion exchange mechanism can be achieved only when hydrophobic interactions are suppressed. The possible effect of hydrophobic interactions on retention times of proteins was evaluated using monolithic column 8 under isocratic conditions. The mobile phase was 5 mmol/L sodium phosphate buffer at pH 6.0 containing various concentrations of sodium chloride. As shown in Figure 4.5A, a linear dependence between logarithm of retention factor and logarithm of salt concentration in the mobile phase indicates that the separation was governed by a pure ion exchange mechanism.[15] The column exhibited high efficiency for the separation of proteins without undesirable hydrophobic interactions. For example, an efficiency of approximately 71,000 plates/m was achieved for separation of proteins when 0.8 mol/L NaCl in 5 mmol/L sodium phosphate at pH 6.0 was used as mobile phase (Figure 4.5B).

The effects of acetonitrile (ACN) in the mobile phase on the retention times of peptides (CES P0050) and on peak capacity were also used to evaluate hydrophobic interactions. As shown in Figure 4.6, the retention times of peptides varied slightly with 0, 10, and 20% (v/v) ACN in the mobile phase. The peak capacity (14, 15, and 15 in Figures 4.6A, B, and C) also varied only slightly. Similar retention times and constant peak capacity indicates that there are negligible hydrophobic interactions between peptides and the monolith, which confirms the low hydrophobicity of the monolith. A good efficiency of approximately 52,900 plates/m for the separation of peptides was obtained when 1 mol/L NaCl in 5 mmol/L sodium phosphate at pH 3.0 was used as the mobile phase.
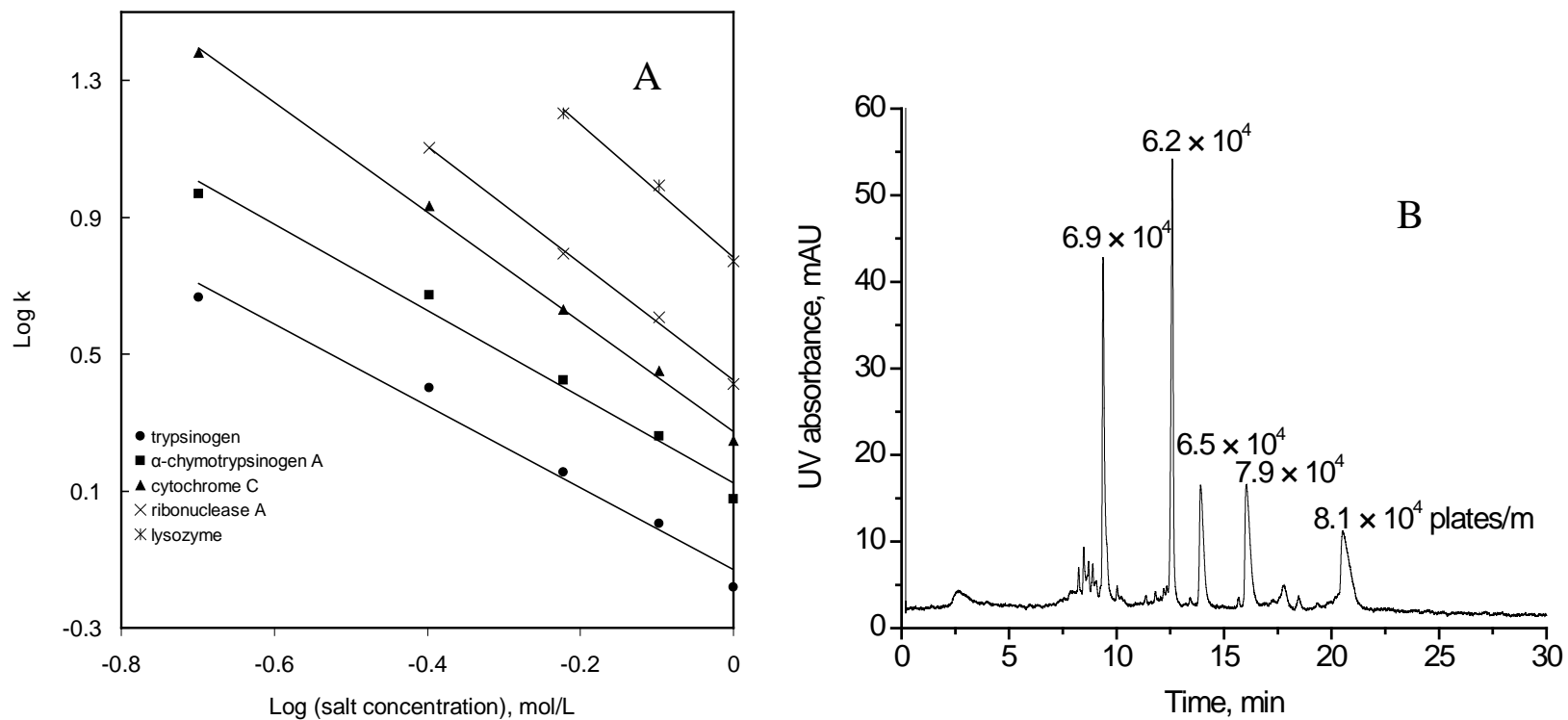
Figure 4.5. (A) Relationship between retention factor (k) and salt concentration and (B) representative chromatogram (0.8 mol/L NaCl concentration) for isocratic separation of proteins. Conditions: 8.0 cm × 75 µm I.D. column 8; buffer was 5 mmol/L phosphate with various salt concentrations at pH 6.0; 40 µL/min pump flow rate; on-line UV detection at 214 nm. Numbers in B represent separation efficiencies in plates/m. Peaks according to elution order are trypsinogen, α-chymotrypsinogen A, cytochrome C, ribonuclease A, and lysozyme.

Figure 4.6. Effect of ACN in the mobile phase on the separation of peptides. Conditions: 16.0 cm × 75 μm I.D. column 8; buffer A was 5 mmol/L phosphate at pH 3.0 containing (A) 20, (B) 10, and (C) 0% (v/v) ACN, buffer B was 1 mol/L NaCl in buffer A; 2-min isocratic elution of 100% buffer A, followed by linear gradient from 100% buffer A to 100% buffer B in 10 min; 40 μL/min pump flow rate; on-line UV detection at 214 nm. Peak identifications are the same as in Figure 4.4 A.

4.3.6 Effect of pH on the Separation of Synthetic Peptides and Proteins

The pH of the mobile phase has an important effect on the separation of peptides and proteins in the ion-exchange mode by controlling the extent of ionization of the ion-exchange functional groups and the analytes. Since phosphoric acid is a medium acid, pH has a negligible effect on its ionization. The synthetic peptides in CES P0050 are all undecapeptides that have no acidic residues. Therefore, they have the same charges in acidic to neutral buffers. In theory, pH should have no appreciable effect on the separation of the peptides. Nevertheless, the retention times and peak capacities were less at pH 3.0 compared to pH 7.0 when the pH effect on separation of the synthetic peptides using monolithic column 8 was investigated using salt gradient elution (data not shown). Peak 4 eluted even later than 70 min at pH 7.0. This pH effect on separation of peptides was reported earlier.[5,6] Hodges[16] explained that the effect was due to a reduction in the column capacity to retain charged species as the pH became more acidic, which is not desirable.

Although mobile phase pH has a negligible effect on the ionization of the ion exchanger, it significantly affects the ionization of proteins. Figure 4.7 shows the effects of pH on retention time, peak capacity, and resolution between α-chymotrypsinogen A and cytochrome C using monolithic column 8. With an increase in pH, the retention time of each protein decreased. Ribonuclease A eluted before α-chymotrypsinogen A and cytochrome C when the pH was 8.0 or higher, while it eluted later at pH values of 6.0 and 7.0. This effect can be used to optimize various separations. Peak capacities of 15, 17, 17, and 16 were obtained for proteins at pH 6.0, 7.0, 8.0, and 9.0, respectively. The slight variation in peak capacity from pH 6.0 to 9.0 indicates that the column was stable at different pH values. The resolution between α-chymotrypsinogen A and cytochrome C decreased from 3.8 to 2.0 at pH 6.0 and 9.0, respectively.
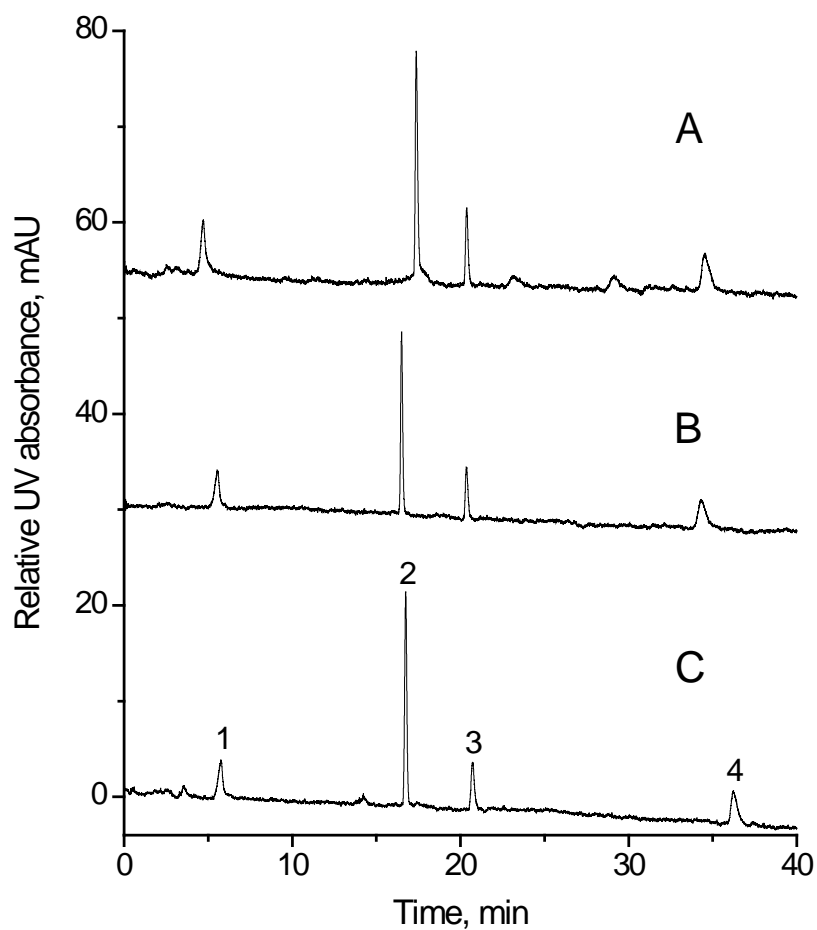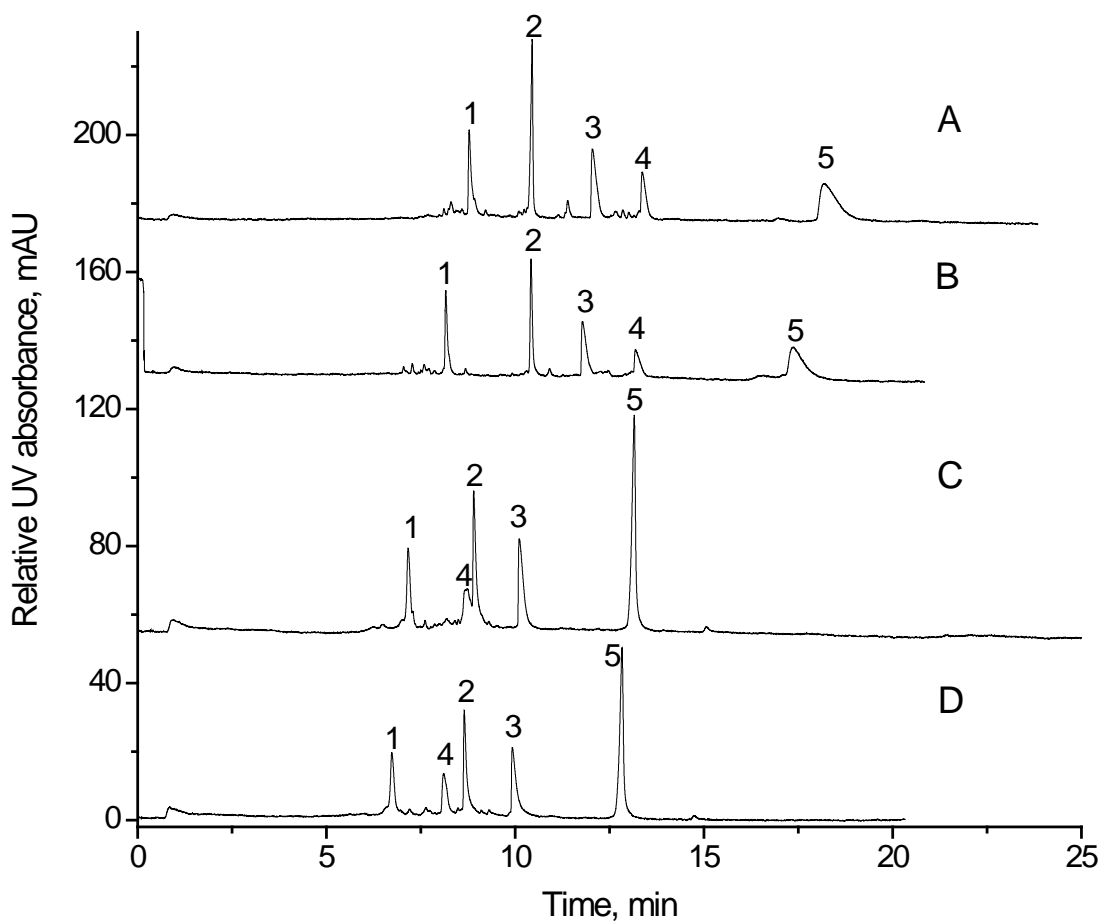
Figure 4.7. Effect of mobile phase pH on the separation of proteins. Conditions: 10.5 cm × 75 µm I.D. column 8; buffer A was 5 mmol/L phosphate at pH (A) 6.0, (B) 7.0, (C) 8.0, and (D) 9.0, buffer B was 1 mol/L NaCl in buffer A; 2-min isocratic elution of 100% buffer A, followed by linear gradient from 100% buffer A to 100% buffer B in 10 min; 40 µL/min pump flow rate; on-line UV detection at 214 nm. Peak identifications are the same as in Figure 4.4B.

4.3.7 Separation of Peptides and Protein Digest

Monolithic column 8 was applied to separate peptide mixture H2016 using salt gradient elution (Table 4.6). The structures and characteristics of these natural peptides were described previously.[9] Five peaks were separated without ACN in the mobile phase. With an increase in gradient rate from 5% to 20% B/min, the peak capacity decreased from 20 to 5. Acceptable resolution of methionine enkephalin and leucine enkephalin was obtained. Methionine enkephalin (Mw 573) and leucine enkephalin (Mw 555) have the same charge and chain length, and similar molecular weights and hydrophobicities. Ionic interaction is less for methionine enkephalin than for leucine enkephalin, due to its greater molecular weight, thus, leading to earlier elution. The resolution between methionine enkephalin and leucine enkephalin changed from 1.1 to 1.4 to 0.78 when using gradient rates of 5%, 10%, and 20% B/min, respectively. This monolith provided better resolution of methionine enkephalin and leucine enkephalin than the poly(AMPS-co-PEGDA monolith),[5] but worse than the poly(SPMA-co-PEGDA)[6] and poly(PAHEMA-co-PEGDA)[9] monoliths reported earlier.

Monolithic column 8 was also used to separate a peptide mixture containing D-Leu-Gly, Gly-Gly-Tyr-Arg, Gly-Tyr, angiotensin II, and leucine enkephalin under isocratic elution conditions. With 1 mol/L NaCl in 5 mmol/L sodium phosphate at pH 3.0 as the mobile phase, an efficiency of 13,228 plates/m was achieved (Figure 4.8A).

The column was also used to separate a cytochrome C digest under gradient elution conditions. The separation was carried out in 5 mmol/L sodium phosphate mobile phase with a linear gradient of sodium chloride. The separation is shown in Figure 4.8B. Ten major peaks were obtained. Although the peaks were not identified, the number of peaks are consistent with a

Table 4.6. Effect of salt gradient on the separation of peptides.[a]

Gradient rate	Peak 1		Peak 2		Peak 3		Peak 4		Peak 5		Resolution[d]	Peak capacity[e]
	t_R[b]	w_d	t_R	w_d	t_R	w_d	t_R	w_d	t_R	w_d		
2.5% B/min	12.6	1.46	14.8	1.52	16.0	1.67	18.1	1.72	69.3	4.02	1.48	19 ± 10
5.0% B/min	10.5	1.45	12.7	1.47	14.1	1.68	16.9	1.69	53.1	3.80	1.50	10 ± 4.9
10% B/min	9.49	1.38	11.1	1.00	12.4	1.28	14.3	1.14	46.0	3.50	1.35	6 ± 3.8
20% B/min	8.44	0.78	9.22	0.83	10.4	0.96	12.0	1.08	40.2	3.10	0.97	4 ± 2.7

[a] Conditions: 10.2 cm × 75 µm I.D. column 8; 100% A to 100% B in 40, 20, 10, and 5 min, followed by 100% B, where A was 5 mmol/L phosphate buffer at pH 3.0 and B was 1 mol/L NaCl in A, 40 µL/min pump flow rate, on-line detection at 214 nm. [b] retention time in min. [c] peak width in min. [d] resolution between peaks 1 and 2. [e] calculated from gradient time/peak width. Peaks 1-4 represent methionine enkephalin, leucine enkephalin, Val-Tyr-Val, Gly-Tyr, and angiotensin II, respectively.
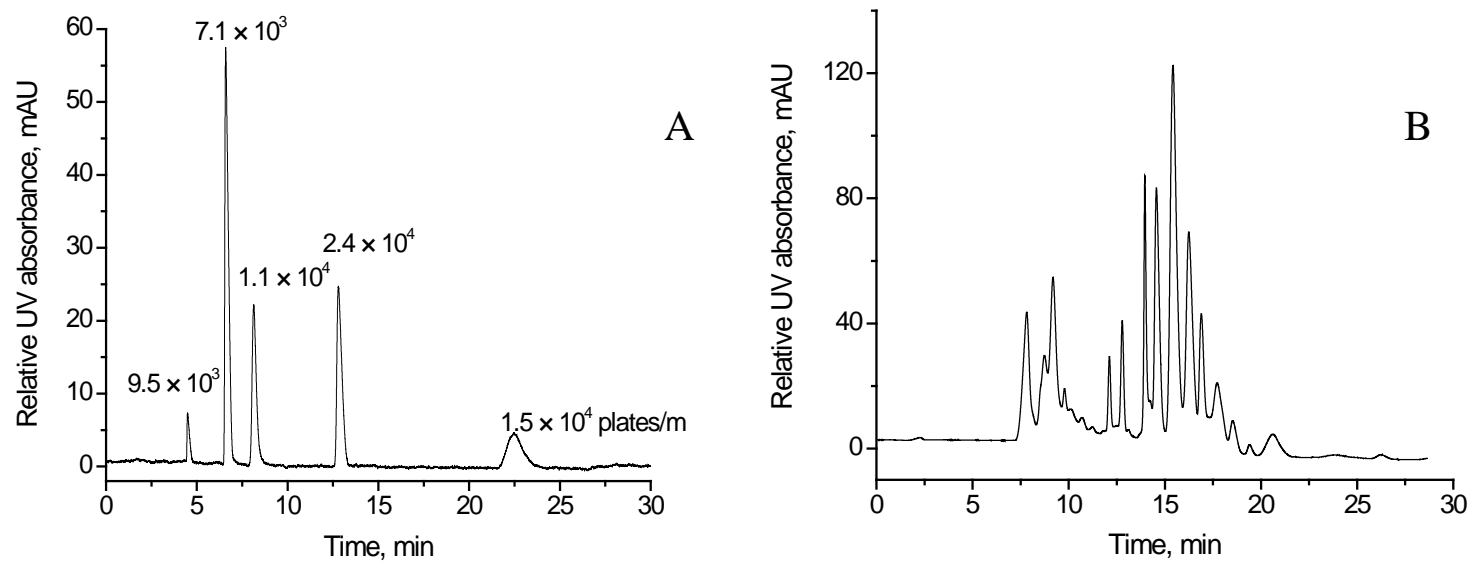
Figure 4.8. Separation of peptides and a protein digest. Conditions: 16.0 cm × 75 µm i.d. column 8; buffer A was 5 mmol/L phosphate at pH 3.0, buffer B was 1 mol/L NaCl in buffer A; (A) isocratic separation of 100% buffer B; (B) linear gradient from 100% buffer A to 100% buffer B in 10 min; 40 µL/min pump flow rate; on-line UV detection at 214 nm. Peak identifications: A: (1) leucine enkephalin, (2) Gly-Tyr, (3) D-Leu-Gly, (4) angiotensin II, and (5) Gly-Gly-Tyr-Arg; B: cytochrome C digest.

previous literature report.[7] This column would be effective as the first dimension in two-dimensional proteomics applications.

4.3.8 Reproducibility of the Monoliths

The run-to-run and column-to-column reproducibilities were measured using column 8. For three consecutive separations of proteins, interspersed with 20 min equilibrations with 5 mmol/L sodium phosphate at pH 9.0, the RSDs of retention times for the five proteins were 1.47%, 1.5%, 0.46%, 0.94%, and 1.0%. The RSDs of peak widths for the five proteins were 3.1%, 8.37%, 6.2%, 0.83%, and 5.7%. These results indicate good run-to-run reproducibility, confirming the stability of the monolithic material. Column-to-column reproducibility was performed using three columns to separate CES P0050 under isocratic conditions with 20% (v/v) ACN in the mobile phase at pH 3.0. The RSDs of retention times for the four peptides were 3.5%, 3.0%, 2.6%, and 2.0%. The RSDs of peak widths for the four peptides were 16%, 15%, 9.4%, and 13%, which is not excellent, but good for research laboratory separations.

4.3.9 Separations of Deamidation Variants of Ribonuclease A

Deamidation of asparagine (Asn) residues is a common structural modification of recombinant proteins. It is observed in protein-based pharmaceuticals, including human growth hormone,[17] monoclonal antibodies,[18] and acidic fibroblast growth factor.[19] It affects the activity or the stability of the therapeutical protein.[20] Hence, monitoring the deamidation variants in proteins is important for quality control in pharmaceutical production. Donato et al.[21] used a cation exchange column, Mono S, followed by hydrophobic interaction chromatography to resolve two deamidation variants and ribonuclease A. It was concluded that the kinetics of deamidation were first order with a half life, $T_{1/2}$, of 178 h. Weitzhandler et al.[20] used a weak cation exchange column, ProPac WCX-10, to separate the two deamidation variants and the

native ribonuclease A. Kinetics of first order were observed with $T_{1/2}$ of 159 h. With monolithic column 8, deamidation variants having Asp and isoAsp at Asn[67] were separated from each other and from ribonuclease A (Figure 4.9). A first order reaction was observed with $T_{1/2}$ of 195 h (Figures 4.10A and 4.10B). Compared to the $T_{1/2}$ values of 159 and 178 h, the measured 195 h is larger, which might result from the use of an old ribonuclease A sample. Normally, the deamidation rate decreases with incubation time. As can be seen in Figure 4.9, an untreated sample already had some deamidation variants. Thus, a large $T_{1/2}$ would be expected.

4.3.10 Characterization and Merits of the Single Monomer Monolith

All BMEP monoliths were synthesized in 75 μm I.D. fused silica capillaries. Column pressure drops were measured using different solvents (i.e., water, methanol, and ACN) to evaluate the mechanical stabilities, particularly of monolithic column 8. A linear dependence of flow rate on column back pressure was observed (Figure 4.11), indicating that these monoliths were not compressed at least up to 3 mm/s (back pressure < 2000 psi).

Permeability measurements can be used to study the swelling and shrinking of a monolith. If a monolith swells, its throughpores decrease in size, resulting in lower permeability, and vice versa. The permeability was calculated using Darcy's law, $K= \eta uL/\Delta P$, where η is the dynamic viscosity of the mobile phase, L is the column length, u is the linear velocity of the mobile phase, and ΔP is the column pressure drop. The permeabilities of monolithic column 8 were measured as 9.86×10^{-15} m^2, 51.3×10^{-15} m^2, and 20.2×10^{-15} m^2 for water, methanol, and ACN, respectively. The permeability of the monolith was 5.2 times higher in methanol and 2.0 times higher in ACN than in water. These results indicate that the monolith swelled in aqueous solution. Due to the highly cross-linked structure of the monolith, the swelling may not result from the body of the monolith, but from the ionized functional groups due to the solvent effect.
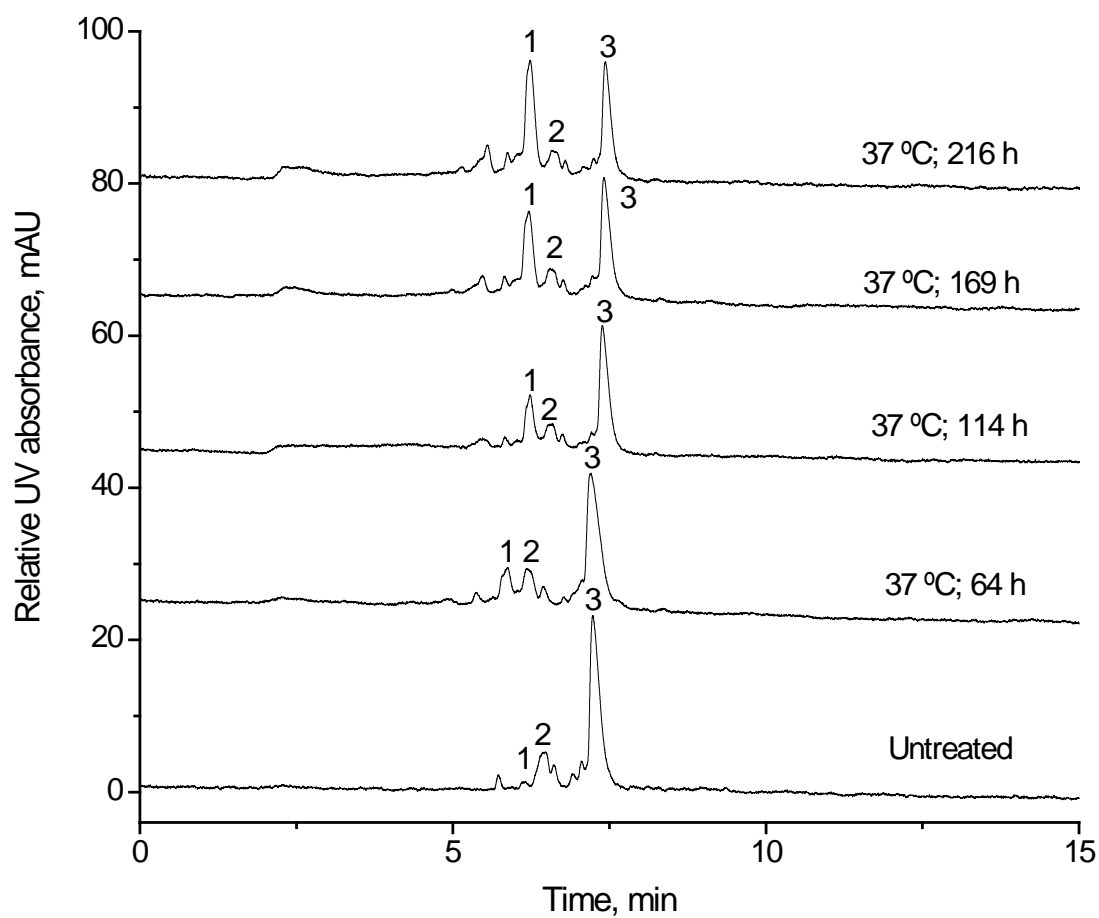
Figure 4.9. Separation of deamidation variants of ribonuclease A. Conditions: 16.0 cm × 75 µm I.D. column 8; buffer A was 5 mmol/L phosphate at pH 6.0, buffer B was 1 mol/L NaCl in buffer A; linear gradient from 80% buffer B to 90% buffer B in 15 min; 40 µL/min pump flow rate; on-line UV detection at 214 nm. Peak identifications: (1) and (2) are deamidation products (DP), and (3) is the native ribonuclease A.

Figure 4.10. (A) Formation of deamidation products as a function of the full incubation time of 216 h and (B) formation of deamidation products as a function of the first 169 h.

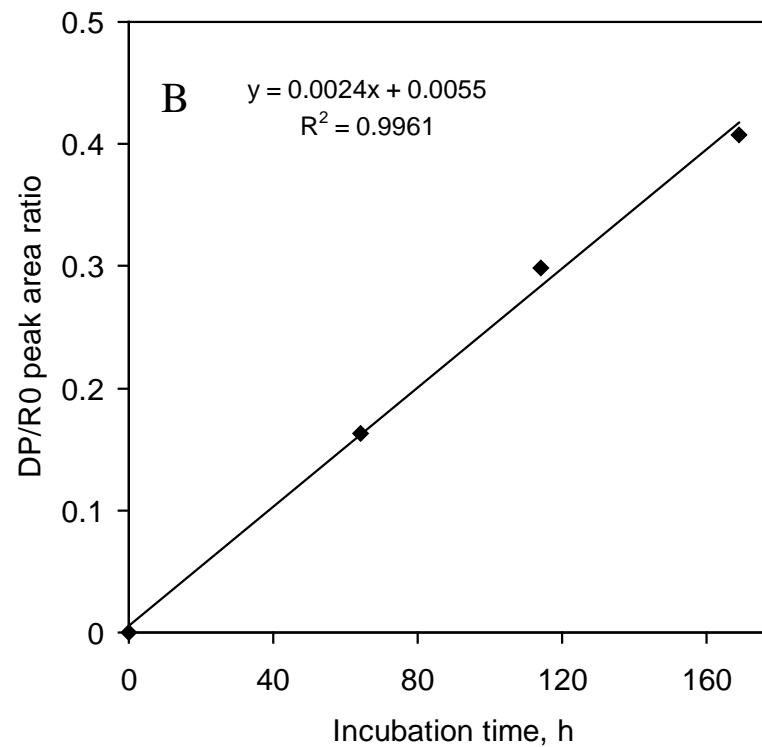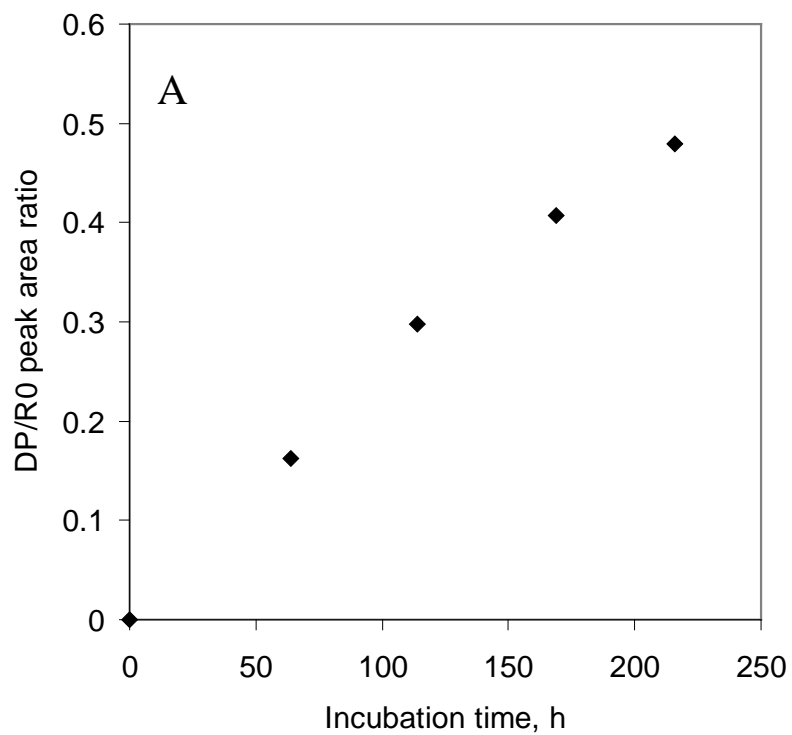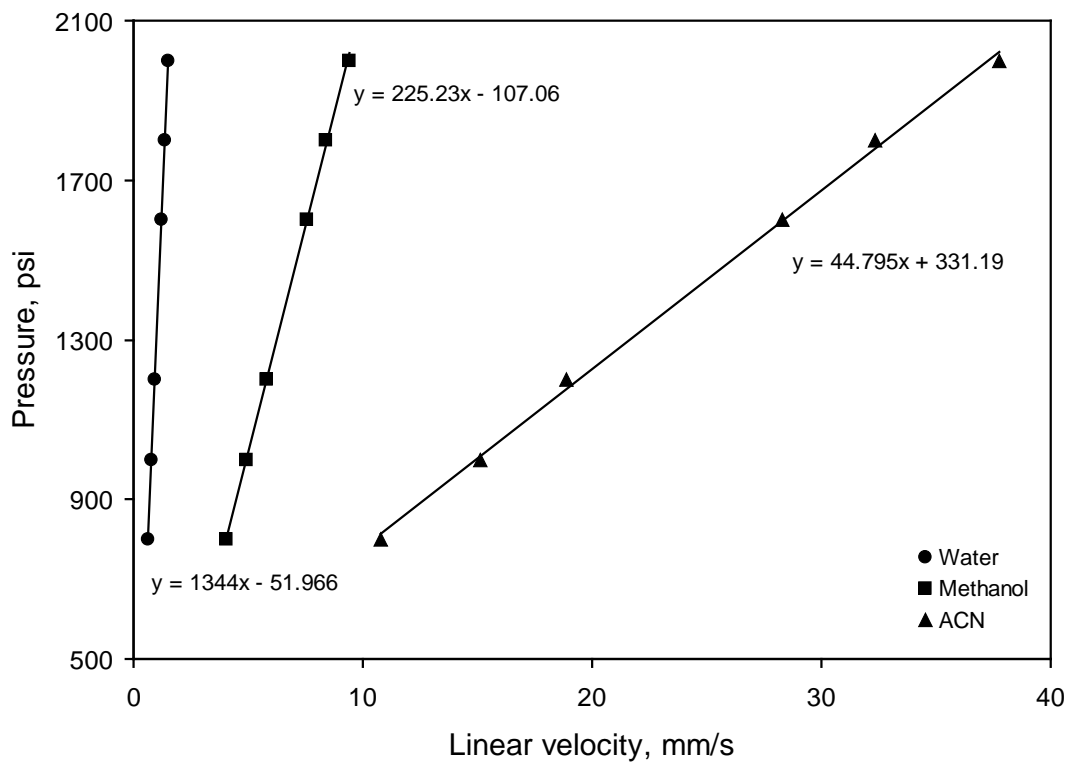Figure 4.11. Effect of mobile phase flow rate on column back pressure for 10.0 cm × 75 µm I.D. column 8. Flow rates were measured for pressures of 800, 1000, 1200, 1600, 1800, and 2000 psi.

During testing with different solvents, no detachment of the monolith from the capillary wall was observed. The flow rate reached a constant value after equilibration with a new solvent in 3 min, indicating that swelling and shrinking was reversible.

4.4 Conclusions

Cation exchange polymeric monoliths were prepared by *in situ* photo-initiated copolymerization in 75 μm I.D. capillaries using BMEP as a single monomer. The resulting monoliths provided relatively high dynamic binding capacities, and permeabilities, and low back pressure. These monolithic columns were used for IEC of peptides and proteins. Good separation of peptides and proteins was achieved, and good stabilities and reproducibilities were observed. The monoliths showed negligible hydrophobicity for separations of peptides and proteins.

Compared to monoliths prepared from two monomers (i.e., monomer and cross-linker), monoliths prepared from only one monomer showed some advantages. The highly cross-linked structure makes them more stable. A single monomer reduces the complexity in preparation of the monolith and, thus, leads to improved reproducibility, as well as ease in finding suitable porogen solvents. Based on the phase separation mechanism,[10] highly cross-linked polymers appear in the early stage of the polymerization process and, therefore, lead to early phase separation. The extent of cross-linking affects swelling of the polymers in the porogens, leading to small nuclei. These pre-globules can capture some of the nuclei generated at later stages to form large pores. Consequently, monoliths prepared with a single monomer have a bimodal pore size distribution. Although polymeric monoliths are mainly used for separation of large molecules such as proteins, monoliths prepared by this method most likely can be used to separate compounds from low to high molecular weights.[1,2,14]

4.5 References

1. Lubbad, S. H.; Buchmeiser, M. R. *J. Sep. Sci* **2009**, *32*, 2521-2529.

2. Greiderer, A.; Ligon Jr., S. C.; Huck, C. W.; Bonn, G. K. *J. Sep. Sci.* **2009**, *32*, 2510-2520.

3. Gu, B.; Li, Y.; Lee, M. L. *Anal. Chem.* **2007**, *79*, 5848-5855.

4. Vidic, J.; Podgornik, A.; Štrancar, A. *J. Chromatogr. A* **2005**, *1065*, 51-58.

5. Gu, B.; Chen, Z.; Thulin, C. D.; Lee, M. L. *Anal. Chem.* **2006**, *78*, 3509-3518.

6. Chen, X.; Tolley, H. D.; Lee, M. L. *J. Sep. Sci.* **2009**, *32*, 2565-2573.

7. Krenkova, J.; Gargano, A.; Lacher, N. A.; Schneiderheinze, J. M.; Svec, F. *J. Chromatogr. A* **2009**, *1216*, 6824-6830.

8. http://www.dionex.com/en-us/webdocs/4458-AN125-Cation-Exchange-26Jun09-LPN1045-02.pdf

9. Chen, X.; Tolley, H. D.; Lee, M. L. *J. Chromatogr. A* **1217**, *2010*, 3844-3854.

10. Viklund, C.; Svec, F.; Fréchet, J. M. J. *Chem. Mater.* **1996**, *8*, 744-750.

11. Burke, T. W. L.; Mant, C. T.; Black, J. A.; Hodges, R. S. *J. Chromatogr.* **1989**, *476*, 377-389.

12. Wang, F.; Dong, J.; Jiang, X.; Y, M.; Zou, H. *Anal. Chem.* **2007**, *79,* 6599-6606..

13. Weitzhandler, M.; Farnan, D.; Horvath, J.; Rohrer, J. S.; Slingsby, R. W.; Avdalovic, N.; Pohl, C. *J. Chromatogr. A* **1998**, *828*, 365-372.

14. Greiderer, A.; Trojer, L.; Huck, C. W.; Bonn, G. K. *J. Chromatogr. A* **2009**, *1216*, 7747-7754.

15. Bouhallab, S.; Henry, G.; Boschetti, E. *J. Chromatogr. A* **1996**, *724*, 137-145.

16. Mant, C. T.; Hodges, R. S. *J. Chromatogr.* **1985**, *326*, 349-356.

17. Johnson, A. B.; Shirokawa, J. M.; Hancock,W. S.; Spellman, M. W.; Basa, L. J.; Aswad, D.

W. *J. Biol. Chem.* **1989**, *624*, 14262-14271.

18. Cacia, J.; Quan, C. P.; Vasser, M.; Sliwkowski, M. B.; Frenz, J. *J. Chromatogr.* **1993**, *634*, 229-239.

19. Volkin, D. B.; Verticelli, A. M.; Bruner, M. W.; Marfia, K. E.; Tsai, P. K.; Middaugh, C. R.; Sardana, M. K. *J. Pharmaceu. Sci.* **2006**, *84*, 7-11.

20. Weitzhandler, M.; Farnan, D.; Rohrer, J. S.; Avdalovic, N. *Proteomics* **2001**, *1*, 179-185.

21. Donato, A. D.; Ciardiello, M. A.; Nigris, M. D.; Piccoli, R.; Mazzarella, L.; D'Alessio, G. *J. Biol. Chem.* **1993**, *268*, 4745-4751.

CHAPTER 5 WEAK CATION-EXCHANGE MONOLITHIC COLUMNS CONTAINING CARBOXYLIC ACID FUNCTIONAL GROUPS

5.1 Introduction

Compared to strong cation-exchange columns, there are significantly fewer reports of the synthesis of weak cation-exchange columns by copolymerization. Two reasons for this have been proposed. First, monomers containing carboxylic acid functional groups for weak cation-exchange chromatography are less available than monomers for strong cation-exchange chromatography. Second, weak cation-exchange columns are affected more by mobile phase pH, and can even completely lose any separation ability under certain pH conditions. In contrast, strong cation-exchange columns operate over a wider pH range. To best knowledge, only a few reports of weak cation-exchange monolithic columns prepared by copolymerization have been published. For example, Thabano et al.[1,2] synthesized a weak cation-exchange poly(methacrylic acid-co-ethylene glycol dimethacrylate) monolith in the front end of a capillary electrophoresis column for solid phase extraction (SPE) of neurotransmitters. At pH 7.0, which is higher than the pKa of carboxylic acid groups, analytes were adsorbed by the monolithic SPE phase. Elution of the analytes was achieved at pH 3.0. The method allowed adsorbed analytes to be simultaneously focused during elution, giving efficient transfer from the preconcentration zone into the separation section of the capillary. As a result, the detection limits were lowered by two orders of magnitude compared to capillary electrophoresis with conventional hydrodynamic injection. Zhu and Row[3] also prepared a poly(methacrylic acid-co-ethylene glycol dimethacrylate) monolith for on-line SPE before analysis of caffeine and theophylline in human urine.

In this chapter, weak cation-exchange monolithic columns were prepared by direct copolymerization of 2-carboxyethyl acrylate (CEA, Figure 5.1) and polyethylene glycol
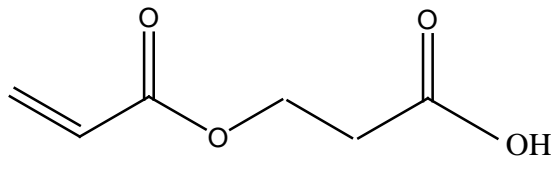
2-Carboxyethyl acrylate (CEA)
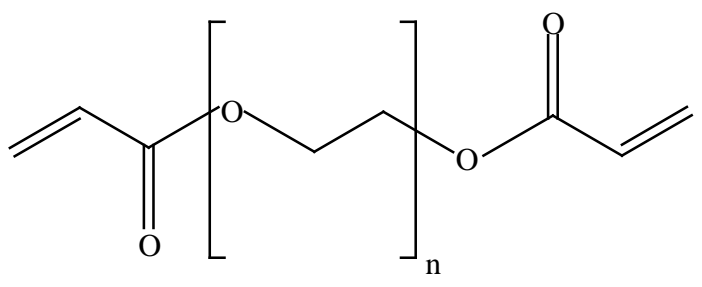
Polyethylene glycol diacrylate (PEGDA)

Figure 5.1. Chemical structures of CEA and PEGDA.

diacrylate (PEGDA, Mn ~ 258, Figure 5.1) in 75 µm I.D. fused-silica capillaries by photoinitiated polymerization. The synthesized monoliths were utilized in IEC to separate standard peptides and proteins. The effects of functional group concentration, salt gradient programming rate, and buffer pH on chromatographic performance were studied.

5.2 Experimental

5.2.1 Reagents and Chemicals

2,2-Dimethoxy-2-phenylacetophenone (DMPA, 99%), 3-(trimethoxysilyl) propyl methacrylate (TPM) (98%), poly(ethylene glycol) diacrylate (PEGDA, Mn ~ 258), uracil, and CEA were purchased from Sigma-Aldrich (Milwaukee, WI, USA). Protein standards (i.e., ribonuclease A from bovine pancreas, cytochrome C from bovine heart, α-chymotrypsinogen A from bovine pancreas, and lysozyme from chicken egg white) were purchased from Sigma-Aldrich. A synthetic peptide standard (CES-P0050) was obtained from Alberta Peptides Institute (Edmonton, Alberta, Canada). Propyl paraben was purchased from Spectrum (Gardena, CA, USA). Porogenic solvents for monolith synthesis and chemicals for mobile phase preparation were HPLC or analytical reagent grade.

5.2.2 Polymer Monolith Preparation

UV-transparent fused-silica capillaries (75 µm I.D. × 360 µm O.D., Polymicro Technologies, Phoenix, AZ, USA) were first silanized with TPM to introduce pendant vinyl groups to anchor the polymer monolith to the capillary wall.[4] The monoliths were prepared as previously described.[4] Each polymerization mixture was prepared in a 4-mL glass vial by mixing initiator, monomer, cross-linker, and porogens (Table 5.1). The mixture was vortexed and ultrasonicated for only 30 s, considering the volatility of ethyl ether, to help form a homogeneous solution and eliminate oxygen. Subsequently, the reaction solution was introduced into the

Table 5.1. Reagent compositions and physical properties of monoliths.

Monolith	Reagent compositions						Physical properties			
	CEA (g)	PEGDA (g)	Methanol (g)	Ethyl ether (g)	DMPA (g)	UV time (s)	DBC (mg/mL)	Permeability ($\times 10^{-15}$ m^2)	Porosity (%)	Retention factor
M1	0.20	0.24	0.30	0.50	0.005	210	86.3	3.23	58.3	0.74
M2	0.20	0.24	0.20	0.60	0.005	210	72.7	6.41	63.4	0.58
M3	0.24	0.20	0.20	0.60	0.005	210	108	8.12	69.6	0.97

capillary by capillary action. The capillary was placed directly under a PRX 1000-20 Exposure Unit UV lamp (TAMARACK Scientific, Corona, CA, USA),which was fitted with a 1000 W Hg/Xe lamp for exposure at a constant intensity of 8 mW/cm^2 for 210 s. The resulting monolith was then flushed with methanol and water sequentially for 30 min each using an LC pump to remove porogens and unreacted monomers. The capillaries were stored in 10% methanol aqueous solutions to prevent the monoliths from drying. Scanning electron microscopy (SEM) images of the monoliths were obtained as previously described.[4]

5.2.3 Capillary LC

Capillary LC of peptides and proteins was performed using an LC system comprised of two ISCO 100 DM syringe pumps and a flow controller. A Valco splitting tee (Houston, TX) was positioned between the static mixer of the syringe pumps and the 60-nL Valco internal loop sample injector. A 40-cm-long capillary (30 µm I.D.) was used as a capillary splitter and a 10-cm-long capillary (30 µm I.D.) was connected between the splitting tee and the injector. The mobile phase flow rate was set at 40 µL/min, and the linear velocity in the monolithic capillary column was approximately 1 mm/s. The mobile phase was 5 mmol/L aqueous phosphate buffer prepared with various pH values. All mobile phases were filtered through a 0.2 µm Nylon membrane filter (Supelco, Bellefonte, PA, USA). A Model UV3000 detector from Thermo Separations (San Jose, CA, USA) was used at a wavelength of 214 nm. Data were acquired with ChromQuest 2.5.1 software (Thermo Separations). Detailed chromatographic conditions are given in the figure captions.

For evaluation of the relative hydrophobicities of the monoliths, capillary reversed-phase LC elution measurements of propyl paraben and uracil were performed. The mobile phase was 20% (v/v) acetonitrile in 5 mmol/L phosphate buffer at pH 6.0. The pump flow rate was 40

µL/min, and the detection wavelength was 214 nm. Uracil was used as an unretained marker. The retention factor for propyl paraben was obtained from the equation, $k = (t_p - t_u)/t_u$, where k is the retention factor, and t_p and t_u are the retention times of propyl paraben and uracil, respectively. To investigate the permeabilities of the resulting monolithic columns, pressure drop measurements were made using 5 mmol/L phosphate buffer at pH 6.0 as the permeating fluid at flow rates of 50 nL/min to 300 nL/min.

5.2.4 DBC measurements

The DBC was examined via frontal analysis following a procedure described previously.[5] The column was first equilibrated with 5 mmol/L sodium phosphate buffer at pH 6.0, and then a solution of 3.00 mg/mL lysozyme in buffer was pumped through the column at a flow rate of 40 µL/min. The mobile phase flow rate in the monolithic capillary column was measured using a calibration capillary (Eksigent, Livermore, CA, USA). The binding capacity was calculated at 50% of the final absorbance value of the breakthrough curve and expressed in mg/mL of column volume.

5.3 Results and Discussion

5.3.1. Preparation of Polymeric Monoliths

CEA was selected as a monomer to prepare weak cation-exchange monoliths because it contains the desired carboxylic acid functional group. Ostuni et al. proved that a surface coated with PEG effectively resisted the adsorption of proteins.[6] PEG and PEG-containing materials have been used in many applications, including capillary gel electrophoresis matrices and artificial organ coatings.[7,8] PEG materials have demonstrated suppression of nonspecific interactions.[4,9] Therefore, PEGDA was selected as cross-linker to prepare the weak cation-exchange monoliths.

Methanol is a common solvent used in preparation of monoliths containing PEG functional groups due to its good solubility.[4,9-11] Therefore, methanol was chosen as the initial porogen solvent to prepare the poly(CEA-co-PEGDA) monoliths. With methanol as the only porogen solvent, a white translucent gel structure was observed, which indicated that small pores occupied most of the column volume and confirmed that methanol was a small-pore forming solvent. In order to increase the pore size, an addition of a larger-pore forming solvent was required. Ethyl ether is also an effective porogen solvent for monoliths synthesized from PEG-based monomers. By combining methanol and ethyl ether as porogen solvents, poly(CEA-co-PEGDA) monoliths were prepared, where ethyl ether served as a macropore forming solvent. It was found that absence of ethyl ether or excess of methanol led to a translucent gel structure.

SEM provided direct images of the poly(CEA-co-PEGDA) monoliths (Figure 5.2). As can be seen, these monoliths were uniform and firmly bonded to the capillary wall. The morphology of monolith M1 was different from those of M2 and M3, which have similar morphologies. The through-pores of the monoliths are obvious. Conventional polymer monolithic morphology with mostly discrete microglobules is observed in Figure 5.2B. Spherical units are aggregated into large clusters in monoliths M2 and M3 (Figures 5.2D and 5.2F).

5.3.2 Stability of Poly(CEA-co-PEGDA) Monoliths

Monoliths (M1, M2, and M3 in Table 5.1) were synthesized in 75 µm I.D. fused-silica capillaries. Column pressure drops were measured using 5 mmol/L phosphate buffer at pH 6.0 to evaluate the mechanical stabilities of the synthesized monoliths. A linear dependence of flow rate on column back pressure was observed (Figure 5.3), indicating that these monoliths were not compressed at least up to a linear velocity of 1.5 mm/s.
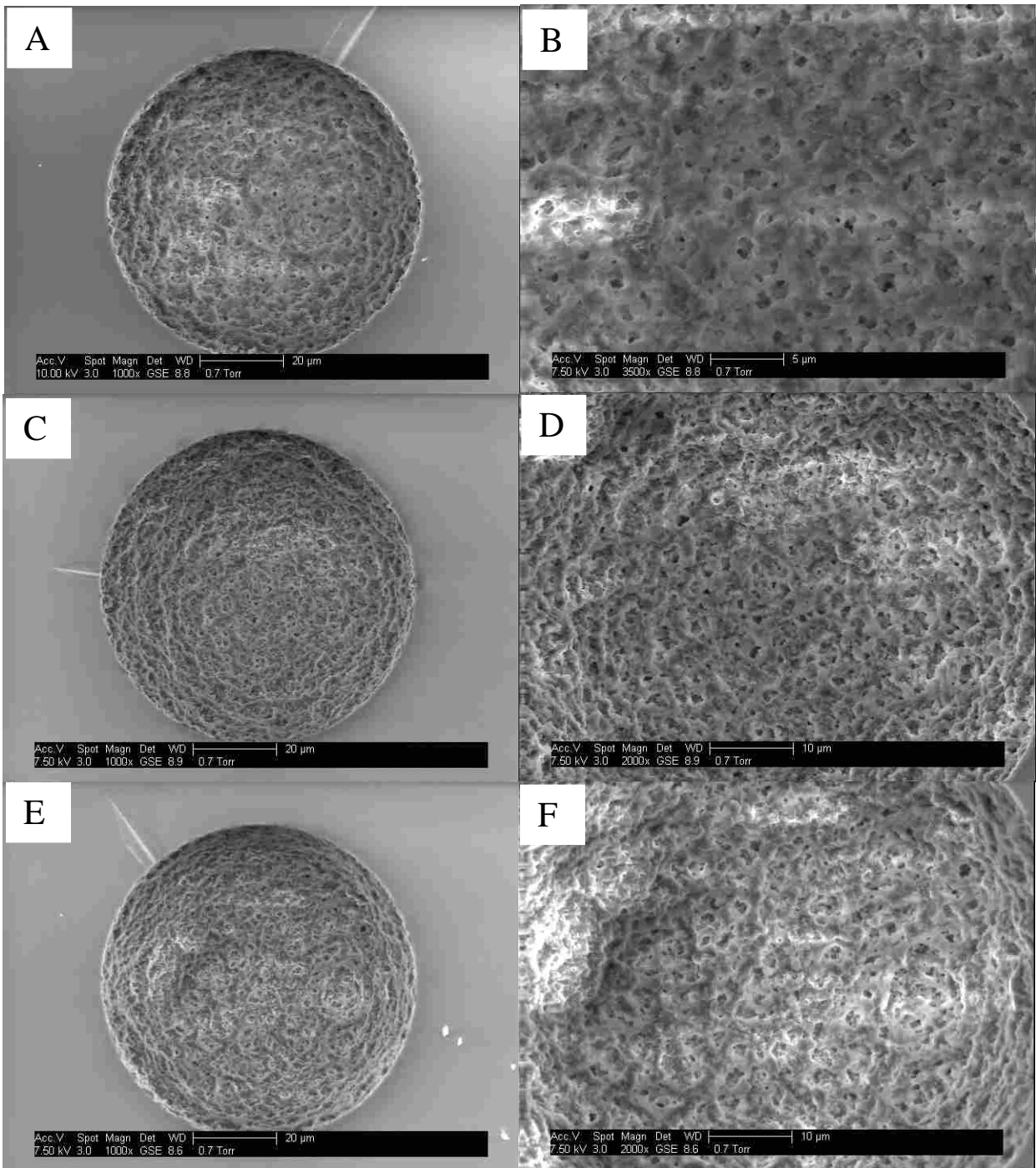
Figure 5.2. Scanning electron micrographs of (A) monolith M1 (scale bar, 20 µm), (B) monolith M1 (scale bar, 5 µm), (C) monolith M2 (scale bar, 20 µm), (D) monolith M2 (scale bar, 10 µm), (E) monolith M3 (scale bar, 20 µm), and (F) monolith M3 (scale bar, 10 µm).
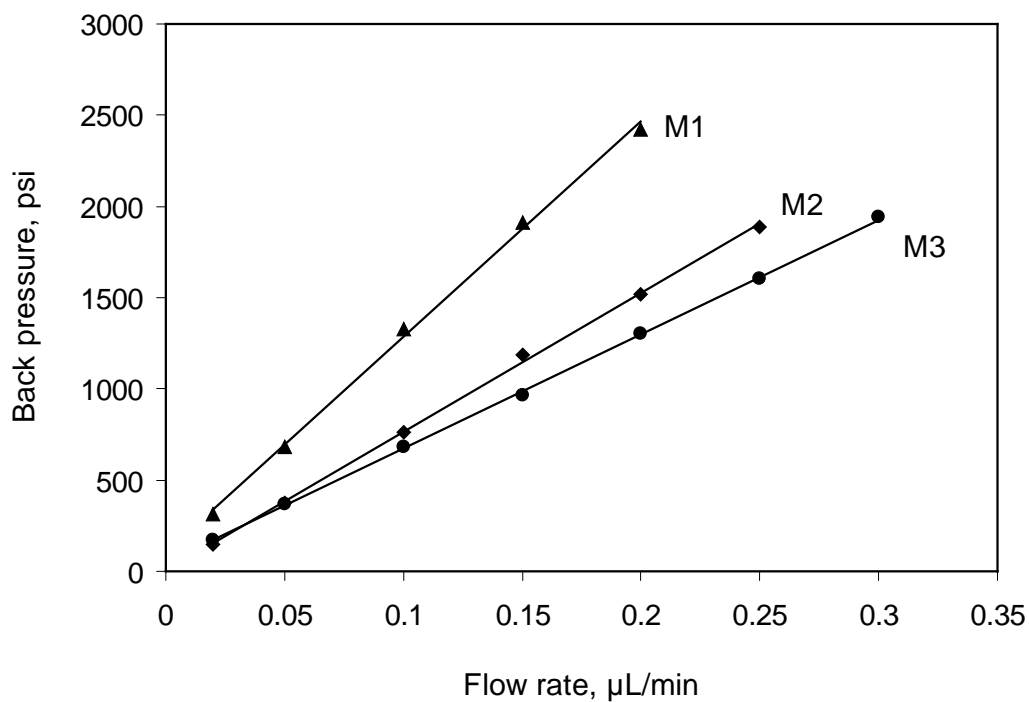
Figure 5.3. Back pressure dependency on flow rate for column M1, M2, and M3. Conditions: 9.30, 10.0, and 10.3 cm × 75 µm I.D. column for M1, M2, and M3, respectively; mobile phase, 5 mmol/L phosphate buffer at pH 6.0.

Permeability represents the ability of a liquid to flow through a chromatographic column. The permeability was calculated using Darcy's law, $K = \eta uL/\Delta P$, where η is the dynamic viscosity of the mobile phase, L is the column length, u is the linear velocity of the mobile phase, and ΔP is the column pressure drop. Obviously in Table 5.1, the permeability of M1 is less than that of M2, which is less than that of M3. The larger permeability of M2 over M1 confirmed that ethyl ether is a macropore forming solvent. Compared M2 to M3, a decrease in cross-linker led to an increase in permeability. Thus, it can be concluded that an increase in cross-linker in the monomers leads to a higher cross-linked structure with lower porosity and lower permeability. This is consistent with reports that a high proportion of cross-linker in the monomer mixture decreases the average pore size by early formation of highly cross-linked globules with a reduced tendency to coalesce.[12] Greater retention factors of analytes on M3 compared to M2 indicated that CEA is more hydrophobic than PEGDA.

5.3.3 DBC of Poly(CEA-co-PEGDA) Monoliths

DBC is an important property of ion-exchange columns, which affects column resolution and loadability. Using frontal analysis, the DBC was measured as reported previously.[5] A 3.00 mg/mL lysozyme solution was used to determine the DBC of the poly(CEA-co-PEGDA) monolithic columns. Using frontal analysis, the DBC values were measured to be 86.3, 72.7, and 108 mg/mL of column volume for monoliths M1, M2, and M3, respectively. The sharp frontal analysis curves indicated rapid adsorption of lysozyme on these monoliths (Figure 5.4). The DBC of the poly(CEA-co-PEGDA) monoliths was superior to those of weak cation-exchange monolithic columns that have been reported previously.[13,14] The DBC of the monolith grafted with acrylic acid was less than 30 mg/mL.[13] The DBC values of the poly(CEA-PEGDA) monolith are larger than those of some commercial columns, such as 6 mg/mL for a ProPac
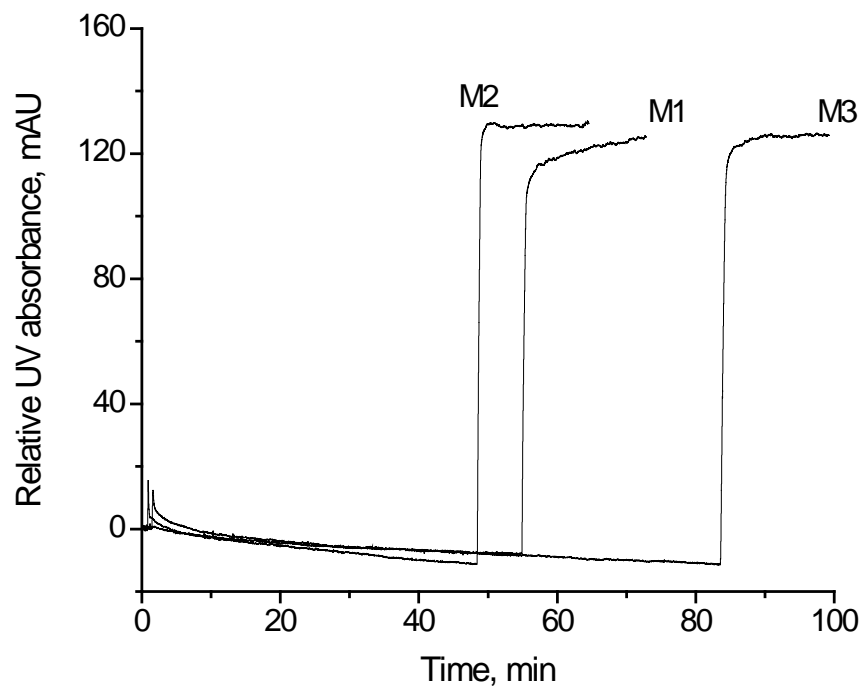
Figure 5.4. Breakthrough curves for lysozyme on monoliths. Conditions: 9.3, 10.0, and 10.3 cm × 75 µm

I.D. for columns M1, M2, and M3, respectively; 5 mmol/L phosphate at pH 6.0 mobile phase; 3.00

mg/mL lysozyme in the mobile phase; 40 µL/min pump flow rate; on-line UV detection at 214 nm.

WCX column,[14] 19.3 mg/mL for a ProSwift WCX-1S column (http://www.dionex.com), and 9 mg/mL for a monolithic CIM CM disk (http://www.biaseparations.com).

5.3.4 Effects of Porogen Solvents and Monomer Concentration on the Separation of Proteins

Selection of the porogen solvent(s) has a great effect on the morphology of the resulting monolith, thus, affecting significantly separation performance. Methanol is a "good" solvent, which leads to late phase separation during polymerization and results in small pores.[12] With more methanol in the porogens, the back pressure of the monolith increases, while the total porosity decreases (M1 and M2 in Table 5.1). M1 and M2 were used to separate a protein mixture containing ribonuclease A, cytochrome C, α-chymotrypsinogen A, and lysozyme (Figures 5.5A and 5.5B). It is obvious that proteins eluted earlier with higher resolution in M2 than in M1. The longer elution times for M1 may result from the higher DBC value of M1 and higher hydrophobicity of M1, which could also result in lower resolution of proteins.

The monomer concentration in the monolith alters both the monolith morphology and the monolith composition. With a higher ratio of monomer/cross-linker in the preparation of the monolith, the back pressure of the monolith decreased and the porosity increased (M2 and M3 in Table 5.1). With an increase in concentration of CEA in the monolith, the elution times for proteins increased (Figures 5.5B and 5.5C). It is reasonable to conclude that more carboxylic acid groups are exposed on the surface of the monolith, thus, leading to higher DBC value when higher CEA concentration is used in the monolith preparation. Unfortunately, ribonuclease A, cytochrome C, and α-chymotrypsingen A coeluted, possibly due to hydrophobic interactions between the proteins and monolith (Figure 5.5C). The tailing of the lysozyme peak in M3 is
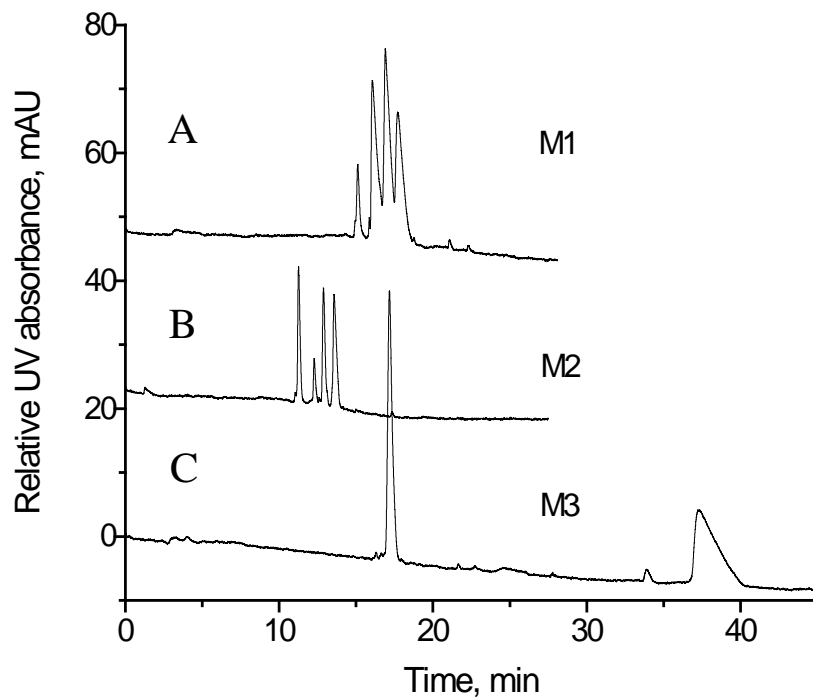
Figure 5.5. Separations of protein mixture. Conditions: 10.0 cm × 75 µm I.D. for (A) M1, (B) M2, and (C) M3 columns; buffer A was 5 mmol/L phosphate at pH 6.0, buffer B was 1 mol/L NaCl in buffer A; linear gradient from buffer A to buffer B in 10 min, followed by 100% buffer B; 40 µL/min pump flow rate; on-line UV detection at 214 nm. Peaks according to the elution order are α-chymotrypsinogen A, cytochrome C, ribonuclease A, and lysozyme.

obvious while M2 showed no obvious tailing of lysozyme, confirming that significant

hydrophobic interactions in M3 destroyed the separation of proteins.

5.3.5 Hydrophobic Interactions

Hydrophobic interactions between analytes and the column are detrimental for ion

exchange chromatography. Analyte retention is strongly affected by hydrophobic interactions

when using a high concentration of salt in the mobile phase. A pure ion exchange mechanism

can be achieved only when hydrophobic interactions are suppressed. The possible effect of

hydrophobic interactions on retention times of proteins was evaluated for M2 under isocratic

conditions. The mobile phase was 5 mmol/L sodium phosphate buffer at pH 6.0 containing

various concentrations of sodium chloride. As shown in Figre 5.6A, a linear dependence between

logarithm of retention factor and logarithm of salt concentration in the mobile phase indicates

that the separation was governed by a pure ion exchange mechanism.[15] The column exhibited

high efficiency for the separation of proteins without undesirable hydrophobic interactions. For

example, an efficiency of approximately 37,000 plates/m was achieved for separation of proteins

when 0.8 mol/L NaCl in 5 mmol/L sodium phosphate at pH 6.0 was used as mobile phase

(Figure 5.6B).

CES P0050 is a mixture of four undecapeptides designed for evaluation of particle

packed cation exhange columns.[16] The structures and physical properties of these peptides were

described previously.[4,16] The effects of acetonitrile (ACN) in the mobile phase on the retention

times of peptides (CES P0050) and on peak capacity were also used to evaluate hydrophobic

interactions. As shown in Figure 5.7, the retention times of peptides varied slightly with 0, 10,

and 20% (v/v) ACN in the mobile phase. The peak capacity (n = gradient time/peak width) also

varied only slightly. Similar retention times and constant peak capacity indicate that there are
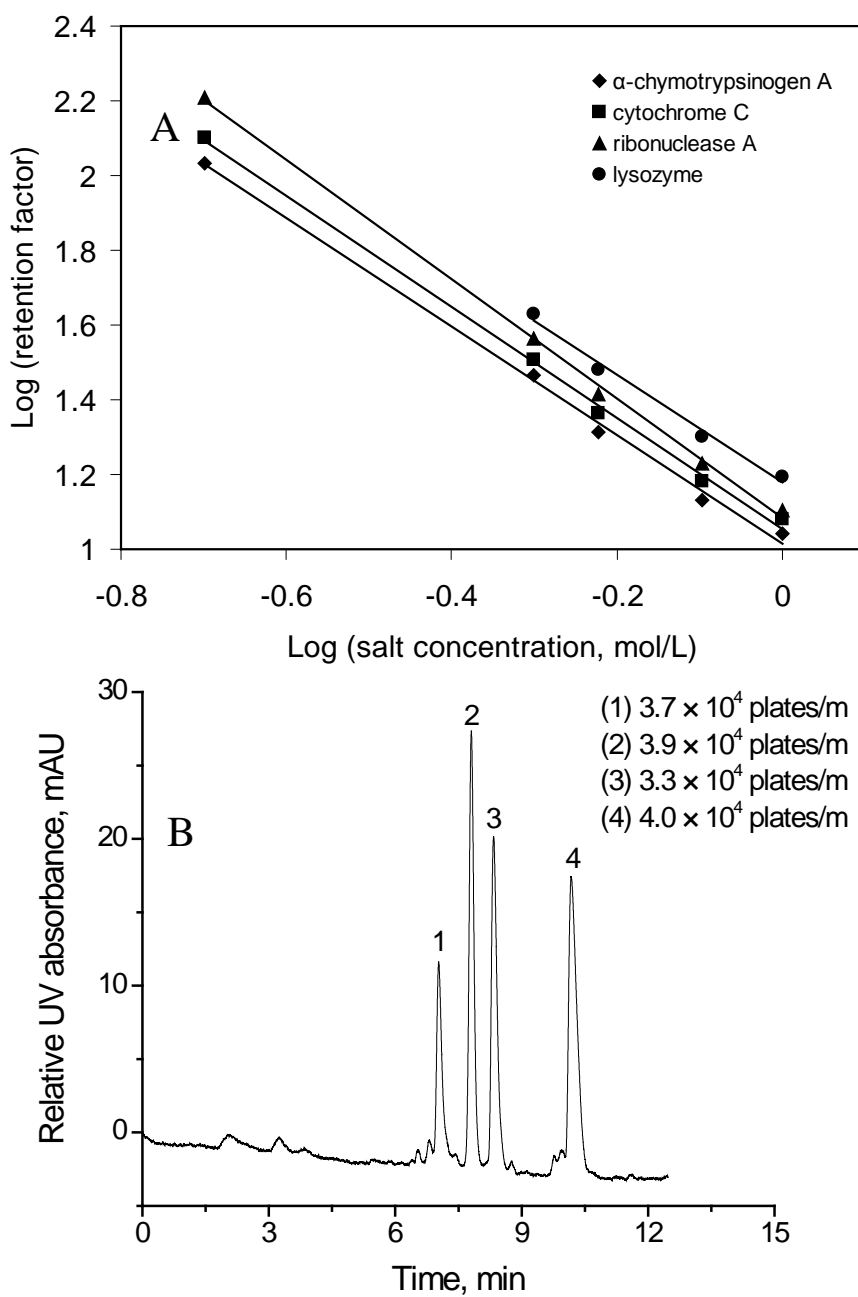
Figure 5.6. (A) Relationship between retention factor (k) and salt concentration and (B) representative chromatogram (0.8 mol/L NaCl concentration) for isocratic separation of proteins. Conditions: 10.0 cm × 75 µm I.D. column M2; buffer was 5 mmol/L phosphate with various salt concentrations at pH 6.0; 40 µL/min pump flow rate; on-line UV detection at 214 nm. Numbers in B represent the separation efficiency in plates/m. Peaks are (1) α-chymotrypsinogen A, (2) cytochrome C, (3) ribonuclease A, and (4) lysozyme.
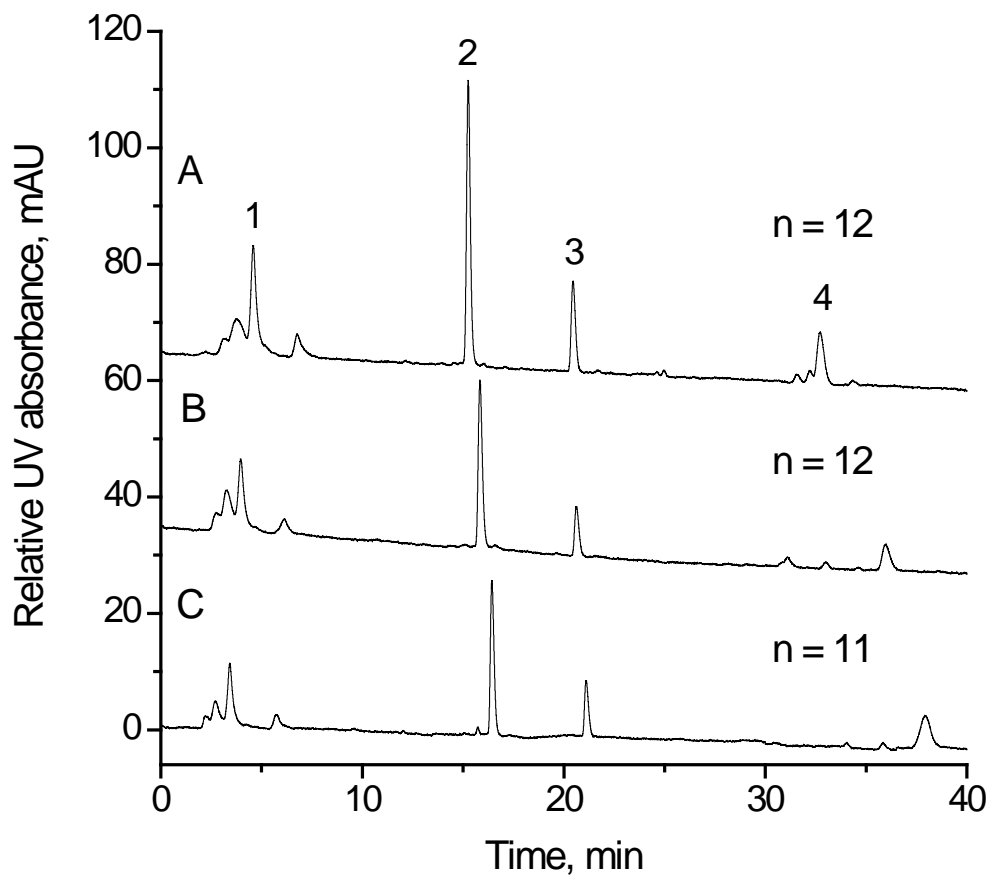
Figure 5.7. Effect of ACN in the mobile phase on the separation of peptides. Conditions: 10.0 cm × 75 µm I.D. column M2; buffer A was 5 mmol/L phosphate at pH 6.0 containing (A) 20, (B) 10, and (C) 0% (v/v) ACN, buffer B was 1 mol/L NaCl in buffer A; linear gradient from 100% buffer A to 100% buffer B in 10 min, followed by 100% buffer B; 40 µL/min pump flow rate; on-line UV detection at 214 nm. Peak identifications: (1) Ac-Gly-Gly-Gly-Leu-Gly-Gly-Ala-Gly-Gly-Leu-Lys-amide, (2) Ac-Lys-Tyr-Gly-Leu-Gly-Gly-Ala-Gly-Gly-Leu-Lys-amide, (3) Ac-Gly-Gly-Ala-Leu-Lys-Ala-Leu-Lys-Gly-Leu-Lys-amide, (4) Ac-Lys-Tyr-Ala-Leu-Lys-Ala-Leu-Lys-Gly-Leu-Lys-amide.

negligible hydrophobic interactions between peptides and the monolith. Compared to other weak cation-exchange monolithic columns,[17] monolithic column M2 exhibited very low hydrophobicity.

5.3.6 Effect of pH and Salt Gradient Rate on the Separation of Proteins

The pH of the mobile phase has an important effect on the separation of proteins in the ion-exchange mode by controlling the extent of ionization of the ion exchange functional groups and the analytes. For the poly(CEA-co-PEGDA) monolithic column M2, pH affected both the ion exchange functional groups and proteins. As shown in Figure 5.8, the retention times of proteins decreased with an increase in pH from 6.0 to 9.0. However, the effects for different proteins were not similar. This behavior was also previously described before.[18,19] Ribonuclease A eluted after α-chymotrypsinogen A and cytochrome C at pH 6.0, while it eluted between α-chymotrypsinogen A and cytochrome C at pH 7.0 and 8.0, but before them at pH 9.0. This effect can be used to optimize separations.

The effects of salt gradient rate on protein retention times, resolution, and peak capacity were examined using column M2 (Figure 5.9). Retention times and peak widths of proteins were reduced for steep salt gradient rates, exhibiting typical ion exchange behavior. Baseline separation was obtained with either steep (10% B/min, Figure 5.9B) or shallow (5% B/min, Figure 5.9C) salt gradient rates. With a salt gradient rate of 10% B/min, a peak capacity of 15 and resolution of 1.60 between α-chymotrypsinogen A and cytochrome C were measured. When the gradient rate was reduced to 5% B/min, the peak capacity increased to 39 and the resolution increased to 2.26. These results showed the expected trend that a shallow salt gradient rate yields better resolution and higher peak capacity. However, even with isocratic separation with 100% B/min (Figure 5.9A), the proteins can be baseline separated with excellent resolution.
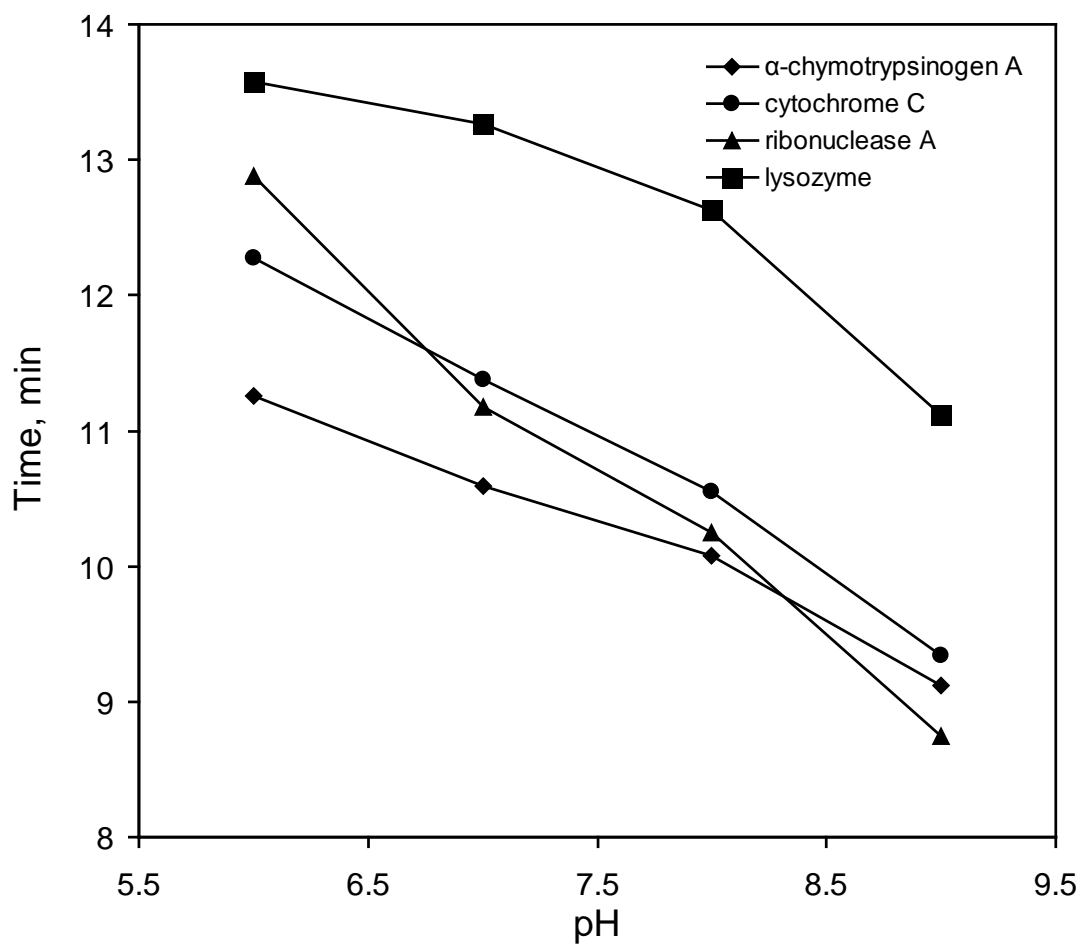
Figure 5.8. Effect of pH on the retention of proteins. Conditions: 10.0 cm × 75 µm I.D. column M2;

buffer A was 5 mmol/L phosphate at pH 6.0, 7.0, 8.0, and 9.0, buffer B was 1 mol/L NaCl in buffer A;

Other conditions are the same as in Figure 5.5.
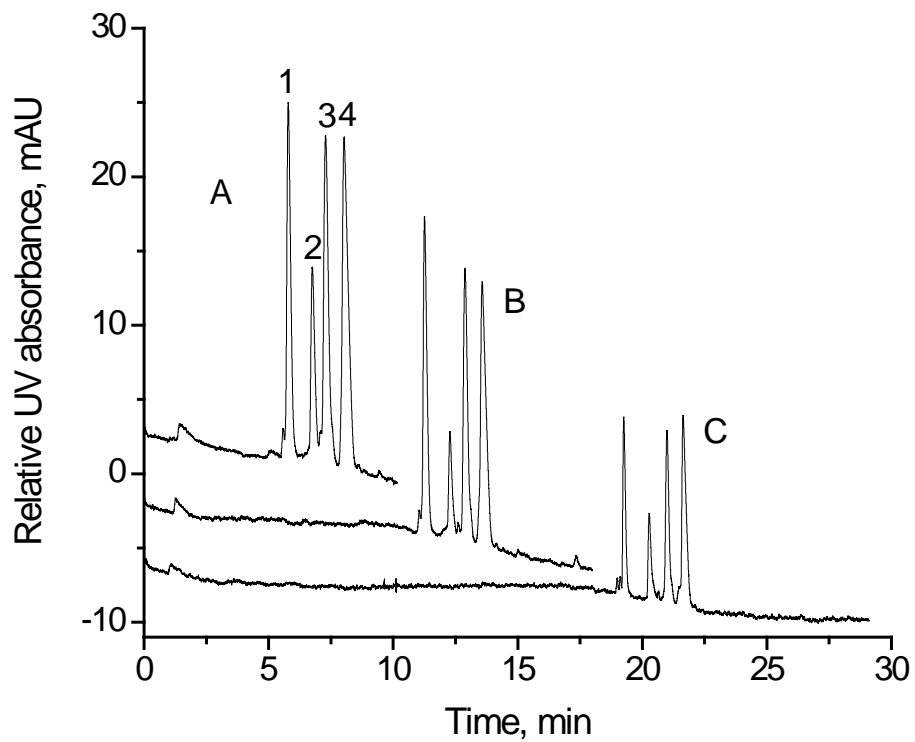
Figure 5.9. Separations of proteins with various salt gradient rates. Conditions are the same as in Figure 5.5, except that isocratic 100% buffer B for (A) and linear gradient from 100% buffer A to 100% buffer B in (B) 10 min, and (C) 20 min. Peak identifications: (1) α-chymotrypsinogen A, (2) cytochrome C, (3) ribonuclease A, and (4) lysozyme.

5.3.7 Reproducibility of Monoliths

The run-to-run and column-to-column reproducibilites were determined for monolithic column M2 (Table 5.2). For three consecutive runs interspersed with 30 min equilibrations under separation conditions listed in Figure 5.9B, the relative standard deviation (RSD) of the retention times was in the range of 0.93-1.97% for run-to-run reproducibility, which demonstrated that reproducible separations were achieved. Similarly, column-to-column reproducibility measurements gave RSD values of retention times of proteins ranging from 1.57 to 4.63% (n=3).

5.4. Conclusions

Stable weak cation-exchange monoliths were prepared by direct photo-initiated copolymerization of functional CEA monomer and PEGDA cross-linker in 75 µm I.D. capillaries in the presence of methanol and ethyl ether as porogen solvents. The resulting monoliths were evaluated for separation of peptides and proteins in the ion exchange mode. Good separations of peptides and proteins were achieved. Meanwhile, good stability and reproducibility of monolithic columns were obtained. It can be concluded that a high DBC value and low hydrophobicity contribute primarily to the good separation performance for peptides and proteins.

Table 5.2. Reproducibilities of the monolithic column M2.

Proteins	Run-to-run	Column-to-column
	RSD% of retention time	RSD% of retention time
α-Chymotrypsingen A	1.24	2.85
Cytochrome C	1.97	2.46
Ribonuclease A	1.27	4.63
Lysozyme	0.93	1.57

5.5 References

1. Thabano, J. R. E.; Breadmore, M. C.; Hutchinson, J. P.; Johns, C.; Haddad, P. R. *J. Chromatogr. A* **2007**, *1175*, 117-126.

2. Thabano, J. R. E.; Breadmore, M. C.; Hutchinson, J. P.; Johns, C.; Haddad, P. R. *Analyst* **2008**, *133*, 1380-1387.

3. Zhu, T.; Row, K. H. *Chromatographia* **2009**, *69*, 1477-1480.

4. Gu, B.; Chen, Z.; Thulin, C. D.; Lee, M. L. *Anal. Chem.* **2006**, *78*, 3509-3518.

5. Wang, F.; Dong, J.; Jiang, X.; Ye, M.; Zou, H. *Anal. Chem.* **2007**, *79*, 6599-6606.

6. Ostuni, E.; Chapman, R. G.; Holmlin, R. E.; Takayama, S.; Whitesides, G. M. *Langmuir* **2001**, *17*, 5605-5620.

7. Lee, J. H.; Kopecek, J.; Andrade, J. D. *J. Biomed. Mater. Res.* **1989**, *23*, 351-368.

8. Tan, H.; Yeung, E. S. *Electrophoresis* **1997**, *18*, 2893-2900.

9. Chen, X.; Tolley, H. D.; Lee, M. L. *J. Sep. Sci.* **2009**, *32*, 2565-2573.

10. Chen, X.; Tolley, H. D.; Lee, M. L. *J. Chromatogr. A* **2010**, *1217*, 3844-3854.

11. Gu, B.; Li, Y.; Lee, M. L. *Anal. Chem.* **2007**, *79*, 5848-5855.

12. Viklund, C.; Svec, F.; Fréchet, J. M. J.; Irgum, U. *Chem. Mater.* **1996**, *8*, 744-750.

13. Krenkova, J.; Gargano, A.; Lacher, N. A.; Schneiderheinze, J. M.; Svec. F. *J. Chromatogr. A* **2009**, *1216*, 6824-6830.

14. Weitzhandler, M.; Farnan, D.; Horvath, J.; Rohrer, J. S.; Slingsby, R. W.; Avdalovic, N.; Pohl, C. *J. Chromatogr. A* **1998**, *828*, 365-372.

15. Bouhallab, S.; Henry, G.; Boschetti, E. *J. Chromatogr. A* **1996**, *724*, 137-145.

16. Burke, T. W. L.; Mant, C. T.; Black, J. A.; Hodges, R. S. *J. Chromatogr.* **1989**, *476*, 377-389.

17. Gatschelhofer, C.; Mautner, A.; Reiter, F.; Pieber, T. R.; Buchmeiser, M. R.; Sinner, F. M. *J. Chromatogr. A* **2009**, *1216*, 2651-2657.

18. Yang, Y.; Harrison, K.; Kindsvater, J. *J. Chromatogr. A* **1996**, *723*, 1-10.

19. Wei, Y.; Huang, X.; Liu, R.; Shen, Y.; Geng, X. *J. Sep. Sci.* **2006**, *29*, 5-13.

CHAPTER 6 HYDROPHILIC INTERACTION ZWITTERIONIC MONOLITHIC COLUMNS FOR CAPILLARY LIQUID CHROMATOGRAPHY

6.1 Introduction

Since the completion of the human genome project, intense research in the life sciences has continued in areas referred to as genomics, proteomics, and metabolomics. Metabolites include many low-molecular-weight compounds, such as amino acids, nucleotides, steroids, lipids, and carboxylic acids that play vital roles in metabolic processes in the cell. Theses compounds are usually weakly retained in reversed-phase liquid chromatography (RPLC), which is the most widely used LC separation mode due to its versatility and ability to separate a wide variety of compounds.[1,2] As a complementary technique, hydrophilic interaction chromatography (HILIC) often provides excellent separation of polar compounds.[3]

Initially investigated by Alpert,[4] HILIC continues to grow in interest due to its complementary selectivity to RPLC and good compatibility with mass spectrometry. Similar to normal phase liquid chromatography (NPLC), HILIC is also based on the use of a stationary phase that is more hydrophilic than the mobile phase. However, an aqueous-organic mobile phase, usually containing more than 60% organic solvent, is used in HILIC instead of the completely non-aqueous mobile phase characteristic of NPLC. NPLC suffers from poor reproducibility, low solvating power for polar compounds, and poor ionization efficiency for mass spectrometry (MS). Due to the high organic solvent content in the mobile phase and ease of spraying, HILIC provides high MS sensitivity. The low viscosity of the mobile phase makes fast separation possible without generating high back pressures.

Retention in HILIC is believed to be caused by partitioning of the analytes between the bulk mobile phase and a water-rich layer immobilized on the stationary phase surface.[5] However,

a simple retention mechanism is not possible for most compounds. In addition to a partition mechanism, hydrogen bonding, dipole-dipole, ion-dipole, and ion-ion interactions are involved.[6-8] The dominating mechanism is dependent on the nature of the stationary phase, the buffer conditions, including organic solvent content, the type and concentration of salt, and the pH.[9]

Good separations of low-molecular weight polar compounds, such as carbohydrates, peptides, drugs and pharmaceuticals have been reported using HILIC.[10-14] Several reviews of HILIC have been published.[15-18] Various types of HILIC stationary phases have been developed including silica,[19-22] amino,[23] amide,[24,25] polyhydroxyethyl A,[26] diol,[27] cyclodextrin[28] and sulfoalkylbetain.[29] Among these stationary phases, those containing sulfoalkyl betain zwitterionic functional groups are attractive due to the weak electrostatic interactions between charged analytes and zwitterionic functional groups. Recently, commercial zwitterionic HILIC columns have been introduced.[29,30]

Several monolithic HILIC columns have been reported.[30-34] Jiang et al. reported two reasons for the slow development of monolithic columns for HILIC.[35] First, new optimized conditions must be determined due to the limited solubility of polar monomers in commonly used porogens and, second, only a few polar monomers are commercially available.

Zwitterionic ion-exchangers combine both anion- and cation-exchange groups in a single particle, thus, expanding ion exchange selectivity. In fact, simultaneous separation of anions and cations has been reported.[36] The combination of positively and negatively charged groups results in reduced shrinking and swelling and improved mechanical stability of the stationary phase compared to traditional ion-exchangers.[37] Zwitterionic ion-exchangers have been incorporated in both polymeric particles and monoliths. Jiang et al. prepared a series of polymer-based zwitterionic separation materials by a two-step reaction.[38-40] These materials were able to

separate inorganic anions and cations independently and simultaneously using aqueous solutions of perchloric acid and perchlorate salts as eluents. Similar materials were also used to separate both acidic and basic proteins in the ion-exchange mode.[41]

Viklund et al. prepared a zwitterionic monolith by photoinitiated copolymerization of N,N-dimethyl-N-methacryloxyethyl-N-(3-sulfopropy)ammonium betain (SPE, Figure 6.1) and ethylene dimethacrylate (EDMA) in a 2.7 mm I.D. glass column.[42] They also thermally grafted SPE on a rigid carrier poly(trimethylolpropane trimethacrylate-EDMA) monolith. Cytochrome C and lysozyme were separated in the ion-exchange mode using the grafted monolith. Recently, Jiang et al. synthesized a series of polymeric zwitterionic monolithic columns for HILIC by thermal-initiated copolymerization.[35,43,44] Acrylamides, benzoic acids, pyrimines, and peptides were well separated in the HILIC mode. Most monoliths reported for HILIC were prepared by thermal-initiated copolymerization instead of photo-initiated copolymerization. Compared to over 12 h for thermal-initiation copolymerization,[35] only several minutes were required for photo-initiated copolymerization.

In this study, a porous poly[SPE-co- poly(ethylene glycol) diacrylate (PEGDA)] monolithic column was synthesized by photo-initiated copolymerization of SPE and PEGDA inside a 75-μm-I.D. fused-silica capillary. PEGDA (Mw ~ 258, Figure 6.1), which contains three ethylene glycol units, has been shown to be more biocompatible and hydrophilic compared to EDMA.[45,46] The resulting monoliths were used to separate polar compounds such as amides, benzoic acids, and phenols. The effects of mobile phase pH, salt concentration, and organic solvent content in the mobile phase on separation of polar compounds were investigated.
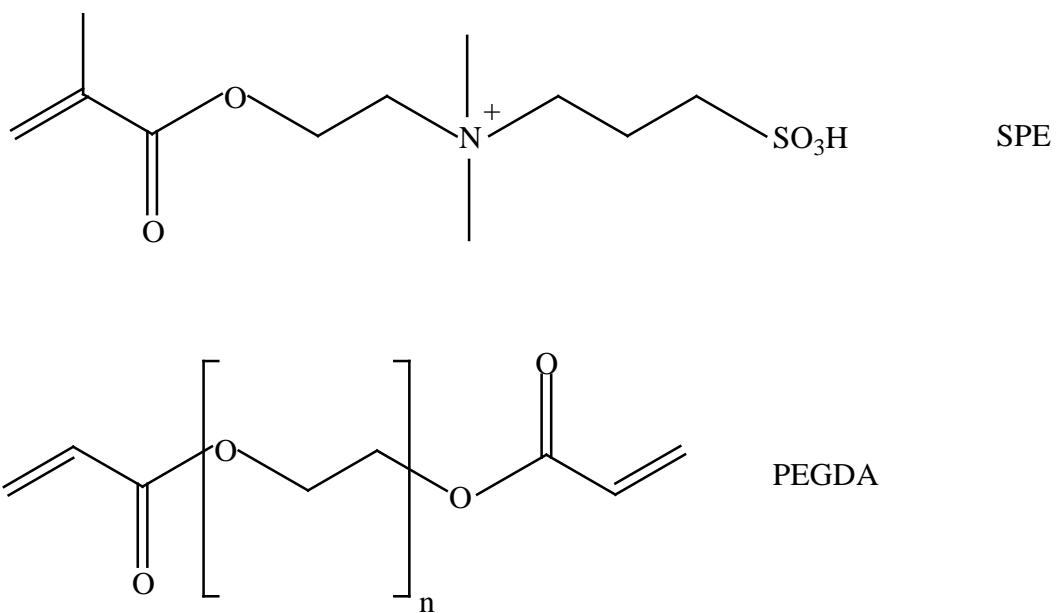
Figure 6.1. Chemical structures of SPE and PEGDA.

6.2 Experimental

6.2.1 Reagents and Chemicals

The hydrophilic functional monomer, SPE (80 wt% solution in water), 2,2-dimethoxy-2-phenylacetophenone (DMPA, 99%), 3-(trimethoxysilyl)propyl methacrylate (98%), and poly(ethylene glycol) diacrylate (PEGDA, Mn ~ 258) were purchased from Sigma-Aldrich (Milwaukee, WI) and used without further purification. Ammonium formate, formic acid, toluene and catechol were purchased from Fisher Scientific (Pittsburgh, PA). Analytes including benzoic acid (B), 2-hydroxybenzoic acid (2-HB), 3-hydroxybenzoic acid (3-HB), 3,4-dihydroxybenzoic acid (3,4-DHB), 2,4-dihydroxybenzoic acid (2,4 –DHB), 3,5-dihydroxybenzoic acid (3,5-DHB), 3,4,5-trihydroxybenzoic acid (3,4,5-THB), hydroquinone, phenol, pyrogallol, resorcinol, thiourea, formamide, N,N-dimethylacrylamide, acrylamide, and methacrylamide were also purchased from Sigma-Aldrich (Milwaukee, WI). All chemicals were of analytical grade and the water used was HPLC grade.

6.2.2. Instrumentation

HILIC was performed using a system previous described,[47] which included an Eksigent Nano 2D LC system (Dublin, CA) with a K-2600 UV detector (Sonntek, Upper Saddle River, NJ). The detection cell was a 3-nL ULT-UZ-N10 flow cell from LC packings (Sunnyvale, CA). A P-720 zero dead volume union (Upchurch, Oak Harbor, WA) was used to connect the column to the detection cell. The detection wavelength was set at 214 nm. The Eksigent V2.08 software was used for data acquisition and handling.

6.2.3. Preparation of Monolithic Columns

In order to anchor the polymer to the capillary wall, UV transparent fused-silica capillaries (75 µm I.D. × 360 µm O.D., Polymicro Technologies, Phoenix, AZ) were treated with

3-(trimethoxysilyl)propyl methacrylate to provide pendant vinyl groups as described previously.[47] SPE and PEGDA monomers, 2-propanol and decanol porogens, and DMPA initiator were mixed in a 4-mL glass vial. The mixture was vortexed and ultrasonicated for 2 min to help dissolve the monomers, eliminate oxygen, and yield a homogeneous solution. In order to obtain monoliths with high chromatographic efficiency and permeability, various ratios of monomers, porogens, and monomers to porogens were tested (Table 6.1). Each homogeneous solution was introduced into the capillary by capillary action. The capillary was placed directly under a PRX 1000-20 UV lamp Exposure Unit (TAMARACK Scientific, Corona, CA) for 3 min. The resulting monolith was then flushed with methanol and water sequentially for 30 min each with an LC pump to remove porogens and unreacted monomers. The capillary was filled with 10% methanol aqueous solution before storing to avoid drying the monolith. Scanning electron microscopy (SEM) images were obtained as previously described,[47] and the morphologies of the monoliths were observed from the SEM images.

6.2.4. Chromatographic Conditions

Due to the poor solubility of phosphate buffer in high organic solvent-containing mobile phases, ammonium formate was selected as a mobile phase buffer. Stock solutions (1 M) were prepared, and the pH was adjusted with formic acid and ammonium hydroxide. The mobile phase was prepared by mixing the desired amounts of ammonium formate solution, acetonitrile (ACN), and water. All samples were prepared in ammonium formate solutions containing 80% (v/v) ACN. The reported mobile phase pH refers to the aqueous portion only.

6.2.5. Inverse Size-Exclusion Chromatography (ISEC)

The liquid chromatographic system described previously was used for ISEC.[47] The mobile phase was THF and UV-sbsorption detection was at 254 nm. Polystyrene standards with

Table 6.1. Compositions of polymerization solutions used for the preparation of poly(SPE-co-PEGDA) monoliths.

Column	Monomers (%, w/w)		Porogens (%, w/w)		Monomers (%, w/w)	Porogens (%, w/w)	N_{max} (plates/m)	Permeability K ($\times 10^{-15}$ m^2)[a]
	SPE	PEGDA	Isopropanol	Decanol				
C1	45.5	55.5	80.0	20.0	30.6	69.4	8.31×10^3	16.7
C2	45.5	55.5	70.0	30.0	30.6	69.4	9.63×10^3	9.54
C3	45.5	55.5	60.0	40.0	30.6	69.4	15.4×10^3	6.79
C4	45.5	55.5	50.0	50.0	30.6	69.4	11.8×10^3	5.87
C5	45.5	55.5	40.0	60.0	30.6	69.4	14.8×10^3	3.54
C6	45.5	55.5	30.0	70.0	30.6	69.4	10.3×10^3	3.54
C7	45.5	55.5	60.0	40.0	40.0	60.0	1.71×10^3	7.39
C8	45.5	55.5	60.0	40.0	20.0	80.0	0.729×10^3	25.0
C9	55.5	45.5	60.0	40.0	30.6	69.4	9.60×10^3	7.20
C10	35.0	65.0	60.0	40.0	30.6	69.4	1.38×10^3	5.92

narrow molecular weight distributions and average molecular masses of 201, 2,460, 6,400, 13,200, 19,300, 44,100, 75,700, 151,500, 223,200, 560,900, 1,045,000, 1,571,000 and 1,877,000 were purchased from Scientific Polymer Products (Ontario, NY, USA) and prepared in THF (1 mg/mL each).

6.3. Results and Discussion

6.3.1. Optimization of Monolith Preparation

SPE was selected as monomer, since it is known to be hydrophilic.[38] SPE has positive and negative charged functionalities that can participate in both hydrophilic and ion exchange interaction mechanisms. PEGDA, which has an acrylate group at each end of the molecule and a three-unit ethylene glycol connecting chain, is a good cross-linker that has been shown to be more biocompatible and more hydrophilic than EDMA.[47] Therefore, PEGDA was chosen as the cross-linker.

While theories have been proposed for macroporous particle synthesis using suspension polymerization,[48,49] these theories are not suitable for monolith preparation. Generally, the morphology of a monolith is controlled by porogen solvent, temperature, monomer ratio, and ratio between monomers and porogen solvents.[50] Monoliths were started by reference to the poly(SPE-co-EDMA) monolith reported by Jiang et al.,[35] which was prepared in methanol by thermally initiated copolymerization. When EDMA was replaced by PEGDA, no monolith was observed. This indicated that methanol was a poor solvent, leading to large pore formation. Therefore, 2-propanol was substituted for methanol as the porogenic solvent, and a monolith was observed. Finally, a long chain alcohol, decanol, was selected to complement the short chain alcohol, 2-propanol, as a secondary porogenic solvent.

The effect of porogenic solvent on the preparation of monoliths was investigated (Table 6.1, C1-C6). Figures 6.2a, b, c, and d show scanning electron micrographs of monoliths C3, C2, and C5. It was observed that the morphologies of these monoliths were unique. In Figures 6.2a and b, spherical units are aggregated into large clusters. Conventional polymer monolithic morphology with discrete microglobules was formed. When the decanol percentage in the porogens increased from 20 to 30 and further to 60 wt%, the microglobules became fused and disappeared. In Figure 6.2d, the morphology appears to be a hybrid between a conventional polymer monolith with distinct particulate structure and a silica monolith with a skeletal structure. The throughpores in these monoliths are obvious. It was observed that the column backpressure increased with an increase in decanol in the porogens, indicating that decanol is a micropore-forming solvent.

Column efficiency was measured in 20% ACN aqueous solutions using uracil as the test analyte at a flow rate of 200 nL/min. C3 exhibited the highest chromatographic efficiency. The effect of porogens to monomer ratio on the preparation of monoliths was studied as well. Comparing C3 to C7, the chromatographic efficiency decreased dramatically from ~ 15,000 to ~1,700 plates/m as the porogen weight percentage decreased from 69.4% to 60.0%, and dropped even further to 700 plates/m when the porogen weight percentage increased from 69.4% to 80.0%. When the weight percentage of PEGDA varied from 45.5 to 65.0% (columns C3, C9, and C10), the chromatographic efficiency varied only slightly. Based on the above experiments, column C3, which was synthesized from 30.6 wt% monomers (SPE/PEGDA, 45.5:55.5, w/w) and 69.4 wt% porogens (isopropanol/decanol, 60:40, w/w), was finally selected for further experiments.
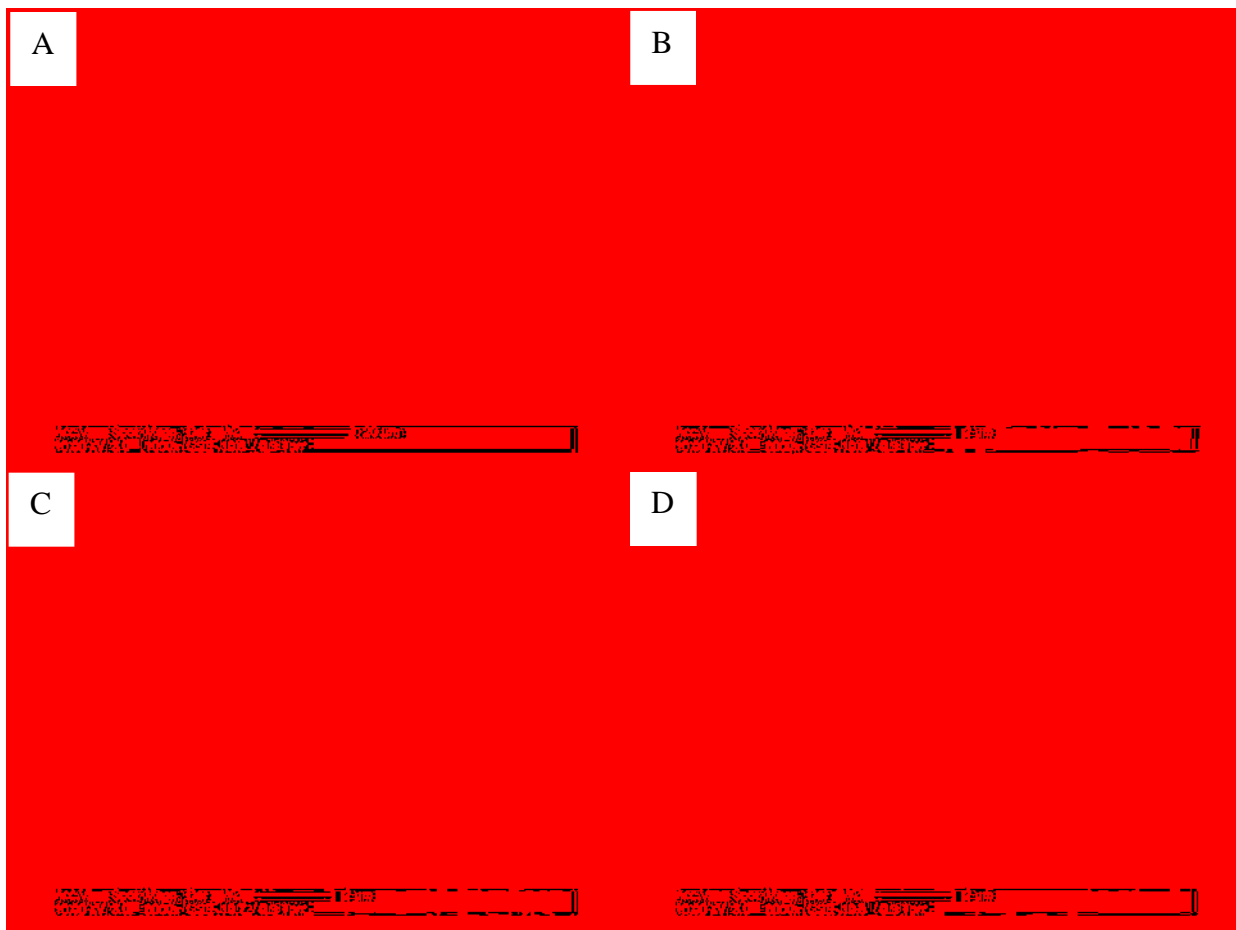
Figure 6.2. Scanning electron micrographs of monolithic columns (A) C3 (scale bar, 2 μm); (B) C3 (scale bar, 20 μm); (C) C2 (scale bar, 2 μm) and (D) C5 (scale bar, 2 μm).

6.3.2. Characterization of the Optimized Monolith

Mechanical Stability. To evaluate the mechanical stability of the synthesized monolith, the pressure drop across the column length was measured using different solvents including water, methanol, and ACN. A linear dependence of flow rate on back pressure was observed for all solvents, showing that the monolithic bed was stable at least up to approximately 2 mm/s.

Permeability. Permeability can be used to determine the swelling and shrinking of a monolith. In theory, column permeability decreases when a monolith swells, and vice versa. An ideal monolith should show no excessive swelling or shrinking in mobile phases of different polarity. The permeability was calculated using Darcy's law, $K = \eta uL/\Delta P$, where η is the dynamic viscosity of the mobile phase, L is the column length, u is the linear velocity of the mobile phase, and ΔP is the pressure drop along the length of the column. The calculated permeability values for column 3 with water, methanol and ACN were 9.20×10^{-15}, 16.4×10^{-15}, and 20.9×10^{-15} m^2, respectively. The permeability with ACN was 2.27 times higher than with water and 1.27 times higher than with methanol. The higher permeability with ACN indicates that the monolith swelled in polar solvents. However, even when it swelled in water, no detachment of the monolith from the capillary wall was observed. The column flow rate returned to the same value for a particular solvent after flushing with three column volumes of that solvent, indicating that swelling and shrinking were reversible.

Porosity and Pore Size Distribution. The porosity and pore size distribution of the monolith were investigated by ISEC. ISEC was originally designed to derive structural information about the pores in packed columns from retention data for specific probe compounds.[51] Guiochon et al. used ISEC to characterize the pore structures of silica monoliths and conventional packed columns.[52] Several definitions have arisen from these studies, including

the total porosity (ε_T), external porosity (ε_e) and internal porosity (ε_i). These porosities can be determined from ISEC data. The total porosity of the column was determined by the smallest injected molecule, toluene (M_n 92). The monolith pore size distribution was obtained from the relationship $M_w = 2.25\, d^{1.7}$, where M_w is the molecular mass of a polystyrene standard and d is the pore size diameter in Å. An ISEC plot for the poly(SPE-co-PEGDA) monolith shown in Figure 6.3 was obtained following this method. From Figure 6.3A, the total porosity was measured to be 74.9%; the excluded molecule mass was considered to be 7.6×10^4, which corresponds to 46 nm; the external porosity was calculated to be 69. 6%; and the internal porosity was 5.3%. The relatively large total porosity led to the low flow resistance of the monolithic column.

The accumulated pore size distribution derived from the ISEC plot is shown in Figure 6.3B. The pore volume fraction of pores larger than 304 nm was 88.2%, and of pores between 50 nm and 304 nm was 4.7%. The pore volume of pores less than 2 nm was approximately 4% and of pores between 2 nm to 50 nm was approximately 3.1%. It is obvious that most of the pore volume fraction was from pores larger than 304 nm. The mesopore volume fraction was only 3.1%.

6.3.3. Retention Mechanism

The mixture of toluene, formamide, and thiourea was used to investigate the HILIC properties of the poly(SPE-co-PEGDA) monolith. The mobile phase was 5 mmol L^{-1} ammonium formate at pH 5.0, containing various amounts of ACN from 25% to 95%. The influence of ACN content in the mobile phase on retention factors for the three test compounds is shown in Figure 6.4. Thiourea, which is commonly used as a dead time marker in RPLC, eluted after toluene and formamide when the content of ACN in the mobile phase was higher than 60%. When it was over 75%, toluene, a nonpolar compound, eluted first, and formamide and thiourea eluted
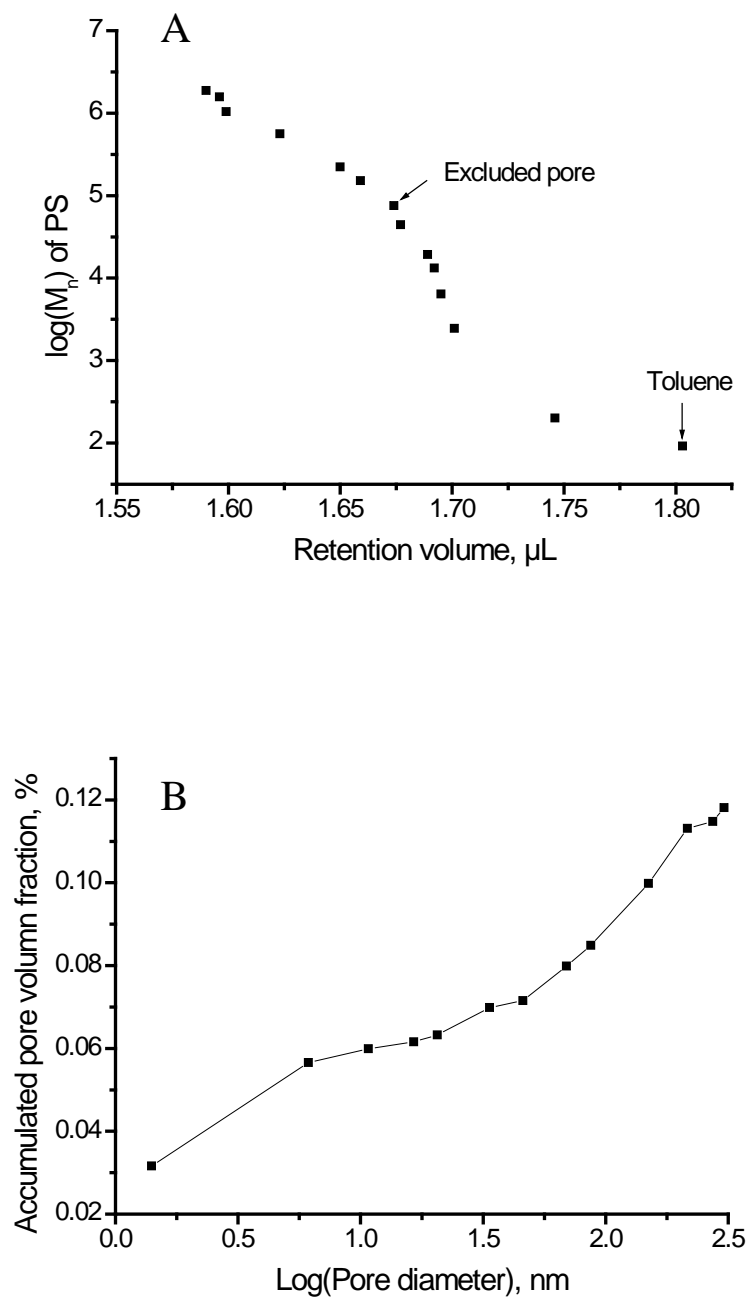
Figure 6.3. (A) ISEC plot and (B) accumulated pore size distribution for monolithic column C3.

Conditions: 54.5 cm × 75 µm I.D. column; THF mobile phase, 1500 psi constant pressure, 0.30 µL/min

mobile phase flow rate and 254 nm detection.

according to their polarities. The retention of toluene decreased dramatically when the content of

ACN increased from 25% to 60%, and then it decreased slightly when the ACN content was

further increased to 95%. In contrast to toluene, the retention of thiourea leveled off when the

ACN content varied from 25% to 60%, and then increased as the ACN content increased to 95%.

Formamide behaved similar to thiourea with less increase. These results are similar to reports by

other researchers,[35,43] demonstrating a typical HILIC mechanism when the content of ACN in the

mobile phase was higher than 60%.

6.3.4. Reproducibility

A mixture of toluene, formamide, and thiourea was used to evaluate the reproducibility of

the poly(SPE-co-PEGDA) monolith. With a mobile phase of 60% ACN in 5 mmol L^{-1}

ammonium formate at pH 5.0, good stability was demonstrated with relative standard deviations

(RSD, n=5) of 0.62, 0.12 and 0.13% for retention times of toluene, formamide, and thiourea,

respectively. After two months of use and hundreds of runs, the column efficiency exhibited no

deterioration, which confirmed the robustness of the monolithic column.

6.3.5. Separation of Amides

Considering the hydrophilic environment provided by the poly(SPE-co-PEGDA) monolith, a

mixture of amides including formamide, methacrylamide, acrylamide, and N,N-

dimethacrylamide was used as a structurally related neutral compound mixture, which is difficult

to separate by RPLC. Acceptable separation of these amides was obtained with 98% ACN in the

mobile phase (Figure 6.5A). The elution order from less to more polar confirmed the HILIC

separation mechanism. As expected, the elution times of these amides increased with 100% ACN

as the mobile phase, and the resolution between them also increased (Figure 6.5B).
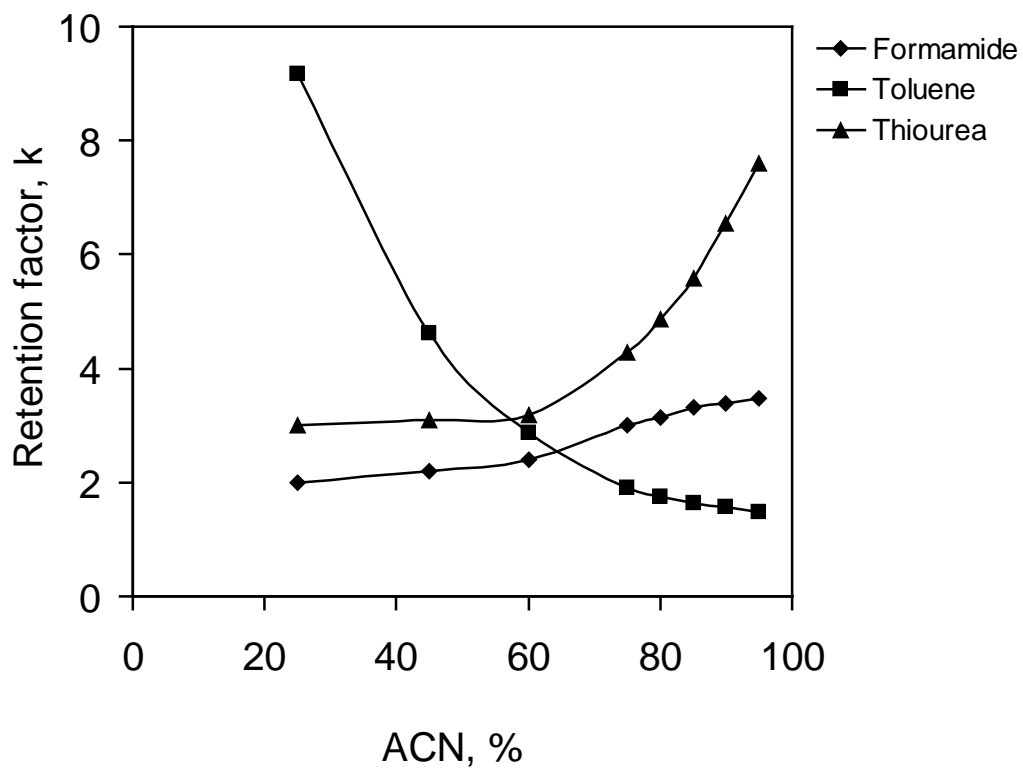
Figure 6.4. Relationship between retention factor and ACN concentration for three test analytes on monolithic column C3. Conditions: 15.5 cm × 75 µm I.D. column; 5 mmol L^{-1} ammonium formate (pH 5.0) in ACN/H_2O mobile phase; 214 nm detection; 400 nL/min flow rate; 60 nL injection volume.
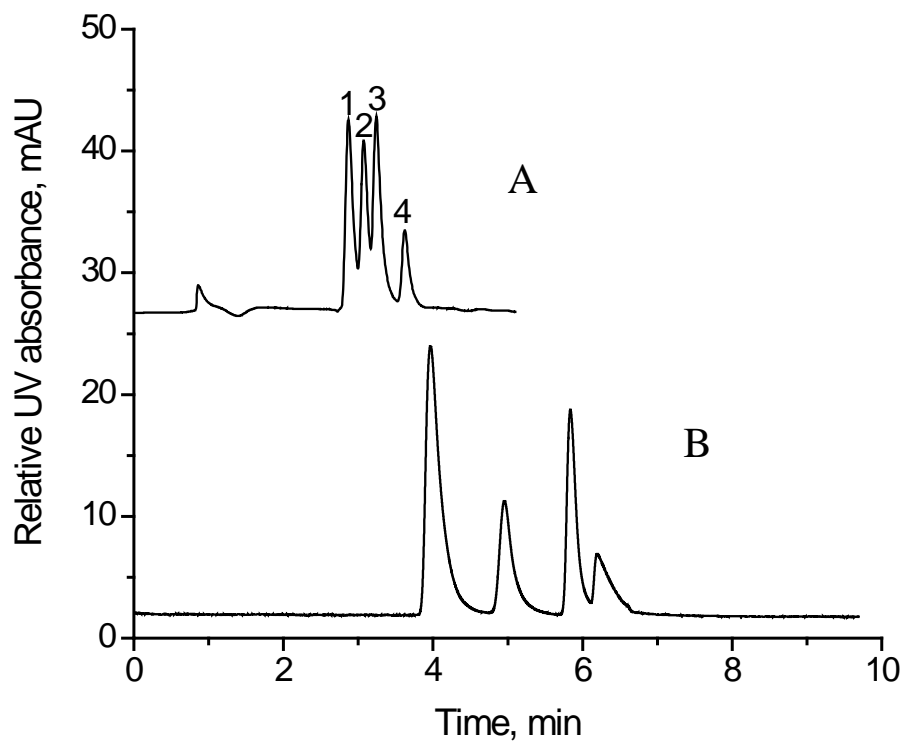
Figure 6.5. Separation of neutral amides. Conditions: 15.5 cm × 75 µm I.D. column; (A) 5 mmol L^{-1} ammonium formate (pH 5.0) in 98% ACN/H$_2$O mobile phase and (B) ACN mobile phase; 214 nm detection; 400 nL/min flow rate; 60 nL injection volume. Peak identifications: (1) N,N-dimethacrylamide, (2) methacrylamide, (3) acrylamide, and (4) formamide.

6.3.6. Separation of Phenols

A mixture of phenols including phenol, catechol, hydroquinone, resorcinol and pyrogallol was selected to further evaluate the poly(SPE-co-PEGDA) monolith. A separation is shown in Figure 6.6A, for which an efficiency of over 40,000 plates/m was obtained. Obviously, retention times increased with an increase in number of hydroxyl groups in the molecule. Phenol, which is the least polar compound due to only one hydroxyl group, eluted first, followed by the other three compounds (i.e., catechol, hydroquinone and resorcinol with two hydroxyl groups) eluting according to polarity. Finally, the most polar compound, pyrogallol, containing three hydroxyl groups eluted.

The effect of ACN content on retention of the phenolic compounds is shown in Figure 6.6B. The retention of phenols increased when the ACN content increased from 75% to 95%, showing that the ACN content has an effect on the retention factors of polar compounds. The retention factor for phenol increased less than the other compounds, indicating that ACN content has a greater effect on more polar compounds, consistent with hydrophilic interactions between the phenols and the monolithic stationary phase.

6.3.7. Separation of Benzoic Acids

Since SPE contains both positive and negative charges, the poly(SPE-co-PEGDA) monolith may exhibit ionic interactions with charged compounds in addition to hydrophilic interactions. Varying the organic solvent concentration, pH, and salt concentration in the mobile phase would be expected to affect the selectivity, resolution and peak shapes. The separation of seven benzoic acids is shown in Figure 6.7A. A column efficiency of over 75,000 plates/m was
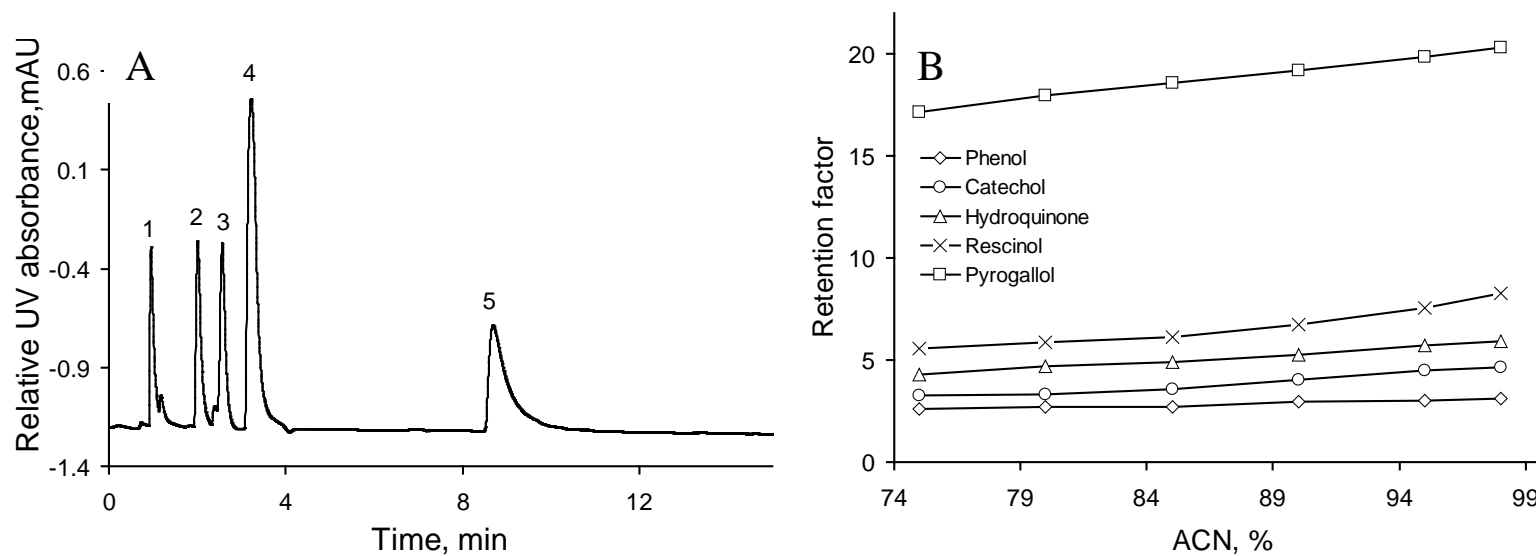
Figure 6.6. (A) Separation of phenols and (B) effect of ACN content on the retention factors of phenols. Conditions: (A) 8.7 cm and (B) 15.5 cm × 75 µm I.D. column; 5 mmol L^{-1} ammonium formate (pH 5.0) in 98% ACN/H$_2$O mobile phase; 214 nm detection; 400 nL/min flow rate; 60 nL injection volume. Peak identifications: (1) phenol, (2) catechol, (3) hydroquinone, (4) resorcinol, and (5) pyrogallol.

obtained. Obviously, compounds containing more hydroxyl groups eluted later.

The effect of ACN concentration on the retention times of benzoic acids is shown in Figure 6.7B. Resolution and selectivity were influenced by the amount of ACN in the mobile phase. Hydrophilic interactions were increased by an increase in ACN in the mobile phase, indicated by an increase in retention factor. These polar benzoic acids behaved similarly. Retention times increased slightly with an increase in ACN concentration from 75% to 90%, and then increased dramatically from 90% to 95%. Baseline separation was obtained throughout this range.

The effect of mobile phase pH on the separation of benzoic acids using the poly(SPE-co-PEGDA) monolith was investigated by changing the pH of the salt solution before mixing with ACN. A 1 M ammonium formate solution was adjusted to pH values of 3.0, 4.0, 5.0, 6.5, and 8.0 using formic acid and ammonium hydroxide. The effect of pH on retention of benzoic acids is shown in Figure 6.8A using 85% ACN in 5 mmol L^{-1} ammonium formate. In addition to participating in hydrophilic interactions, the poly(SPE-co-PEGDA) monolith can also provide ionic interactions with analytes carrying negative charges. Obviously, the retention factors of benzoic acids are dependent on the pH of the mobile phase. As the pH of the mobile phase approached or surpassed the pK_a values of the benzoic acids, they became deprotonated, negatively charged, and more hydrophilic, leading to stronger hydrophilic and ionic interactions, and, thus, longer retention.

The effect of mobile phase concentration on retention factors of benzoic acids was investigated by varying the concentration of ammonium formate from 5 to 50 mmol L^{-1} in the mobile phase at pH 3.0 containing 85% ACN. As can be seen in Figure 6.8B, the retention factors of the benzoic acids increased slightly when the concentration of ammonium formate

increased from 5 to 50 mmol L^{-1}, except for 2-hydroxybenzoic acid. Since the pK_a values of

these benzoic acids, except 2-hydroxybenzoic acid are all above or close to 3.0, no ionic

interactions existed between the analytes and the poly (SPE-co-PEGDA) monolith. The increase

in retention factors resulted primarily from an increase in hydrophilicity of the monolith. As

Alpert suggested,[4] the salt in the mobile phase prefers to be in the water-rich liquid layer on the

column surface due to the high content of ACN in the mobile phase. The higher salt

concentration forces more salt ions into the water-rich layer, leading to an increase in

hydrophilicity and longer retention.[35] Since the pK_a value of 2-hydroxybenzoic acid is 2.98, it is

negatively charged at pH 3.0. Thus, both ionic interaction and hydrophilic interaction contribute

to retention. Higher salt concentration in the water-rich layer increased hydrophilic interactions

and decreased ionic interactions. As expected, the opposite effect was observed, i.e., the

retention factor of 2-hydroxybenzoic acid increased slightly when the concentration of

ammonium formate increased from 5 to 10 mmol L^{-1}, and then decreased when the concentration

increased further to 50 mmol L^{-1}.

6.4. Conclusions

Poly(SPE-co-PEGDA) monolithic columns were prepared in fused silica columns by

photo-initiated copolymerization of SPE and PEGDA in a binary porogen consisting of 2-

propanol and decanol. The optimized column was successfully used in HILIC. A typical HILIC

mechanism was observed when the mobile phase contained high organic content (ACN > 60%).

The effects of pH, salt concentration, and ACN content in the mobile phase on the separation of

phenols and benzoic acids were studied, showing both ionic and hydrophilic interactions that

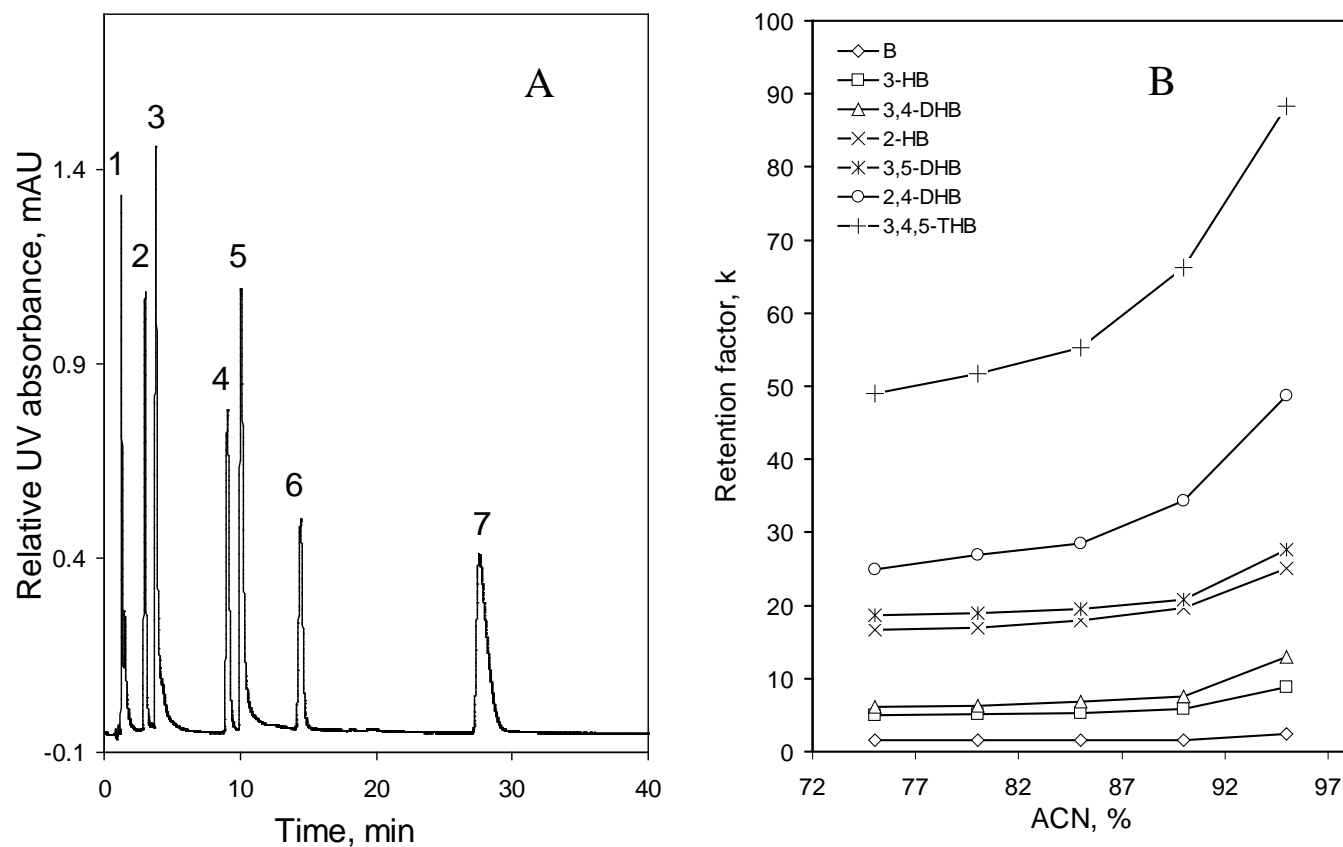significantly affected on retention and selectivity.

Figure 6.7. (A) Separation of benzoic acids and (B) effect of ACN concentration on separation of benzoic acids. Conditions: 8.7 cm × 75 µm I.D. column; 5 mmol L^{-1} ammonium formate (pH 3.0) in 85% ACN/H$_2$O mobile phase; 214 nm detection; 800 nL/min flow rate; 60 nL injection volume. Peak identifications: (1) B, (2) 3-hydroxybenzoic acid, (3) 3,4-dihydroxybenzoic aicd, (4) 2-B, (5) 3,5-dihydroxybenzoic acid, (6) 2,4-dihydroxybenzoic acid, and (7) 3,4,5-trihydroxybenzoic acid.
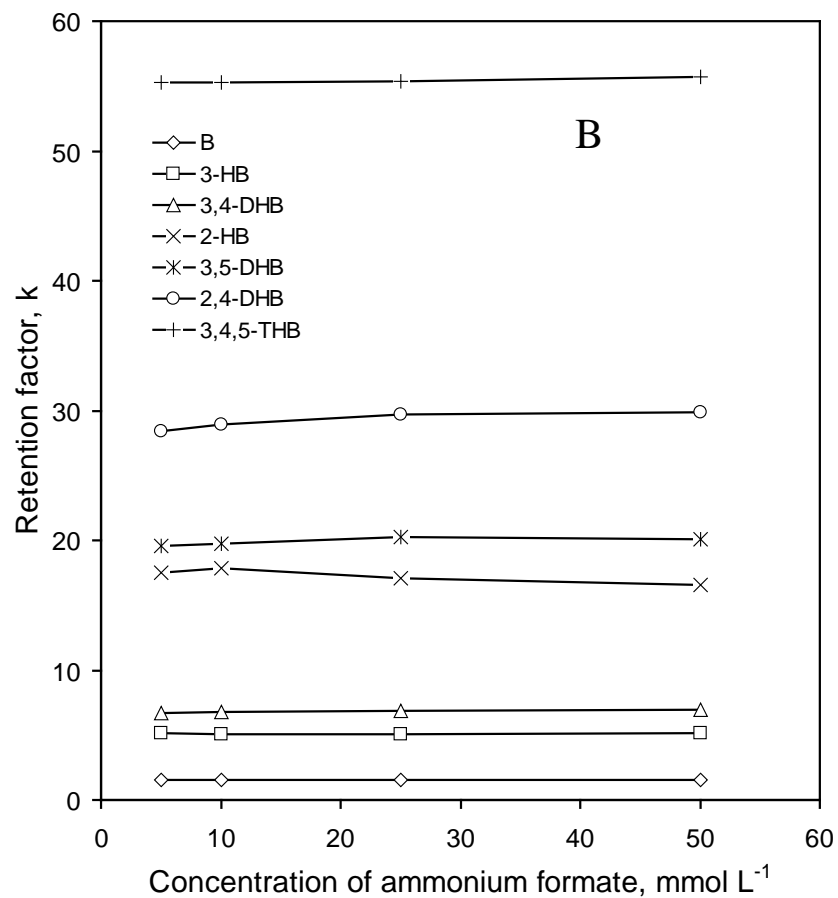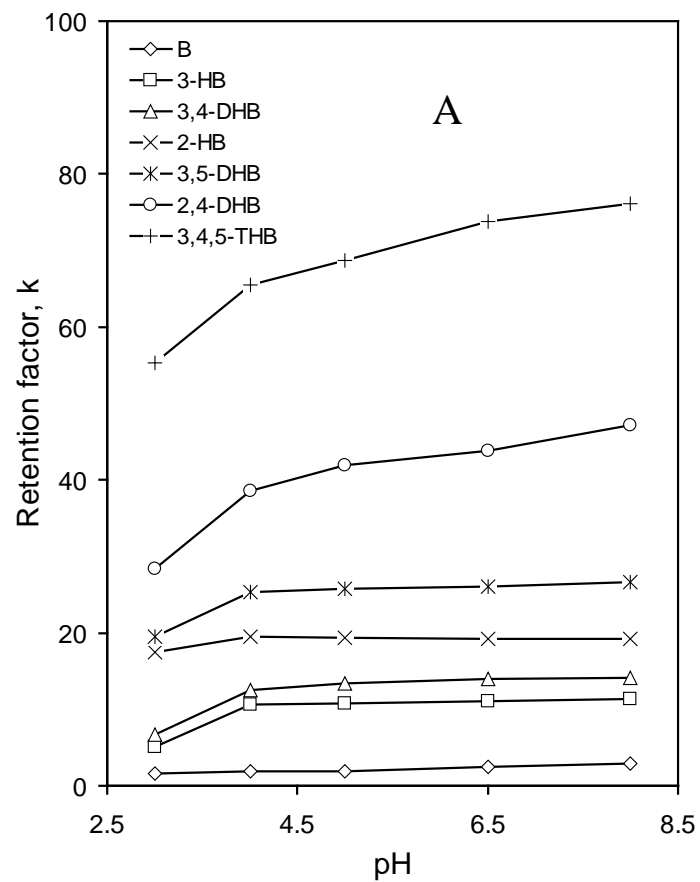
Figure 6.8. (A) Effect of pH on the separation of benzoic acids and (B) effect of salt concentration in the separation of benzoic acids. Other conditions are the same as in Figure 6.7A.

6.5. References

1. Winnik, W. M.; Ortiz, P. A. *J. Chromatogr. B* **2008,** *875*, 478-486.

2. Roberts, J. M.; Diaz, A. R.; Fortin, D. T.; Friedle, J. M.; Piper, S. D. *Anal. Chem.* **2002**, *74*, 4927-4932.

3. Naidong, W. *J. Chromatogr. B* **2003,** *796*, 209-224.

4. Alpert, A. J. *J. Chromatogr.* **1990**, *499*, 177-196.

5. Hemström, P.; Irgum, K. *J. Sep. Sci.* **2006**, *29*, 1784-1821.

6. Yoshida, T. *J. Biochem. Biophys. Meth.* **2004**, *60*, 265-280.

7. Berthod, A.; Chang, S. S. C.; Kullman, J. P. S.; Armstrong, D. W. *Talanta* **1998**, *47*, 1001-1012.

8. Jiang, Z.; Reilly, J.; Everatt, B.; Smith, N. W. *J. Chromatogr. A* **2009**, *1216*, 2439-2448.

9. Guo, Y.; Gaiki, S. *J. Chromatogr. A* **2005**, *1074*, 71-80.

10. Churms, S. C. *J. Chromatogr. A* **1996**, *720*, 75-91.

11. Olsen, B. A. *J. Chromatogr. A* **2001**, *913*, 113-122.

12. Troyer, J. K.; Stephenson, K.; Fahey, J. W. *J. Chromatogr. A* **2001**, *919*, 299-304.

13. Ng, E. S. M.; Yang, F.; Kameyama, A.; Palcic, M. M.; Hindsgaul, O.; Schreimer, D. C. *Anal. Chem.* **2005**, *77*, 6125-6133.

14. Zywicki, B.; Catchpole, G.; Dreper, J.; Fiehn, O. *Anal. Biochem.* **2005**, *336*, 178-186.

15. Jandera, P. *J. Sep. Sci.* **2008**, *31*, 1421-1437.

16. Boersema, P. J.; Mohammed, S.; Heck, A. J. R. *Anal. Bioanal. Chem.* **2008**, *391*, 151-159.

17. Ikegami, T.; Tomomatsu, K.; Takubo, H.; Horie, K.; Tanaka, N. *J. Chromatogr. A* **2008**, *1184*, 474-503.

18. Jinno, K.; Quiming, N. S.; Denola, N. L.; Saito, Y. *Anal. Bioanal. Chem.* **2009**, *393*, 137-

153.

19. Song, Q.; Naidong, W. *J. Chromatogr. B* **2006**, *830*, 135-142.

20. Eerkes, A.; Addison, T.; Naidong, W. *J. Chromatogr. B* **2002**, *768*, 277-284.

21. Li, R. P.; Huang, J. *J. Chromatogr. A* **2004**, *1041*, 163-169.

22. Godejohann, M. *J. Chromatogr. A* **2007**, *1156*, 87-93.

23. Person, M.; Hazotte, A.; Elfakir, C.; Lafosse, M. *J. Chromatogr. A* **2005**, *1081*, 174-181.

24. Risley, D. S.; Yang, W. Q.; Peterson, J. A. *J. Sep. Sci.* **2006,** *29*, 256-264.

25. Charlwood, J.; Birrell, H.; Bouvier, E. S. P.; Langridge, J.; Camilleri, P. *Anal. Chem.* **2000**, *72*, 1469-1474.

26. Fu, H. J.; Jin, W. H.; Xiao, H.; Huang, H. W.; Zou, H. F. *Electrophoresis* **2003**, *24*, 2084-2091.

27. West, C.; Lesellier, E. *J. Chromatogr. A* **2006**, *1110*, 200-213.

28. Liu, Y.; Urgaonkar, S.; Verkade, J. G.; Armstrong, D. W. *J. Chromatogr. A* **2005**, *1079*, 146-152.

29. Oertel, R.; Neumeister, V.; Kirch, W. *J. Chromatogr. A* **2004**, *1058*, 197-201.

30. Omaetxebarria, M. J.; Hägglund, P.; Elortza, F.; Hooper, N. M.; Arizmendi, J. M.; Jensen, O. N. *Anal. Chem.* **2006**, *78*, 3335-3341.

31. Wang, X.; Lu, H.; Lin, X.; Xie, Z. *J. Chromatogr. A* **2008**, *1190*, 365-371.

32. Lin, J.; Lin, J.; Lin, X.; Xie, Z. *J. Chromatogr. A* **2009**, *1216*, 801-805.

33. Wang, X.; Lin, X.; Xie, Z.; Giesy, J. P. *J. Chromatogr. A* **2009**, *1216*, 4611-4617.

34. Persson, J.; Hemström, P.; Irgum, K. *J. Sep. Sci.* **2008**, *31*, 1504-1510.

35. Jiang, Z.; Smith, N. W.; Ferguson, P. D.; Taylor, M. R. *Anal. Chem.* **2007**, *79*, 1243-1250.

36. Pietrzyk, D. J.; Senne, S. M.; Brown, D. M. *J. Chromatogr.* **1991**, *546*, 101-110.

37. Nesterenko, P. N.; Haddad, P. R. *Anal. Sci.* **2000**, *16*, 565-574.

38. Jiang, W.; Irgum, K. *Anal. Chem.* **1999**, *71*, 333-344.

39. Jiang, W.; Irgum, K. *Anal. Chem.* **2001**, *73*, 1993-2003.

40. Jiang, W.; Irgum, K. *Anal. Chem.* **2002**, *74*, 4682-4687.

41. Gong, B.; Bo, C.; Zhu, J.; Yan, C. *J. Appl. Poly. Sci.* **2009**, *113*, 984-991.

42. Viklund, C.; Irgum, K. *Macromolecules* **2000**, *33*, 2539-2544.

43. Jiang, Z.; Reilly, J.; Everatt, B.; Smith, N. W. *J. Chromatogr. A* **2009**, *1216*, 2439-2448.

44. Jiang, Z.; Smith, N. W.; Ferguson, P. D.; Taylor, M. R. *J. Sep. Sci.* **2009**, *32*, 2544-2555.

45. Zhao, Z.; Malik, A.; Lee, M. L. *Anal. Chem.* **1993**, *65*, 2747-2752.

46. Tan, H.; Yeung, E. S. *Electrophoresis* **1997**, *18*, 2893-2900.

47. Gu, B.; Chen, Z.; Thulin, C. D.; Lee, M. L. *Anal. Chem.* **2006**, *78*, 3509-3518.

48. Sederel, W. L.; Jong, G. J. *J. Appl. Polym. Sci.* **1973**, *17*, 2835-2846.

49. Guyot, A.; Bartholin, M. *Prog. Polym. Sci.* **1982**, *8*, 277-331.

50. Svec, F.; Fréchet, J. M. J. *Chem. Mater.* **1995**, *7*, 707-715.

51. Halász, I.; Martin, K. *Angew. Chem. (Int. Engl.)* **1978**, *17*, 901-908.

52. Al-Bokari, M.; Cherrak, D.; Guiochon, G. *J. Chromatogr. A* **2002**, *975*, 275-284.

CHAPTER 7 FUTURE DIRECTIONS

7.1 Introduction

Several polymeric monolithis have been prepared by *in situ* photo-initiated copolymerization. These monoliths were evaluated for IEC of biomolecules and HILIC of small molecules. High peak capacities and high efficiencies were obtained compared to commercial packed columns. However, considerable work remains to be done to achieve the full potential of this relative new column type.

7.2 Preparation of Polymeric Monoliths Using the Grafting Method for IEC

Gu et al.[1] prepared several monoliths with different monomers and PEGDA as cross-linker. The hydrophobicities of these monoliths were systematically evaluated. The authors concluded that the contribution of hydrophobicity from the monomer mainly resulted from the linking group that connected the sulfonic acid functionality with the polymerization functionality. Among the three monoliths, namely poly(AMPS-co-PEGDA), poly[sulfoethyl methacrylate (SEMA)-co-PEGDA], and poly[vinylsulfonic acid (VS)-co-PEGDA], the poly(VS-co-PEGDA) monolith showed the lowest hydrophobicity due to the lower hydrocarbon content of VS compared to AMPS and SEMA. However, some limitations were observed. For example, although the poly(AMPS-co-PEGDA) monolith exhibited high dynamic binding capacity for both peptides and proteins, and it performed well for peptide separations, it did not separate proteins very well. The separation of peptides was good even without any ACN in the mobile phase to reduce hydrophobic interactions. The performance of the poly(VS-co-PEGDA) monolith for peptide and protein separation was better than the poly(SEMA-co-PEGDA) monolith, although the poly(VS-co-PEGDA) monolith had a lower dynamic binding capacity for peptides. Obviously, the hydrophobicities of the monomer and the monolith cannot totally

explain the results. The dynamic binding capacity, pore size distribution, and hydrophobicity all contribute to the separation.

Grafting can be used to modify an existing monolith without affecting the pore size or morphology of the monolith. I suggest that selected monomers be grafted onto an existing (i.e., standardized) monolith to study the effect of hydrophobicity on the separation of peptides and proteins. Since the resulting monoliths would have the same pore size distribution, only the dynamic binding capacity and hydrophobicity would affect the separation. Thus, the effect of hydrophobity of the monomer on the separation could be clearly elucidated. A poly[poly(ethylene glycol) methyl ether acrylate (PEGMEA)-co-PEGDA] monolith could be used as the parent monolith for grafting because it has been demonstrated to resist adsorption of proteins.[2] AMPS, SEMA, VS, 2-propene-1-sulfonic acid and 2-methyl-2-propene-1-sulfonic acid could be photo-grafted onto the poly(PEGMEA-co-PEGDA) monolith. The resulting monoliths could then be tested to determine the effect of monomer hydrophobicity. Dynamic binding capacity could also be measured. Chromatographic separations of peptides and proteins in the IEC mode could be used to evaluate performance.

7.3 Preparation of Methylacrylate-Based Hypercross-linked Monoliths

Generally, polymer monoliths exhibit small surface areas due to lack of mesopores. Thus, they are not suitable for efficient separation of small molecules such as alkylbenzenes. Several papers have reported rather low efficiencies observed for small molecules using polymeric monoliths.[3-5] Several approaches, including termination of the polymerization reaction at an early stage[6,7] and use of high polymerization temperature,[8] have been used to improve the separation performance of polymeric monoliths for small molecules. However, it is difficult to

prepare polymeric monoliths containing both large through pores and small pores in a single step.

Davankov et al. reported hypercross-linked polymeric materials that exhibit large surface areas.[9,10] The hypercross-linked polymeric materials were obtained under conditions in which the rigid polymeric network was formed in the presence of large amounts of good porogens. Linear polystyrene was used to obtain a rigid polymer, which was then cross-linked via Friedel-Crafts alkylation to afford materials containing mostly small pores. Later, this method was used to prepare poly(styrene-divinylbenzene) particles containing both the original pores and an extensive network of additional micro- and meso-pores generated during hypercross-linking.[11,12] Recently, Urban et al.[13] prepared a hypercross-linked monolith based on a monolithic poly(styrene-co-vinylbenzyl chloride-co-divinylbenzene) precursor. A surface area of 663 m^2/g was obtained, which was more than 1 order of magnitude larger than that of the precursor monolith. Isocratic separation of alkylbenzenes was achieved and a size exclusion effect was also observed; however, the separation efficiency was not very good.

I suggest that hypercross-linked monoliths be synthesized based on methacrylate monomers. First, a precursor monolith would be prepared using photo copolymerization of PEGMEA and PEGDA. Then, divinylbenzyl would be photografted on the monolith. The grafted monolith would be flushed with 1,2-dichloroethane (DCE). A filtered solution of $FeCl_3$ in DCE would be pumped through the monolithic column in an ice bath. Finally, the hypercrosslinking reaction would be carried out using both thermo-initiated and photo-initiated polymerization. The resulting monoliths would finally be evaluated for chromatographic separation of small molecules such as the alkylbenzenes.

7.4 Preparation of Hybrid Monoliths

Monolithic columns are mainly classified into silica-based and organic polymer-based. These two types of monoliths have their own inherent drawbacks, which include mechanical and solvent instability of polymer-based monoliths and pH sensitivity of silica-based monoliths. Organic-inorganic hybrid monolithic columns could overcome the separate drawbacks of polymer- and silica-based monolithic columns. A hybrid monolith would combine the merits of both organic polymer- and inorganic silica-based monoliths.

I suggest that hybrid monoliths could be synthesized via copolymerization of methacryl-substituted polyhedral oligomeric silsesquioxane (POSS) (Figure 7.1) and decyl methacrylate (DMA) or stearyl methacrylate (SMA). POSS is a cagelike silsesquioxane, which has an inorganic-organic architecture containing an inner inorganic framework made of silicon and oxygen.[14] The rigid silicon and oxygen framework would enhance the mechanical and thermal stability of the resultant hybrid monolith. Before the preparation of the hybrid monolith, a fused silica capillary would be pretreated to introduce vinyl bonds onto the inner surface to anchor the monolithic matrix as previous described.[2] A polymerization mixture consisting of DMA or SMA, POSS-MA, initiator, and porogens would be sonicated before being introduced into the capillary. The monolith then would be copolymerized by both thermal and photo initiation. The resulting monoliths would be used to separate small and large molecules such as peptides and proteins in the RPLC mode.

7.5 Post Modification Preparation of Monoliths

Modification of a monolith with reactive functionalities is a useful tool to obtain new monoliths, which can be applied in a variety of separation modes. Glycidyl methacrylate-based monoliths have been widely used for this approach since they offer access to various reactions.[15]
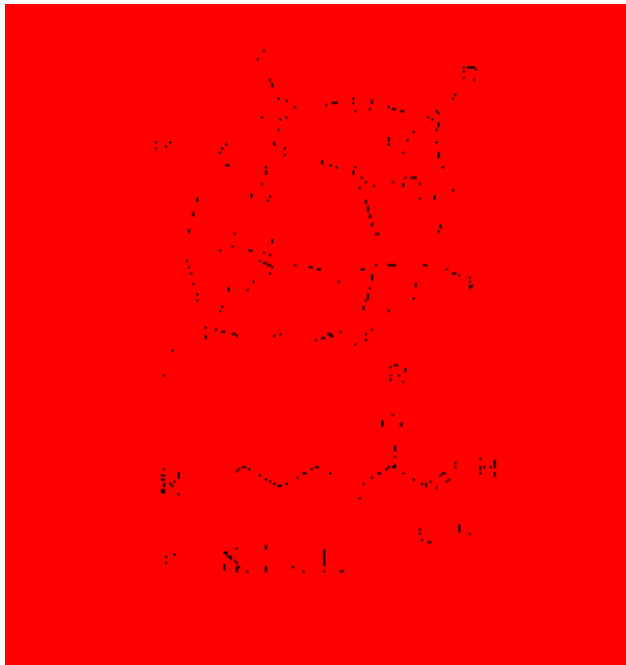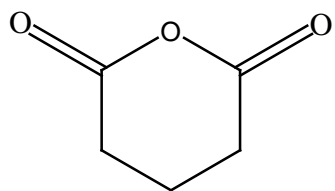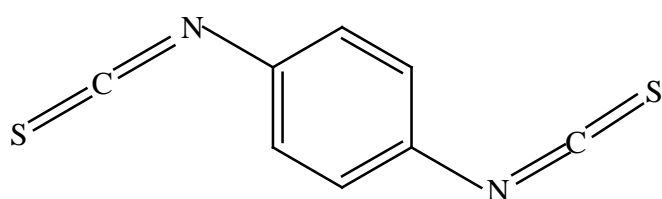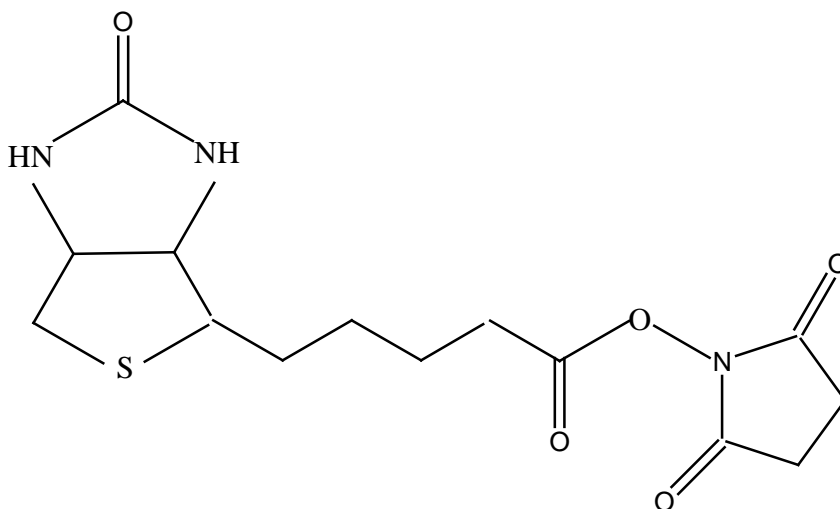
Figure 7.1. Chemical structure of POSS-MA.

I suggest that monoliths could be prepared based on post modification of poly(GMA-co-EDMA) monoliths for chromatographic use in the IEC and RP modes. The Poly(GMA-co-EDMA) monoliths would be prepared as described previously.[16] The monolith would be flushed sequentially with ethylenediamine and methanol, and then with glutaric anhydride (GA), 1,4-diisothiocyanate (PDITC), or biotin NHS ester (BNE) to obtain new monoliths. Reaction of GA, PDITC, and BNE (structures in Figure 7.2) would introduce amine groups in the modified monolith.[17] The synthesis schematics are shown in Figure 7.3. The resulting monoliths would be evaluated for IEC and RPLC separations.

GA

PDITC

BNE

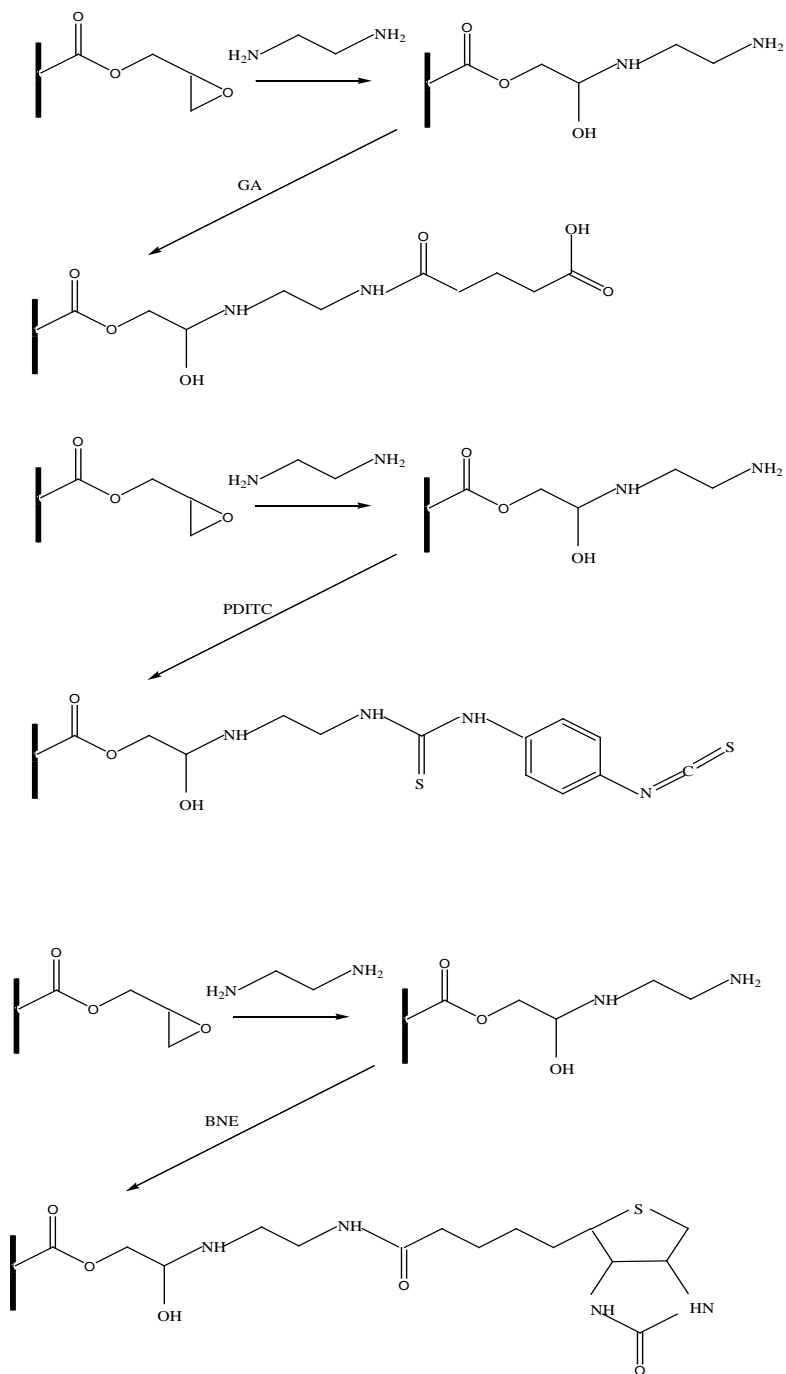Figure 7.2. Chemical structures of GA, PDITC, and NBE.

Figure 7.3. Schematic of the preparation of monoliths modified with GA, PDITC, and NBE.

7.6 References

1. Gu, B.; Li, Y.; Lee, M. L. *Anal. Chem.* **2007**, *79*, 5848-5855.

2. Gu, B.; Armenta, J. M.; Lee, M. L. *J. Chromatogr. A* **2005**, *1079*, 382-391.

3. Moravcova, D.; Jandera, P.; Urban, J.; Planeta, J. *J. Sep. Sci.* **2004**, *27*, 789-800.

4. Huo, Y.; Schoenmakers, P. J.; Kok, W. T. *J. Chromatogr. A* **2007**, *1175*, 81-88.

5. Hirano, T.; Kitagawa, S.; Ohtani, H. *Anal. Sci.* **2009**, *25*, 1107-1113.

6. Wang, Q.; Svec, F.; Fréchet, J. M. J. *Anal. Chem.* **1995**, *67*, 670-674.

7. Trojer, L.; Bisjak, C. P.; Wieder, W.; Bonn, G. K. *J. Chromatogr., A* **2009**, *1216*, 6303-6307.

8. Meyer, U.; Svec, F.; Fréchet, J. M. J.; Hawker, C. J.; Irgum, K. *Macromolecules* **2000**, *33*, 7769-7775.

9. Davankov, V. A.; Tsyurupa, M. P. *React. Polym.* **1990**, *13*, 27-42.

10. Davankov, V. A.; Tsyurupa, M.; Ilyin, M.; Pavlova, L. *J. Chromatogr. A* **2002**, *965*, 65-73.

11. Ahn, J. H.; Jang, J. E.; Oh, C. G.; Ihm, S. K.; Cortez, J.; Sherrington, D. C. *Macromolecules* **2006**, *39*, 627-632.

12. Germain, J.; Hradil, J.; Svec, F.; Fréchet, J. M. J. *Chem. Mater.* **2006**, *18*, 4430-4435.

13. Urban, J.; Svec, F.; Fréchet, J. M. J. *Anal. Chem.* **2010**, *82*, 1621-1623.

14. Li, G. Z.; Wang, L. C.; Toghiani, H.; Daulton, T. L.; Koyama, K.; Pittman, C. U. *Macromolecules* **2001**, *34*, 8686-8693.

15. Buchmeiser, M. R. *Polymer* **2007**, *48*, 2187-2198.

16. Xu, Y.; Cao, Q.; Svec, F.; Fréchet, J. M. J. *Anal. Chem.* **2010**, *82*, 3352-3358.

17. Saini, G.; Gates, R.; Asplund, M. C.; Blair, S.; Attavar, S.; Linford, M. R. *Lab Chip* **2009**, *9*, 1789-1796.